ปฏิกิริยารีดักชันแบบเลือกเกิดที่ใช้ตัวเร่งปฏิกิริยาของก๊าซไนโตรเจนออกไซด์โดยก๊าซแอมโมเนียบนตัวเร่งปฏิกิริยา V_2O_5-WO_3/TiO_2ที่ส่งเสริมด้วยแมงกานีสและโลหะอีกตัว (ซีเรียม, ทองแดง หรือ เหล็ก)

นายอิสกันต์ อรัญญาเกษมสุข

วิทยานิพนธ์นี้เป็นส่วนหนึ่งของการศึกษาตามหลักสูตรปริญญาวิศวกรรมศาสตรมหาบัณฑิต
สาขาวิชาวิศวกรรมเคมี ภาควิชาวิศวกรรมเคมี
คณะวิศวกรรมศาสตร์ จุฬาลงกรณ์มหาวิทยาลัย
ปีการศึกษา 2551

SELECTIVE CATALYTIC REDUCTION OF NO BY NH_3 OVER V_2O_5-WO_3/TiO_2 CATALYST PROMOTED BY Mn AND ANOTHER METAL (Ce, Cu OR Fe)

Mr. Izkun Arunyakasemsuk

A Thesis Submitted in Partial Fulfillment of the Requirements
for the Degree of Master of Engineering Program in Chemical Engineering
Department of Chemical Engineering
Faculty of Engineering
Chulalongkorn University
Academic Year 2008

Thesis Title	SELECTIVE CATALYTIC REDUCTION OF NO BY NH_3 OVER V_2O_5-WO_3/TiO_2 CATALYST PROMOTED BY Mn AND ANOTHER METAL (Ce, Cu OR Fe)
By	Mr. Izkun Arunyakasemsuk
Field of study	Chemical Engineering
Thesis Advisor	Akawat Sirisuk, Ph.D.

Accepted by the Faculty of Engineering, Chulalongkorn University in Partial Fulfillment of the Requirements for the Master's Degree

……...… Dean of the Faculty of Engineering
(Associate Professor Boonsom Lerdhirunwong, Dr.Ing.)

THESIS COMMITTEE

…….. Chairman
(Associate professor Paisan Kittisupakorn, Ph.D.)

…….……. Advisor
(Akawat Sirisuk, Ph.D.)

…….. Examiner
(Assistant Professor Joongjai Panpranot, Ph.D.)

…….. External Examiner
(Kriangsak Kraiwattanawong, D.Eng..)

อิสกันต์ อรัญญาเกษมสุข: ปฏิกิริยารีดักชันแบบเลือกเกิดที่ใช้ตัวเร่งปฏิกิริยาของก๊าซไนโตรเจนออกไซด์โดยก๊าซแอมโมเนียบนตัวเร่งปฏิกิริยา V_2O_5-WO_3/TiO_2 ที่ส่งเสริมด้วยแมงกานีสและโลหะอีกตัว (ซีเรียม, ทองแดง หรือ เหล็ก) (SELECTIVE CATALYTIC REDUCTION OF NO BY NH_3 OVER V_2O_5-WO_3/TiO_2 CATALYST PROMOTED BY MN AND ANOTHER METAL (Ce, Cu OR Fe)) อ.ที่ปรึกษาวิทยานิพนธ์หลัก: ดร.อัครวัต ศิริสุข, 89 หน้า.

ในงานวิจัยนี้ทำการศึกษาปฏิกิริยารีดักชันของก๊าซไนตริคออกไซด์แบบเลือกเกิดด้วยก๊าซแอมโมเนีย บนตัวเร่งปฏิกิริยา V_2O_5-WO_3/TiO_2 และตัวเร่งปฏิกิริยา V_2O_5-WO_3/TiO_2 ที่ปรับปรุงด้วยแมงกานีสและโลหะอีกตัว (ซีเรียม ทองแดง และ เหล็ก) โดยเตรียมไททาเนียมไดออกไซด์ด้วยวิธีโซล-เจล และเติมโลหะวานาเดียมและทังสเตนบน TiO_2 ด้วยวิธีการเคลือบฝังแบบเปียกในการวิเคราะห์ตัวเร่งปฏิกิริยาโดยใช้เทคนิคหลายอย่างได้แก่ nitrogen adsorption, XRD, NH_3-TPD, XPS และ ICP-OES ตัวเร่งปฏิกิริยา V_2O_5-WO_3/TiO_2 ถูกใช้ในปฏิกิริยารีดักชันของก๊าซไนตริคออกไซด์แบบเลือกเกิดด้วยก๊าซแอมโมเนียที่ช่วงอุณหภูมิ 100-450°C โดยสามารถการเปลี่ยนก๊าซ NO ได้เกือบทั้งหมดที่อุณหภูมิ 250-350°C และตัวเร่งปฏิกิริยา V_2O_5-WO_3/TiO_2 ที่ประกอบด้วยโลหะวานาเดียมร้อยละ3 โดยน้ำหนัก และโลหะทังสเตนร้อยละ12 โดยน้ำหนักเป็นตัวเร่งปฏิกิริยาที่ดีที่สุด เพราะสามารถให้ค่าความว่องไวสูงในช่วงอุณหภูมิกว้าง

ในการเพิ่มความว่องไวของตัวเร่งปฏิกิริยา V_2O_5-WO_3/TiO_2 ภายใต้สภาวะที่มีไอน้ำนั้น เราเติมโลหะแมงกานีสและโลหะอีกตัว (ซีเรียม ทองแดง และเหล็ก) ลงบนตัวเร่งปฏิกิริยา ด้วยวิธีการเคลือบฝังแบบแห้งภายใต้สภาวะที่มีไอน้ำนั้น ความว่องไวของตัวเร่งปฏิกิริยา V_2O_5-WO_3/TiO_2 ลดลง เนื่องจากไอน้ำและแอมโมเนียเข้าดูดซับกับตำแหน่งของการเกิดปฏิกิริยาบนตัวเร่งปฏิกิริยาแบบแข่งขัน อย่างไรก็ตาม ตัวเร่งปฏิกิริยา V_2O_5-WO_3/TiO_2 ที่ปรับปรุงด้วยโลหะแมงกานีสและซีเรียมหรือ โลหะแมงกานีส และเหล็กยังคงความว่องไวไว้ได้เท่าเดิม ในสภาวะที่มีไอน้ำ

ภาควิชา วิศวกรรมเคมี ลายมือชื่อนิสิต .....

สาขาวิชา วิศวกรรมเคมี ลายมือชื่ออ.ที่ปรึกษาวิทยานิพนธ์หลัก .....

ปีการศึกษา 2551

5070524421 : MAJOR CHEMICAL ENGINEERING
KEYWORDS : SELECTIVE CATALYTIC REDUCTION (SCR)/ VANADIUM OXIDE / TUNGSTEN OXIDE /TITANIUM (IV) OXIDE /AMMONIA

IZKUN ARUNYAKASEMSUK: SELECTIVE CATALYTIC REDUCTION OF NO BY NH_3 OVER V_2O_5-WO_3/TiO_2 CATALYST PROMOTED BY Mn AND ANOTHER METAL (Ce, Cu OR Fe). ADVISOR: AKAWAT SIRISUK., 89 pp.

In this work selective catalytic reduction (SCR) of nitrogen oxide by ammonia over V_2O_5-WO_3/TiO_2 catalysts and V_2O_5-WO_3/TiO_2 catalysts that were promoted with manganese and another metal (cerium, copper, and iron) was investigated. Titanium dioxide was prepared by a sol-gel method and vanadium and tungsten were added to TiO_2 by wet impregnation method. Various techniques including nitrogen adsorption, XRD, NH_3-TPD, XPS, and ICP-OES were employed to characterize the catalysts. V_2O_5-WO_3/TiO_2 catalysts ware then used in the SCR of NO by NH_3 at a temperature ranging from 100-450°C. Almost complete conversion of NO was achieved by most catalysts 250-350°C. Among the nine catalysts the V_2O_5-WO_3/TiO_2 catalyst containing 3 wt.% vanadium and 12 wt.% tungsten (3V12W) was the best one, which maintained high activity in the widest temperature range.

In order to improve the activity of the V_2O_5-WO_3/TiO_2 catalyst under wet condition, manganese and another metal (cerium, copper, and iron) were deposited on the catalyst by an incipient wetness impregnation method. When water vapor was present in the feed stream, the activity of the catalyst became lower because water vapor competed with ammonia for reaction site on the catalyst. However, when the V_2O_5-WO_3/TiO_2 catalysts promoted with manganese and cerium or manganese and iron were employed, the catalysts maintained their activities even when water vapor was present in the feed stream.

Department : Chemical Engineering Student's Signature .....
Field of Study : Chemical Engineering Advisor's Signature .....
Academic Year : 2008

ACKNOWLEDGEMENTS

The author would like to express his greatest gratitude to his advisor, Dr. Akawat Sirisuk, and Professor Piyasan Praserthdam for his invaluable guidance throughout this study. Moreover, I would also grateful to thank Associate professor Paisan Kittisupakorn, as the chairman, Assistant Professor Joongjai Panpranot and Dr. Kriangsak Kraiwattanawong, members of the thesis committee for their kind cooperation.

Many thanks for kind suggestions and useful help from many best friends in Chemical Engineering Department who have provided the encouragement and co-operation throughout this study.

Finally, he also would like to dedicate this thesis to his parents who have always been the source of his support and encouragement.

The financial support from the PTT Public Company Limited is gratefully acknowledged.

CONTENTS

Page

LIST OF TABLES

LIST OF FIGURES

Figure **Page**

Figure **Page**

Figure **Page**

CHAPTER I

INTRODUCTION

Nitrogen oxides (NO_X) are emitted from automobiles and stationary sources such as oil and coal-fired power plants, waste incinerators, industrial ovens, and chemical processes. Nearly all NO_X (95%) derives from transportation (49%) and power plants (46%). NO_X contributes to photochemical smog, acid rain, ozone depletion and green-house effects. The direct health hazards related to NO_X are bronchitis, pneumonia, viral infections, and hay fever [Phil et al. (2007)].

Reduction of NO_X produced by combustion of fossil fuels can be accomplished by adapting various combustion techniques (e.g. low NO_X burner, air staging in the furnace, re-burning, or flue gas recirculation) or by flue gas treatment. For stationary sources, the most important solution is selective catalytic reduction (SCR) of NO_X to N_2 using ammonia as a reductant, which is now considered to be the most effective and common technique to remove the NO_X in the exhaust gas from stationary sources.

The SCR process is based on the reduction of NO_X with NH_3 into water and nitrogen according to the reactions.

$$4NO + 4NH_3 + O_2 \rightarrow 4N_2 + 6H_2O \qquad (1.1)$$

$$2NO_2 + 4NH_3 + O_2 \rightarrow 3N_2 + 6H_2O \qquad (1.2)$$

$$NO + NO_2 + 2NH_3 \rightarrow 2N_2 + 3H_2O \qquad (1.3)$$

If SO_2 is present in the combustion gases, it can be oxidized to SO_3 over the catalyst.

$$SO_2 + \frac{1}{2}O_2 \rightarrow SO_3 \qquad (1.4)$$

Even a very small SO_2 conversion to SO_3 is highly undesirable because of the deposition and the accumulation of ammonium bisulfate salts onto the catalyst (if the temperature of the catalyst is not high enough) and onto the air-preheater downstream from the catalytic reactor.

The majority of commercial SCR installations uses the V_2O_5/TiO_2 composite either as extruded monoliths or deposited on a plate structure. Nevertheless, there are a number of installations that use zeolite technology. The level of V_2O_5 is important and must be controlled to minimize the SO_3 formation. Additionally, modifiers such as molybdenum and tungsten are added to minimize SO_3 formation. Most manufacturers even claim that adding tungsten can improve long term activity.

The well-known industrial catalyst for the SCR process is based on V_2O_5/TiO_2 (anatase phase), promoted with WO_3. The operating temperature for the catalyst is typically 300–400 °C, making it necessary to locate the SCR unit upstream of the desulfurizer and/or particulate control device to avoid reheating the flue gas. Deactivation occurs with a low-resistance catalyst because of high concentrations of SO_2 and ash in the flue gas. Locating the SCR unit at the end of the flue gas pollution abatement units, at which the flue gas is relatively cleaning as it passes through the scrubber and the electrostatic precipitator or bag-house, can prevent deactivation. Since flue gas temperature is low, it is necessary to develop a catalyst that shows high activity at low temperature.

A low temperature SCR process is believed to have low energy consumption and to be economical for retrofitting into the existing units for flue gas cleaning. The key to development of the low temperature SCR process is that catalysts with high resistance to SO_2 poisoning that prevent formation of the ammonium bisulfate salts on the catalyst surface at low temperatures [Phil et al. (2007)].

A number of factors have been claimed to affect the low temperature selective reduction of NO with ammonia over manganese oxide catalysts. To increase the catalytic activity of manganese oxides, various transition metal oxides were

incorporated as a promoter. Fe–Mn based catalyst prepared by a co-precipitation method and found a high catalytic activity at 100–180°C. MnO_X–CeO_2 catalyst was also reported to be active for low-temperature SCR of NO with NH_3. Mixed oxides containing Cu and Mn as main metal element have been reported to be very active for complete oxidation reaction at low temperatures. This can help the facile formation of NO_2 and promote the NO reduction with ammonia at low temperatures [Kang et al. (2006)].

The objective of this research is to investigate selective catalytic reduction of nitrogen oxide by ammonia using V_2O_5-WO_3/TiO_2 catalysts and promoted catalysts were investigated. This thesis is divided into two main parts. The first part discusses characterizations and activity of V_2O_5-WO_3/TiO_2 catalysts in three different conditions. The second part discusses characterization and activities of promoted catalysts under dry and wet conditions. The activity of catalysts for selective catalytic reduction was studied as a function of reaction temperature.

This thesis is arranged as follows:

Chapter II presents principles of SCR of NO by NH_3 using V_2O_5-WO_3/TiO_2 and another metal

Chapter III describes synthesis of titanium dioxide, preparing V_2O_5-WO_3/TiO_2 catalysts, V_2O_5-WO_3/TiO_2 that are promoted with manganese and another metal, and experimental apparatus and setting.

Chapter IV presents experimental results and discussion.

Chapter V presents overall conclusions of this research and recommendations for further research.

CHAPTER II

BACKGROUND INFORMATION

The selective catalytic reduction (SCR) of NO_X with ammonia by V_2O_5/TiO_2 catalyst has been useful employed in industrial process to control the pollution caused by nitrogen oxides emitted from stationary source. In this chapter, we describe the SCR of NO_X by NH_3 and the side-reaction, adsorption and de-sorption studies on V_2O_5 - based catalyst, and proposed intermediate species, reaction schemes and reaction mechanism for the SCR of NO_X by NH_3, and literature review about SCR of NO_X with ammonia.

2.1 Selective catalytic reduction of NO_X by NH_3 and the side-reaction (Kanongchaiyot, 1999)

The acid rains and town smog, which are produced mainly by atmospheric pollutants like SO_X, NO_X, and volatile organic compounds, are among the most serious world ecological problems. In the case of nitrogen oxide emissions, most of NO_X are produced during the combustion process (thermal NO_X) by the oxidation of the atmospheric nitrogen at very high temperatures. NO_X typically consists of a mixture of 95% NO and 5% NO_2. Other NO_X are formed by oxidation of organic nitrogen present in the fuel (fuel NO_X) and HCN formed from fuel nitrogen (prompt NO_X).

$$N_2 + O_2 \rightarrow 2NO \qquad (2.1)$$

$$NO + \tfrac{1}{2}O_2 \rightarrow NO_2 \qquad (2.2)$$

SCR of NO_X using NH_3 was first discovered in 1975. It is discovered that NH_3 can react selectively with NO_X to produce elemental N_2. The major desirable reactions are as followed.

$$4NH_3 + 4NO + O_2 \rightarrow 4N_2 + 6H_2O \qquad (2.3)$$

$$4NH_3 + 2NO_2 + O_2 \rightarrow 2N_2 + 6H_2O \qquad (2.4)$$

The reaction between NO and NH_3 can also proceed in a different way, given rise to the undesired product N_2O.

$$4NH_3 + 4NO + 3O_2 \rightarrow 4N_2O + 6H_2O \quad (2.5)$$

Under typical SCR conditions (a molar ratio of NH_3/NO near 1, few percent oxygen, and T < 400°C), Equation (2.3) accounts for the overall stoichiometry on the best catalyst. Accordingly, the SCR process occurs when N_2 is produced with the selectivity close to 100% and the ratio of converted moles of NO and NH_3 is 1. Unselective behavior occurs when products other than N_2 (namely N_2O) are formed (e.g. via Equation (2.5)) and/or when the ratio of converted NO and NH_3 moles is lower than 1. This implies that ammonia is converted by ways other than Equation (2.3), i.e. partially oxidized by oxygen, instead of NO, through one of the following ways:

$$2NH_3 + 2O_2 \rightarrow N_2O + 3H_2O \quad (2.6)$$

$$4NH_3 + 3O_2 \rightarrow 2N_2O + 6H_2O \quad (2.7)$$

$$4NH_3 + 5O_2 \rightarrow 4NO + 6H_2O \quad (2.8)$$

Equations (2.6) to (2.8) are the so-called selective catalytic oxidation (SCO) of ammonia. Several active SCR catalysts are also active in SCO although at slightly higher temperature. At a temperature below about 100-200°C, the ammonia can also react with the NO_X present in the process gas producing explosive NH_4NO_3:

$$2NH_3 + 2NO_2 + H_2O \rightarrow NH_4NO_2 + NH_4NO_3 \quad (2.9)$$

When sulfur is present in the flue gas, such as in coal-fired boilers or power plants and in petroleum-derived liquid fuels such as distillate or diesel, the oxidation of SO_2 to SO_3 (equations (2.10) and (2.11)) gives rise to formation of H_2SO_4 upon reaction with H_2O, resulting in condensation downstream and excessive corrosion of process equipment.

$$2SO_2 + O_2 \rightarrow 2SO_3 \quad (2.10)$$

$$SO_3 + H_2O \rightarrow H_2SO_4 \quad (2.11)$$

The reaction of NH_3 with SO_3 also results in the formation of NH_4HSO_4 and/or $(NH_4)_2SO_4$ (Equations (2.12) and (2.13)), which deposits on downstream process equipment such as heat exchanger and causes a loss in thermal efficiencies.

$$NH_3 + SO_3 + H_2O \rightarrow NH_4HSO_4 \quad (2.12)$$

$$2NH_3 + SO_3 + H_2O \rightarrow (NH_4)_2SO_4 \quad (2.13)$$

2.2 Metal oxide catalysts for the SCR process (Busca et al., 1998)

The industrial catalysts for the SCR process are based on TiO_2-supported V_2O_5-WO_3 and/or V_2O_5-MoO_3. However, a number of other formulations have been reported to be active and selective for this reaction. Among metal oxides, pure vanadia and vanadia supported on oxides carriers such as alumina, silica, zirconia and titania (which is the support of choice nowadays) have been widely investigated.

Additionally, catalysts based on pure, supported and mixed iron, copper, chromium and manganese oxides also enjoy wide applications and testing in the scientific literature. The same transition metals also have been introduced into zeolitic cavities, such as X, Y, and ZSM5 zeolites, and have been added to TiO_2-pillared clays.

Catalyst components that give rise to high selectivity in partial oxidation (V_2O_5, WO_3, and MoO_3) when supported on TiO_2 also exhibit high selectivity in the SCR reaction. Transition metal oxides that are poorly active in oxidation catalysis (such as TiO_2 and ZrO_2) also exhibit poor activity in SCR catalysis. This is in line with the evidences showing that the SCR reaction is a redox process.

2.3 The active phases and the roles of the support and promoters in the commercial catalysts (Busca et al., 1998)

Several studies have been published concerning the characterization of V_2O_5-WO_3/TiO_2 model and industrial SCR catalysts. On the other hand, fewer data are known on V_2O_5-MoO_3/TiO_2 catalysts. In all cases the best catalysts contain just a few less than a full monolayer of vanadium plus tungsten (or molybdenum) oxides over the anatase TiO_2 support. The amount of vanadium oxide is variable but generally very small (<1% (w/w)), at least in the most recent catalyst formulations.

Indeed, vanadia is responsible for the activity of the catalyst in the NO_X reduction but also for the undesired oxidation of SO_2 to SO_3 in the case of sulfur bearing fuels. WO_3 is employed in a larger amount (about 10% (w/w)) to increase the catalyst activity and thermal stability.

The choice of anatase TiO_2 as the best support for SCR catalysts relies on two main reasons:

1. SO_2 is usually present in the waste gases of power plants. In the presence of oxygen it can be oxidized to SO_3, thus forming metal sulfate by reacting with the oxide catalyst support. TiO_2 is only weakly and reversibly sulfated in the conditions approaching those of the SCR reaction and the stability of sulfates on the TiO_2 surface is weaker than on other oxides such as Al_2O_3 and ZrO_2. Consequently, TiO_2-based industrial catalysts are only partially and reversibly sulfated at their surfaces upon SCR reaction in the presence of SO_2, and this sulfation even enhances the SCR catalytic activity.

2. Supporting vanadium oxides on anatase TiO_2 leads to very active oxidation catalysts, more active than those obtained with other supports. The reason for this activity enhancement is a result of the good dispersion of vanadium oxide on TiO_2 giving rise to isolated vanadyl centers and polymeric polyvanadate species, possibly of the metavanadate-type (Figure 2.1), and also the semiconductor nature of TiO_2, whose conduction band is not very far from the d-orbital levels of vanadyl centers, located in the energy gap.

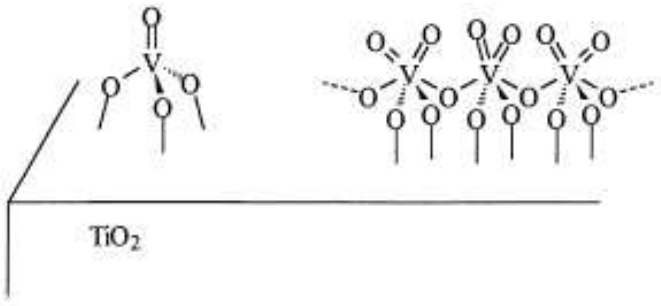

Figure 2.1 Proposed structures for monomeric vanadyl species and polymeric metavanadate species in their dehydrated forms on the surface of V_2O_5/TiO_2 catalysts. (Busca et al., 1998)

Accordingly, anatase TiO_2 is an activating support, giving rise to catalysts that are stable against sulfation or even improved upon sulfation.

In fact, anatase TiO_2 is a metastable titanium dioxide polymorph and tends to convert into the thermodynamically stable form, rutile, at any temperature and pressure. The anatase-to-rutile phase transformation is favored by addition of V_2O_5, which also favors the anatase sintering and loss of surface area. On the contrary, WO_3 and MoO_3 hinder both surface area loss of anatase and its transformation to rutile. This can be another reason for their addition to vanadia-titania, in addition to the effect of such components in the undesired SO_2 oxidation. In fact, WO_3 and MoO_3 compete with and displace SO_3 on the basic sites of the TiO_2 surface and tend to cover it, thus limiting its sulfation. Accordingly, the oxides also reduce the catalytic activity of the SCR catalysts for the SO_2 to SO_3 oxidation. Furthermore, MoO_3 addition has a specific role in the presence of As compounds in the gas, even if the mechanism of this prevention is still largely unclear. In conclusion, MoO_3 and WO_3 act both as stabilizers and as promoters of the SCR catalysts and possibly as inhibitors of the SO_2 oxidation. The mechanism with which tungsten oxide can activate the vanadium oxy-centers for the SCR is still matter of debate. Some authors pointed out that tungsten oxide gives rise to stronger Brønsted acid sites, whose presence favors the reaction. Other authors proposed that the SCR reaction needs two sites, and WO_3 can offer the presence of a second site.

Alternatively, the V_2O_5-WO_3/TiO_2 solid presents quite peculiar electronic features, involving the semiconducting nature of titania and the similarity of the d-levels of tungsten, vanadium, and titanium. In other words, W and V oxide centers, although vibrationally and chemically isolated, interact electronically through the TiO_2 conduction band. This would lead to a further enhancement of the activity and selectivity of the reaction sites, which are vanadyl centers.

In industrial catalysts belonging to the V_2O_5-WO_3/TiO_2 system, with less than 1% of V_2O_5 (w/w), vanadium oxide species are nearly isolated and lie between tungsten oxide species, that are apparently either isolated or more or less polymerized.

2.4 NH_3 adsorption and desorption (Busca et al., 1998)

The nature of the Brønsted acid sites was (Yang et al.,1995) responsible for ammonia adsorption as NH_4 species. Ammonia adsorbs as species on Lewis acid sites of titanium oxide and as NH_4 species on Brønsted acid sites associated with vanadium oxide moieties. In contrast, the interaction of NO with the surface of vanadium oxide is believed to be quite weak. The reaction is initiated by adsorption of ammonia on Brønsted acid sites (V–OH), followed by activation of ammonia via reaction with redox sites (V=O) [Anstrom et al., 2003]. This activated form of ammonia then reacts with weakly adsorbed NO, producing N_2 and H_2O and leading to partial reduction of the catalyst, which is then oxidized by O_2. However, the detailed nature of the steps involved in the reaction of NO with adsorbed NH_4 species is still unclear. In a theoretical study that adsorbed NH_4 species react with NO on the surface of vanadium oxide to give a NH_2NO species, which may then isomerize in the gas phase to give N_2 and H_2O. Several species derived from NH_2NO as reaction intermediates in a theoretical study of the gas-phase reaction of NH_3 and NH_4 species with NO.

2.4.1 V_2O_5-based catalysts

The adsorption-desorption characteristics of ammonia on V_2O_5-based catalysts have been extensively investigated by means of TPD, FTIR and combined TPD-FTIR techniques. The transient response method has also been applied. Ammonia adsorbs on pure V_2O_5, on V_2O_5-TiO_2, on V_2O_5/SiO_2-TiO_2, on V_2O_5-WO_3/TiO_2 and on V_2O_5-MoO_3/TiO_2 in two different strongly held species.

The first, molecularly adsorbed ammonia, through a Lewis-type interaction on co-ordinatively unsaturated cations; and the other one, ammonia adsorbed as ammonium ions, over Brønsted acidic –OH surface hydroxyl groups. Other species, like H-bonded NH_3 on oxide sites through one of its own hydrogen atoms [Lietti et al. (1996)] have also been reported to exist. However, this last species is certainly weakly held, so that it is not supposed to be active in the SCR process. Molecular adsorbed NH_3 species are produced on Ti^{4+}, vanadyl and wolframyl cations and cannot be distinguished spectroscopically. NMR experiments allow to conclude that adsorption on Lewis sites is predominant in V_2O_5-TiO_2. If TiO_2, pure anatase phase supports, only shows Lewis acidity, whereas ammonium ions are formed on V-OH sites. These

suggest that vanadyl sites are Lewis acidic and can convert into Brønsted sites by water adsorption (Figure 2.2). The surface species arising from ammonia adsorption can be depicted as follows, supposing that polymeric vanadates, coordinatively saturated, do not adsorb ammonia (Figure 2.3). In the case of V_2O_5-WO_3/TiO_2 and on V_2O_5-MoO_3/TiO_2, like on WO_3-TiO_2 and on MoO_3-TiO_2 catalysts, Lewis bonded species on wolframyl or molybdenyl species and Brønsted-bonded NH^{4+} species at W-OH sites and Mo-OH are also formed. The thermal stability of NH_3 adsorbed species has also been investigated by FTIR, it has been found that Lewis bonded molecular species are thermally more stable than ammonium ions. It has also been reported that water competes with ammonia on Lewis acid sites, whereas it causes an enhancement of the amount of Brønsted acid sites, as deduced from the increased amount of protonated ammonia species. However ammonia displaces water from Lewis acid sites, due to its greater basicity. As it will be discussed later, authors debate on if protonated or coordinated ammonia species are those active in the SCR process on vanadia/titania based catalysts. Interestingly, no supports from spectroscopic measurements have been derived to the presence of other NH_3-derived species like NH_2O-V (formally, a dissociated form of hydroxylamine, NH_2OH) and V-O-NH-NH-O-V, that have been suggested by some authors to act as intermediate in the SCR reaction and in the SCO reactions.

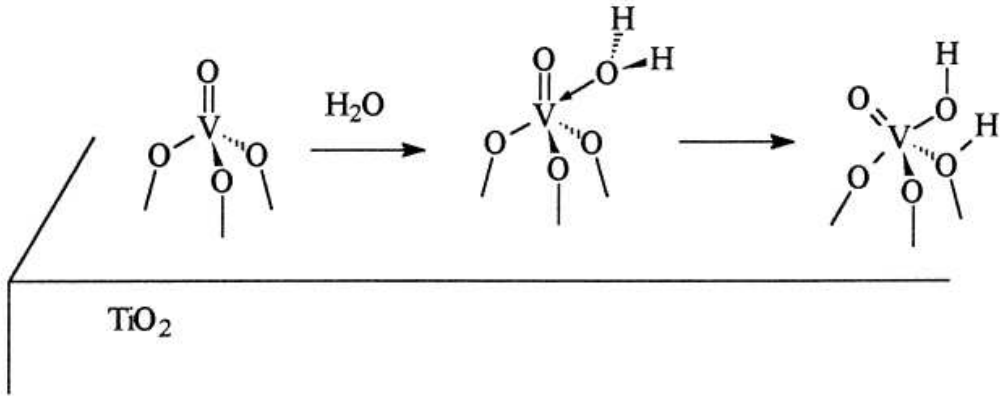

Figure 2.2 The generation of the Brønsted acid sites from surface vanadyl centers.

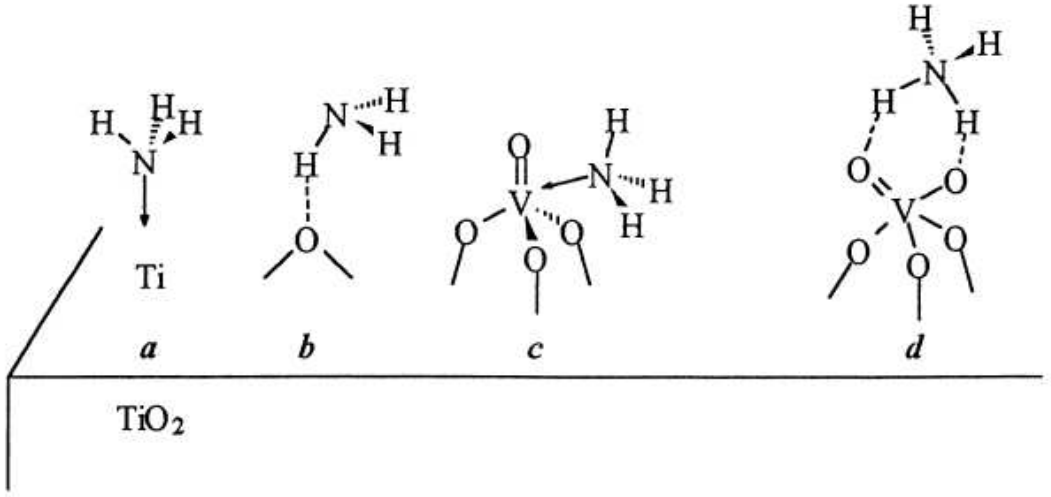

Figure 2.3 Proposed structures for ammonia adsorbed on V_2O_5/TiO_2: (a) Lewis-bonded NH_3 at Ti sites; (b) H-bonded NH_3 on oxide sites; (c) Lewis-bonded NH_3 at vanadyl sites; (d) ammonium ions bonded at V Brønsted acid sites.

The adsorption and desorption of ammonia over V_2O_5/TiO_2 catalysts has also been investigated by TPD. NH_3 strongly adsorbs on pure TiO_2 and vanadia/titania catalysts, and ammonia surface species having different thermal stability exist on the catalyst surface. NH_3 adsorption energies in the range 18-26 kcal/mol have been estimated analysis of the TPD spectra. The data indicate that at the temperatures typical of the SCR process a significant part of ammonia is adsorbed on the catalyst surface. Similar results have been obtained over V_2O_5-WO_3/TiO_2 model catalysts. Both the amounts and the strength of adsorption decreases upon addition of V_2O_5, thus indicating that the V component decreases the catalyst surface acidity. The oxidation of a small fraction of adsorbed ammonia to N_2, N_2O and NO has also been reported to occur at high temperatures during TPD experiments over vanadia/titania catalysts.

This oxidation process may involve either lattice oxygen atoms or traces of gaseous oxygen present in the carrier gas stream, and has been related to the presence of the V components. ESR and XPS data also showed that NH_3 can reduce the vanadia sites over V_2O_5/TiO_2 while conductance measurements showed that ammonia adsorption caused a significant increase in the conductance of V_2O_5/SiO_2-TiO_2

catalysts, so confirming a catalyst reduction by ammonia, in agreement with TPR data.

Although ammonia oxidation by the oxidized vanadia-based surfaces certainly can occur, the identification of the surface species produced by ammonia oxidation is still incomplete and partly tentative. On pure vanadia and on vanadia/titania samples, spectroscopic features that can be assigned to an amide species, $-NH_2$, are observed. Similar species can be observed on several other active SCR catalysts. These species may act as precursors in the NH_3 oxidation to N_2 via their dimeric form, hydrazine N_2H_4, as observed on Cu-based catalysts. The characteristics of NH_3 adsorption-desorption on model V_2O_5/TiO_2 and V_2O_5-WO_3/TiO_2 SCR catalysts have been investigated by the transient response methods [Tronconi et al., 1996]. In line with the existence of several NH_3 adsorption states, it has been found that a simple Langmuir approach could not represent the NH_3 adsorption-desorption data accurately. A nice fit of the data could be obtained by assuming a non-activated NH_3 adsorption and a Temkin-type desorption kinetics. Values of the activation energy for desorption in the range 18-26 kcal/mol have been estimated for the V_2O_5/TiO_2.

2.4.2 Other oxide catalysts

The NH_3 adsorption has been investigated also over other active SCR catalysts, like CuO/TiO_2, CuO-MgO/Al_2O_3, Fe_2O_3, Fe_2O_3/TiO_2, $MnOx/TiO_2$, MgO-Fe_2O_3. Over these catalysts ammonia adsorbs only in a coordinative way at room or lower temperatures. Brønsted acidity cannot be found over these surfaces, some of which display a relevant basic character. Also, manganese sites on $MnOx/Al_2O_3$ do not seem to be associated to Brønsted acidity. Cr_2O_3-based catalysts and $MnOx/TiO_2$ catalysts, also active in the SCR reaction, show weak Brønsted acidity. It is observed that both classes of catalysts are activated in the reduction of NO by NH_3. From these data it has been concluded that the existence of Brønsted acidity is not a requisite for the SCR activity at low temperatures. Lewis bonded and Brønsted bonded ammonia species have also been found on Cu-ZSM5, even if over exchanged, as well as on other Cu-zeolite systems and on Fe-Y and Fe-ZSM5 zeolites. In these cases it has been supposed that the Brønsted acid sites are residual on exchanged OHs of the zeolite, there are retained in spite of the cation over-exchange.

An interesting case is that of TiO_2, that, if pure, only shows Lewis acidity and poor catalytic activity for SCR. However, when sulfated, strong Brønsted acidity is formed and SCR activity is strongly enhanced, although only at very high temperature. From this and other data it has been proposed that Brønsted acidity plays an important role in the SCR reaction. However, it should be noted that sulfation also increases the acid strength of the Lewis sites of titania.

2.5 NO adsorption and desorption (Busca et al., 1998)

2.5.1 V_2O_5-based catalysts

The adsorption of the other SCR reactant, i.e. NO, has also been extensively investigated in the literature over V_2O_5-based catalysts and over other catalytic systems active in the SCR reaction. The data in this case are however not as clear as in the case of ammonia, since the chemistry of nitrogen oxide at the interface of oxide materials is very complex. In principle, NO can adsorb in a molecular forming, giving rise to surface nitrosyls where it interacts with a lone pair of the N atom to the surface metal cationic centers, and can be oxidized by oxide surfaces, giving rise to species like nitrosonium ion (NO^+), nitrite ions (NO^{2-}), adsorbed nitrogen dioxide (NO_2), nitronium ion, (NO^{2+}), and nitrate ions (NO^{3-}). However, it can also act as an oxidizing agent, reducing itself to NO^- and to its dimeric form, the hyponitrite anion, $N_2O_2^{2-}$as well as to N_2O and N_2.

Moreover, it can dimerize to dinitrogen dioxide N_2O_2 (which is possibly an intermediate in its reduction and/or in its oxidation) and to disproportionate giving rise to both reduced and oxidized species. It has been shown that over catalysts like pure V_2O_5, on V_2O_5-TiO_2, V_2O_5-SiO_2, on V_2O_5-Al_2O_3, on V_2O_5-TiO_2-SiO_2, on V_2O_5 -WO_3-TiO_2 and on V_2O_5 -MoO_3-TiO_2, the interaction of NO is very weak. Upon contacting a V_2O_5-TiO_2 sample with NO, observed the formation of a surface nitrosyl species, coordinated to Ti^{4+} sites. On the other hand, NO does not adsorb on an ammonia covered surface since NH_3 blocks the Ti^{4+} adsorption sites due to its greater basicity, and only a minor formation of nitrate species has been observed by nitric oxide oxidation on vanadyl sites. Nitrate and/or nitrite species are observed to form slowly at room temperature and to desorb or decompose easily.

A similar behavior has been found on V_2O_5-ZrO_2, where these species have been supposed to take an important role in the SCR reaction. NO_2 gives more evident adsorbed species on V_2O_5-TiO_2. Conductance measurements showed that NO adsorption causes a slight increase of the conductance of V_2O_5/SiO_2-TiO_2 catalysts only at high vanadia contents and this has been interpreted as due to a slight catalyst reduction with the production of more oxidized nitrogen oxide species like NO^+ or NO_2. On the other hand, NO is able to reoxidize the centers of reduced V_2O_5 and V_2O_5/TiO_2 catalysts and can also adsorb on the TiO_2 support.

In general, NO adsorbs as nitrosyl and dinitrosyl surface species on reduced vanadia surfaces, whereas it does not adsorb over fully oxidized surfaces, with few exceptions. These data show that oxidized NO adsorbed species can be formed at the catalyst surface, although according to many authors NO can also be reduced by reduced catalyst centers. In any case, adsorption is usually negligible at the reaction temperature, particularly in the presence of ammonia. These data allowed to interpret the kinetic data on vanadia-based catalysts (and in particular the apparent zero and first order kinetics with respect to NH_3 and NO, respectively) as due to slow step involving the reaction of gas-phase NO with adsorbed NH_3. Similarly, weak or no adsorption has been found on oxidized supported MoO_3 and WO_3, while quite strong adsorption can occur over these materials after prereduction.

2.5.2. Other oxide catalysts

More extensive and stronger adsorption of NO has been found on other active SCR catalysts, like Fe_2O_3, Fe_2O_3-Cr_2O_3, Cr_2O_3, CuO-TiO_2, CuO/Al_2O_3, MnOx-Al_2O_3 ,and Cr_2O_3/TiO_2 . Adsorbed NO has been identified in various forms in these cases, including nitrosyl, nitrato-, nitrito-, hyponitrito- and other anionic species. These species decompose or desorb at relatively low temperatures (<250°C) and mostly gives back NO. This behavior can differentiate most metal oxide catalysts from Cu-based zeolites where different adsorbed forms of NO in the presence of oxygen give rise to stepwise desorption during TPD experiments. In this case surface spectroscopy pointed out the existence of the formation of quite stable nitrosyl species together with species that apparently contain more oxygen atoms, whose actual nature is not still completely understood, but that are frequently denoted as NO_2 or nitrate-like species. However, also these species decompose giving back mostly NO.

Conductance measurements showed that NO adsorption on Fe_2O_3 gives rise to both reduced and oxidized species. Recently, a study has been published concerning Ce-mordenite catalysts, reported to be active in SCR. Strong NO adsorption has been found by IR.

2.5.2. Adsorption of other related compounds

To better identify potentially involved surface species, or species revealing mechanistic aspects, the dsorption of other N-containing molecules could be investigated too. With this in mind, the interaction of TiO_2, $CuO\text{-}TiO_2$ and $V_2O_5\text{-}TiO_2$ with hydrazine ($NH_2–NH_2$) and hydroxylamine (NH_2OH) vapors has also been investigated by IR spectroscopy. The spectra of the adsorbed species arising from hydrazine and hydroxylamine have also been compared with those arising from ammonia on the same surfaces. In fact, on some surfaces very active in ammonia oxidation, hydrazine ($H_2N–NH_2$) has been identified as an adsorbed species arising from NH_3 with a quite good degree of certainty, by comparison with the spectrum of hydrazine adsorbed directly from the gas-phase. The catalysts where these species have been observed are $CuO\text{-}TiO_2$, $Fe_2O_3\text{-}TiO_2$, $CrOx\text{-}TiO_2$, and also over-exchanged Cu-ZSM5. Species supposed to be an amide species $-NH_2$ was detected on vanadia-titania. Similar species can be observed on several other catalysts active in both SCR and ammonia oxidation, such as Fe_2O_3 and $MgO\text{-}Fe_2O_3$ catalysts. These data, coupled with the known very easy oxy-dehydrogenation of hydrazine in contact with transition metal cations in a high oxidation state, proposed a mechanism for the surface oxidation of ammonia to nitrogen:

$$NH_3 + M^{n+} + O^{2-} \rightarrow M^{(n-1)+}–NH_2 + {}^{-}OH \qquad (2.14)$$

$$2–NH_2 \rightarrow N_2H_4 \rightarrow N_2 + 4H^{+} + 4e^{-} \qquad (2.15)$$

The first step involves the activation of ammonia, possibly via the amide species, followed by a coupling reaction that gives rise to nitrogen. IR studies of the adsorption of hydroxylamine did not confirm the formation of species like $NH_2O\text{-}V$ species (formally a dissociated form of hydroxylamine, NH_2OH) and V–O–NH–NH–O–V, which have been supposed to act as intermediates in the SCR reaction and in the SCO reaction. However such studies supported the identification

of a species, detected by oxidation of both ammonia and hydrazine and hydroxylamine, as a nitroxyl species (HNO).

According to the known chemistry of inorganic nitrogen compounds and to some spectroscopic evidences, it can be supposed that the nitroxyl species is the intermediate in the oxidation of ammonia to both NO and N_2O. Another species detectable by IR from ammonia and hydrazine but not from hydroxylamine has been tentatively identified as an imido species (NH). This species could be intermediate in the oxidation of amide to nitroxyl. However, from its behavior it looks quite inactive.

2.6 The proposed mechanism of selective catalytic reduction for V_2O_5-based catalysts (Busca et al., 1998)

The very popular reaction scheme of Inomata et al. is reproduced. It consists in the reaction of ammonium ion species with gaseous NO, throughout an ``activated complex". The electronic structure of this intermediate and the interaction occurring have not been specified. Moreover, the movements of electrons upon the reactions have not been hypothesized, and no sufficient chemical details are given.

In Figure 2.5 the adsorption of ammonia over a polyvanadate species O=V–O–V=O leads to the intermediate species $V–ONH_2$ (species D) that is proposed as the key intermediate in the SCR reaction and/or ammonia oxidation on vanadia-based catalysts. This species is formally a dissociated form of hydroxylamine (NH_2OH) which actually is a very weak acid (pK_a 13.7). Metal complexes of hydroxylamine (through a coordination of the N atom lone pair to the metal) are known and can also be formed by hydroxylamine adsorption on metal oxide surfaces.

Transition metal complexes of the NH_2O radical-like species have also been supposed to act as intermediates in hydroxylamine oxidation by such cations. Such an oxidation gives rise generally to N_2O or nitrates, but N_2 can also be obtained, depending on the cation and on its concentration. The reaction of Co-hydroxylamine complexes with nitrous acid has been shown to occur, but the product is N_2O. On the other hand, the formation of hydroxylamine (even in its dissociated form), from ammonia by oxidation with oxygen or transition metal cations, is quite unlikely.

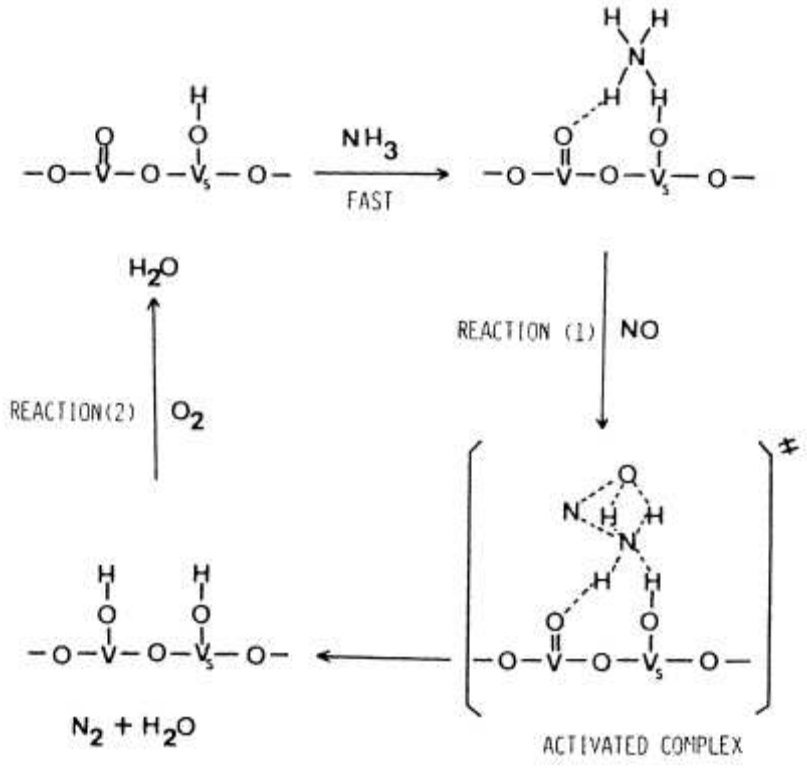

Figure 2.4 Mechanism of the NO–NH_3 reaction on vanadium oxide catalysts.

In fact, hydroxylamine was supposed to be an intermediate in ammonia oxidation to NO on platinum catalysts, but this hypothesis seems to be now ruled out, in particular on transition metal oxides. Hydroxylamine can actually be produced from ammonia by oxidation with hydrogen peroxide over Ti silicalite. In any case, no spectroscopic studies detected hydroxylamine-type species among the ammonia adsorption and oxidation products on any solid surface.

More IR studies of hydroxylamine reaction over SCR catalysts further tend to exclude a role of such species in the reaction. A similar proposed species act as a precursor for NH_3 oxidation to NO (Figure 2.6, steps 1 with 2). Another species to be formed from ammonia on vanadia-based catalysts (depicted as V–ONH_3) and produced by the reaction of V=O+NH_3. This species is supposed to be a precursor for N_2 and N_2O formation from ammonia (steps 3 with 4 and 3 with 5 of Figure 2.6, respectively) or of N_2O from NH_3+NO (steps 3 with 6). The same intermediate is used in the scheme used as a base for their mathematical analysis of transient experiments of ammonia oxidation on V_2O_5-TiO_2.

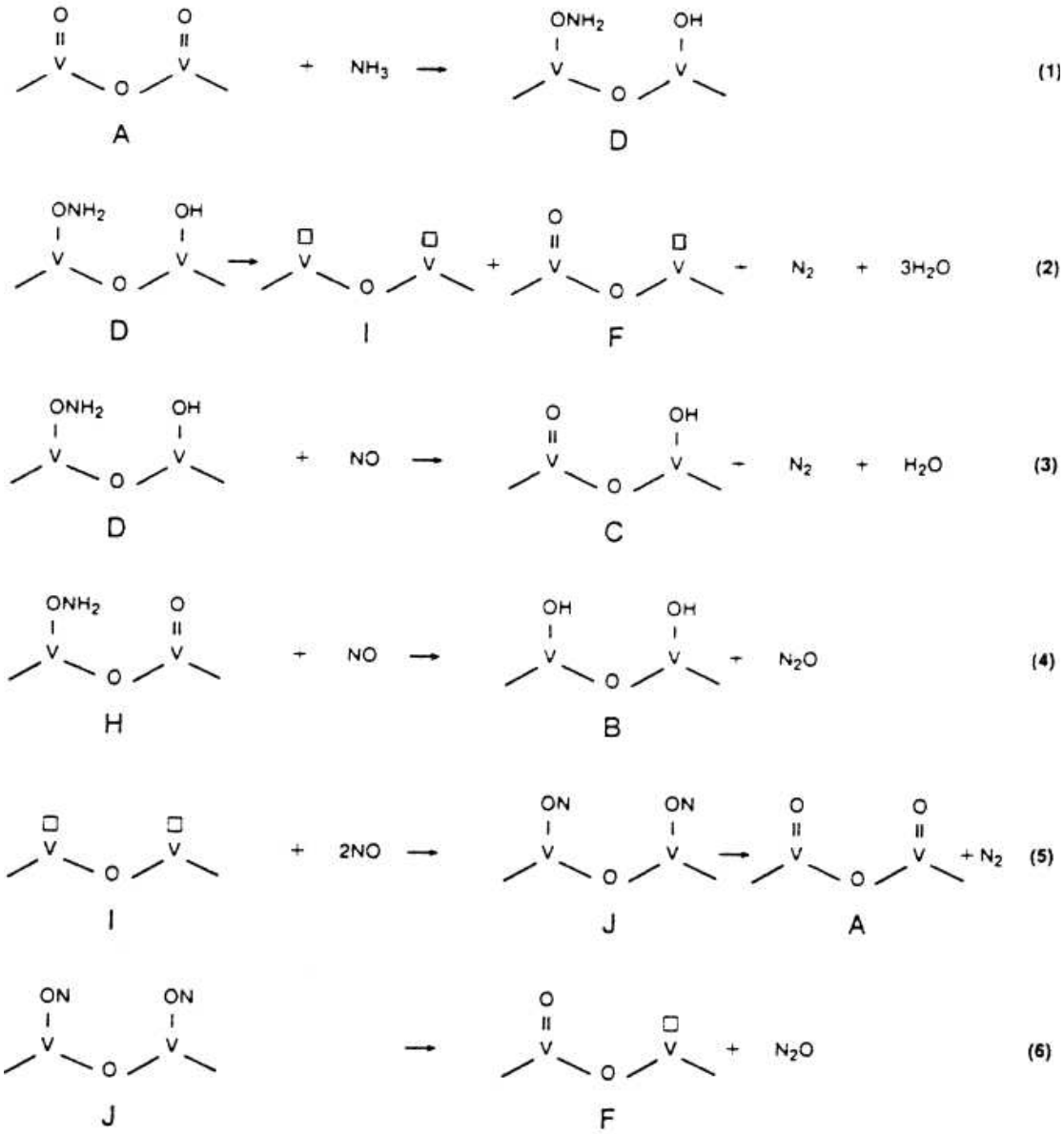

Figure 2.5 Mechanism of the NO–NH_3 reaction on supported vanadium oxide catalysts in the presence of oxygen.

However, the chemical nature of these species is not discussed and is difficult to be interpreted. The reactive NH_3 species involved in the SCR reaction has been depicted as V–ONH_4. This species originates from NH_3+V–OH (step 7 of Figure 2.6) and is thought to be involved in the SCR reaction with gas-phase NO (step 8). It is obvious that the formation of some of the above mentioned species from ammonia

would cause the reduction of the adsorbing vanadium centers, but in this respect, use notations that do not allow to distinguish reduced from oxidized centers; also they do not try to close the catalytic cycles within their reaction schemes.

Catalytic cycle for ammonia oxidation only taking into account the mass or atomic balances, but totally neglecting the electronic and charge balances. Accordingly, the corresponding conclusions are very difficult to be judged on chemical grounds. The other reaction pathway was shown in Figugre 2.7. This mechanism consists of the following steps:

$$NH_3 + M^{n+} + O^{=} \rightarrow M^{(n-1)+}\text{-}NH_2 + {}^{-}OH \quad (2.16)$$

$$M^{(n-1)+}\text{–}NH_2 + NO \rightarrow M^{(n-1)+}\text{–}NH_2 + NO \quad (2.17)$$

$$M^{(n-1)+}\text{–}NH_2NO \rightarrow M^{(n-1)+} + N_2 + H_2O \quad (2.18)$$

$$2M^{(n-1)+} + 1/2O_2 \rightarrow 2M^{n+} + O^{=} \quad (2.19)$$

$$2\,{}^{-}OH \rightarrow H_2O + O^{=} \quad (2.20)$$

Accordingly, ammonia is adsorbed over a Lewis acid site that activates ammonia to an amide NH_2 species (Equation 2.16), resulting in catalyst reduction. This activated ammonia species then react with gas-phase NO giving rise to a nitrosamide intermediate (Equation 2.17) that then decomposes to nitrogen and water (Equation 2.18). The reduced catalyst sites are then regenerated by gas phase oxygen (Equation 2.19). The proper sum of these equations gives the reaction stoichiometry (Equation 2.20).

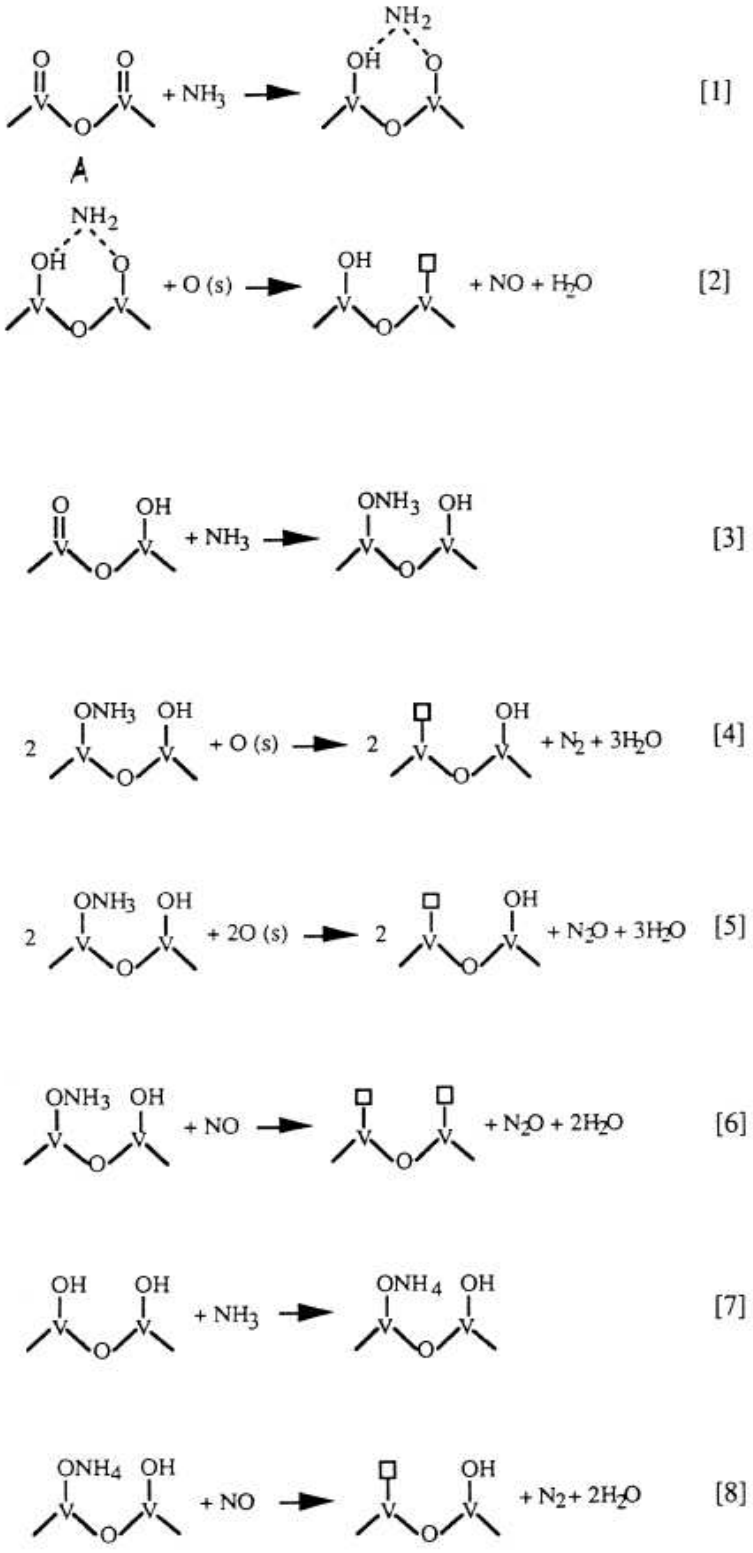

Figure 2.6 Mechanism of the NO–NH_3 reaction on vanadium oxide catalysts in the presence of oxygen.

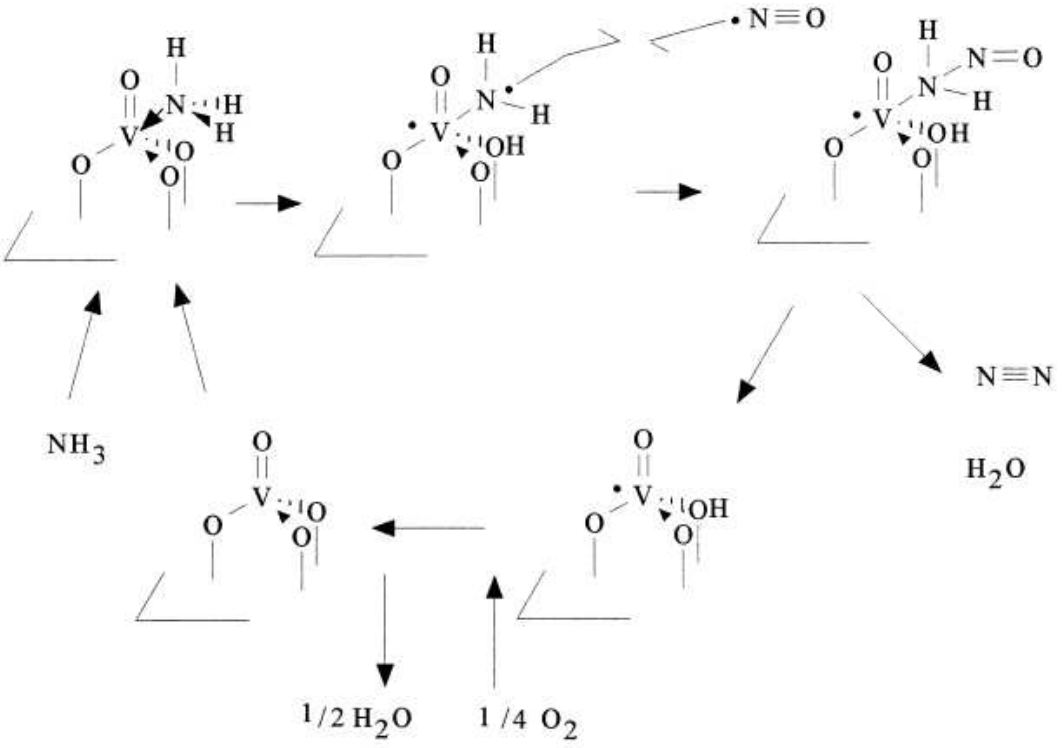

Figure 2.7 Mechanism of the NO–NH_3 reaction on supported vanadium oxide catalysts in the presence of oxygen.

The key reaction step is supposed to involve a radical coupling between the [$M^{(n-1)+}$–NH_2] surface species(whose amide moiety would act as a neutral radical), with the radical molecule NO. This is the first mechanism proposed for vanadia-based catalyst implying an activation of ammonia on Lewis acid sites. However, it is closely related metal and CuOx catalysts and to the detection of nitrosamide as a product of SCR. This mechanism will be referred as the “amide–nitrosamide” mechanism.

The next proposed a mechanism implying the activation of ammonia in the form of an amide species. Although less detail was given on the reaction step, it forecasts also ways for N_2O formation. Kinetic study of the $DeNO_X$-SCR reaction over vanadium oxide catalysts, proposed a reaction mechanism based on the following steps:

$$4NO + 4e^- \rightarrow 2O^{2-} + 2N_2O_{(ads)} \quad (2.21)$$

$$O_2 + 4e^- \rightarrow 2O^{2-} \quad (2.22)$$

$$6V_2O_5 + 2N_2O_{(ads)} + 4NH_{3(ads)} + 4e^- \rightarrow 6V_2O_4 + 4N_2 + 6H_2O + 2O^{2-} \quad (2.23)$$

$$6V_2O_4 + 6O^{2-} \rightarrow 6V_2O_5 + 12e^- \quad (2.24)$$

Steps (equation 2.21) and (equation 2.22) correspond to the chemisorption of NO and O_2, respectively; step (equation 2.23) is the reaction of $N_2O_{(ads)}$ with $NH_{3(ads)}$ whereas step (equation 2.24) is the catalyst reoxidation. This mechanism, however, is not based on experimental evidences, is not consistent with the agreed mechanistic features of the reaction. The basis of in situ on-line FTIR studies under steady-state conditions, Topsøe et al. (1995) proposed the mechanistic scheme shown in Figure 2.8. In this mechanism, the catalytic activity is found to be related to the ammonia adsorbed on the Brønsted acid sites associated with V^{5+}–OH sites. V^{5+}=O groups are also involved in the reaction, and specifically in the activation of adsorbed ammonia. This activation process involves the transfer or partial transfer of a hydrogen from the NH_3 molecule and accordingly reduced V^{4+}–OH sites are produced.

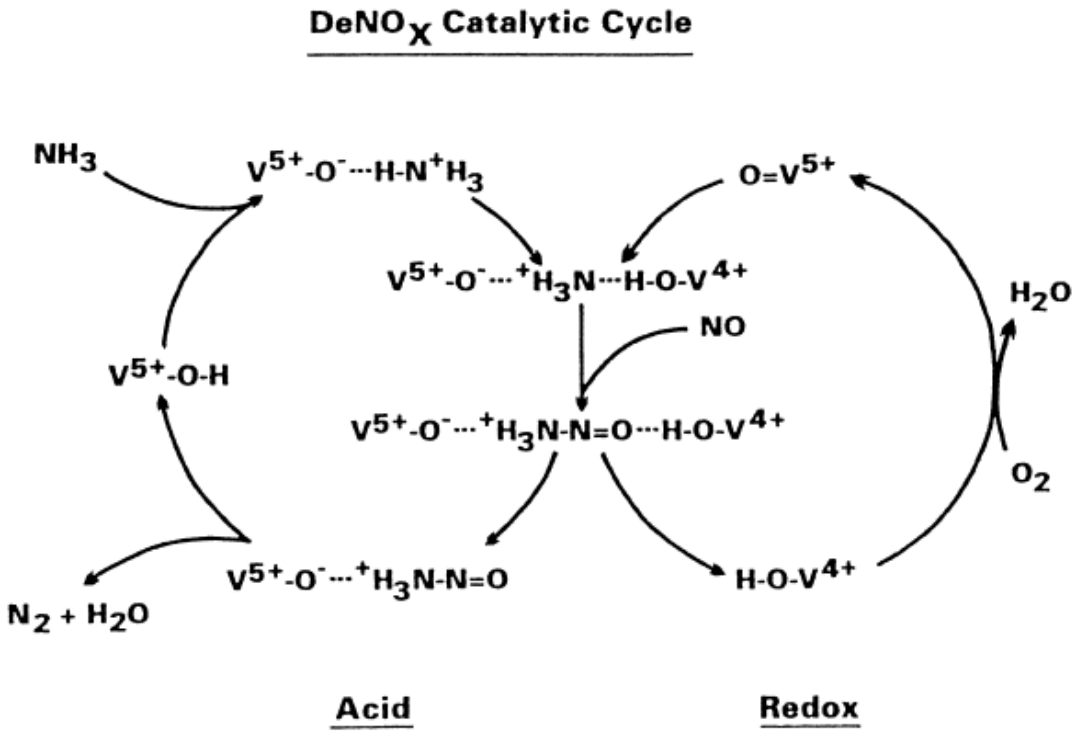

Figure 2.8 Illustrating the catalytic cycle of the SCR reaction over vanadia/titania catalyst in the presence of oxygen proposed by Topsøe et al. (1995).

Once ammonia has been activated, NO from the gas-phase reacts with the activated ammonia complex leading to the formation of an intermediate and then decomposes to nitrogen and water. Regeneration of the active sites (i.e. oxidation of

the reduced V^{4+}–OH sites to V^{5+}=O groups) occurs by gas-phase oxygen. Accordingly, the proposed catalytic cycle consists of both acid-base and redox functions. It is noted that this mechanism can be seen as a modification of the mechanism in Figure 2.7, in which the ammonia adsorption sites are considered to be Brønsted acid sites instead of Lewis acid sites. These authors much emphasized their proposed mechanism that also supposes a kinetic role for a species depicted as NH_3^+, which would be a radical-cation produced by extracting an electron from ammonia.

The possibility of this species to be proposed as an intermediate involved in a slow step (as they in fact suppose) and to react as such with NO is very unlikely on chemical grounds in the opinion of the present authors, and should be supported by more convincing data.

2.7 Effect of vanadia and tungsten loadings of V_2O_5-WO_3/TiO_2 (commercial) catalysts (Djerad et al., 2003)

The state of V_2O_5-WO_3/TiO_2 catalyst is strongly dependent on calcination temperature and V_2O_5 content. High vanadia loading decreases the temperature required for transformation of anatase into rutile. Large amount of tungsten (9% (w/w)) provides thermal stability toWO_3/TiO_2 systems upon addition of vanadia. WO_3 and V_2O_5 crystallites were formed when their concentrations were higher than those corresponding to three monolayers. DTA analyses showed that the presence of V_2O_5 crystallites was not essential for the transformation of anatase into rutile. High reactivity in limited temperature range (225–350°C) had been observed for the catalyst with 8% (w/w) V_2O_5 with large formation of N_2O during the SCR reaction. The catalyst with 3% (w/w) V_2O_5 exhibited a slightly lower reactivity but with a high selectivity to N_2 preserved at all working temperature.

2.8 Effect of sulfation of vanadia–titania (V_2O_5–SO_4^{2-}/TiO_2) binary solid prepared by a sol–gel process (Baraket et al., 2006)

The NO conversion exceeds 99% at high temperature (400–500°C) in presence of vanadia-sulfated-titania catalyst. In fact, sulfate ions affect the properties of oxides in several ways.

Sulfation improves the textural properties. So the sintering is reduced by the presence of sulfates. This explains the stabilization and the increase of the surface of the oxides.

Sulfation generates Lewis and Brønsted acidities at the surface, which are likely govern the SCR reaction at high temperature (350–500°C). Sulfation improves the redox properties of vanadates at the surface. This is due to the existence of strong electronic interaction between vanadia and sulfates. This superficial interaction induces a better reducibility of vanadate at the surface and then a higher reactivity of redox sites.

2.9 Other metal supported on anatase TiO_2

2.9.1 TiO_2-supported MoO_3 (Nova et al., 1998)

A comparison with a WO_3/TiO_2 catalyst having similar molar composition indicates that the WO_3- and MoO_3-containing samples exhibit similar structural and morphological characteristics, but different reactivity. The WO_3/TiO_2 sample is less active but more selective in the SCR reaction than MoO_3/TiO_2 is.

The MoO_3/TiO_2 catalysts are active in the reduction of NO by NH_3. The reactivity of the catalysts increases as the MoO_3 loading increases, whereas the N_2 selectivity decreases due to the formation of undesired N_2O. The formation of N_2O is primarily ascribed to a reaction between NH_3 and NO, and not to the ammonia oxidation reaction.

2.9.2 Ce/TiO_2 catalyst (Xu et al., 2008)

Cerium supported on titanium with different Ce loadings have been prepared by an impregnation method and tested for the selective catalytic reduction of NO by NH_3 in the presence of excess oxygen. The catalysts with 5% Ce and above show high activity in the temperature range 275-400° C at a space velocity of 50,000 h^{-1}. All the catalysts showed an excellent selectivity to N_2 and high tolerance to SO_2 and H_2O under the test conditions.

2.9.3 Addition of transition metals to Mn/TiO_2 (Wu et al., 2007)

Wu and coworkers (2007) investigated the Mn/TiO_2 and the addition of transition metals (including Fe, Cu, Ni and Cr) to the catalyst. Addition of transition

metals led to a significant increase in the activity of the catalysts. And the negative effect of increasing the manganese oxides was weakened when the ratio of Mn/Ti increased from 0.4 to 0.6. Among these transition metals, Fe had the most favorable effect on the catalytic activity.

Manganese oxides were better dispersed in the catalysts with transition metals, and these metals were found to interact with manganese oxides and titania, forming a solid solution. Therefore, the better dispersions of Mn and Ti were obtained, and the surface area and pore volume were higher.

NO_2 and nitrate were active components in the SCR reaction. With the solid solution, NO could be more easily converted to these components, and a higher catalytic activity could be obtained.

The assumption model had been developed to analyzing the nano-structure of the catalyst. From this model, the behavior of the transition metals was simulated. The addition of transition metals could segregate the particles of manganese oxides and titania. And the particles were prevented from sintering so that the manganese oxides were kept in amorphous phase. Therefore, the catalytic activity was significantly improved.

2.9.4 Iron and manganese oxides supported on titania (Qi et al., 2003)

A series of manganese oxide and iron–manganese oxides supported on TiO_2 with different amounts of manganese and iron was studied for low-temperature selective catalytic reduction (SCR) of NO with ammonia in the presence of excess oxygen. The addition of iron oxide not only increased the NO conversion and N_2 selectivity but also increased the resistance to H_2O and SO_2. The Fe-Mn/TiO_2 catalysts yielded high activities and high N_2 product selectivity. The N_2O product selectivity increased with the amount of MnO_X as well as temperature. Crystalline phase of MnO_X was present at ≥15% Mn on TiO_2, and the amount increased with Mn content. In addition, SO_2 and H_2O decreased the activities only slightly, while such effect was reversible. The Fe–Mn/TiO_2 with Mn/Fe = 1 showed the highest activity. This catalyst yielded nearly 100% NO conversion at 120° C at a space velocity of 15,000 h^{-1}. The effect of oxygen was also studied. Reversible transient behaviors

similar to that of other oxide catalysts, including vanadia and chromia, were observed for the Fe–Mn/TiO_2 catalyst.

2.9.5 Thermally stable V_2O_5-WO_3 /TiO_2 SCR catalysts modified with silica and rare-earths (Ce, Tb, Er) (Vargas et al., 2007)

The catalytic activity of silica-free and silica-modified rare earth (Ce, Tb, Er) containing V_2O_5-WO_3 -TiO_2 catalysts in the selective catalytic reduction of NO by ammonia has been investigated as a function of aging temperatures. Rare earths slightly decrease the catalytic activity of catalysts in a fresh state, and this has been attributed to the perturbation of the vanadyl groups with a likely lowering of their Lewis acidity.

However, rare earths (in particular Tb and Er) strongly increase the catalytic activity of catalysts after aging. Silica only does not seem to have a positive effect on thermal stability and activity when vanadium is present. Rare earths strongly increase the thermal resistance of the catalysts and inhibit formation of rutile and surface area loss because they do not penetrate the anatase bulk, tending to cover the external surface. In addition, the negative action of free vanadium on phase stability is decreased due to formation of rare earth vanadates.

2.10 Mechanism of the Fast SCR reaction over Vanadium based catalysts (Nova et al., 2006)

The Fast SCR reaction, for which NH_3 reacts with NO and NO_2, is widely investigated, as it can extend the operating window into the low temperature region. Transient data collected at low temperature study of the reactivity for NH_3–NO/NO_2 mixtures with different NO/NO_X ratio (from 0 to 1) over V_2O_5-WO_3 -TiO_2 had allowed identification of a novel reaction pathway for the Fast SCR reaction. Concerning the reactivity between NO_2 and NH_3, it is proposed that NO_2 via dimerization, disproportion, and reaction with water leads to nitrous and nitric acid, which, in the presence of ammonia adsorbed species, form, respectively, NH_4NO_2, from which nitrogen is readily produced, and NH_4NO_3. In the absence of a suitable reducing agent, ammonium nitrate behaves as a terminal product, or might be

thermally decomposed to N_2O at higher temperatures. But the introduction of NO into the reacting system allowed reduction of ammonium nitrate through reaction between nitric acid (in equilibrium with ammonium nitrate) and NO. Also nitric acid is able to oxidize gaseous NO to NO_2, then being reduced to nitrous acid. In the presence of adsorbed NH_3 nitrous acid produces N_2, via decomposition of NH_4NO_2. The well-known stoichiometry of the Fast SCR reaction was readily recovered once they couple the observed overall reaction summarizing the chemistry of the NO_2/NH_3 system with that describing the addition of NO to this reacting system. So in the full NH_3–NO/NO_2 reacting system (Fast SCR), the selectivity to N_2 is not only ruled by the formation of NH_4NO_2 that decomposes to N_2, but also by the formation of NH_4NO_3 that was reduced to NH_4NO_2 by NO. Accordingly, NO_2 was responsible for the formation of nitrites and nitrates. The key role of NO is to reduce nitrates to nitrites, and eventually ammonia, allowing formation of ammonium nitrite, which was the direct precursor of the desired nitrogen product. The proposed reaction scheme could describe not only the stoichiometry of the Fast SCR reaction, and specifically the optimal equimolar NO to NO_2 feed ratio, but also the selectivity to all of the observed products, namely, N_2, NH_4NO_3, HNO_3, and N_2O. Furthermore, it was in agreement with the observed kinetics of the Fast SCR reaction, which at low temperature was limited by the reaction between HNO_3 and NO. Such reaction pathways provided the basis for the development of a chemically consistent kinetic model of the Fast SCR system.

2.11 Highly porous Pt–V_2O_5–WO_3/TiO_2/SiC filter for simultaneous removal of NO and particulates (Kim et al., 2008)

TiO_2 was coated on the pore surface of SiC filter element to formed a highly porous film having the macro-pores more than 50% in the surface area based-calculation. The filter element was the good catalyst support of the V_2O_5–WO_3–TiO_2 based catalyst for SCR of NO. In order to improve the porosity of TiO_2 film, the coating solution was modified by addition of PEG, PVA, and HPC. However, the effect of polymer addition was small, resulting in the slight increase in the pore size and the decrease in the total surface area of TiO_2 film. The preformed TiO_2 particle

(P25) seemed too large to be affected by the additional polymer during the coating and calcination processes. The presence of Pt in the catalytic filter acted to shift the optimum working temperature (giving an N_X slip concentration below 20 ppm at the face velocity of 2 cm/s) towards the lower temperatures: 160–240° C for V_2O_5–WO_3–TiO_2/SiC catalytic filters with Pt compared to 260–340°C for the catalytic filter without Pt. This effect of Pt over the V_2O_5–WO_3–TiO_2/SiC catalytic filters was a result of an increase in the electron transfer properties of the catalyst system by Pt. However, Pt added-catalytic filters exhibited the high oxidation activity at the temperature over 250° C.

2.12 SO_2-resistant antimony promoted V_2O_5/TiO_2 catalyst for NH_3-SCR of NO_X at low temperatures (Phil et al., 2007)

Quantum chemical calculation study was carried out to select promoters which were capable of decreasing SO_2 deactivation on V_2O_5/TiO_2 catalysts. Among the selected promoters, selenium, antimony, copper, and sulfur exhibited high NO_X conversions at low temperatures. From the sulfur deactivation studies, antimony-promoted V_2O_5/TiO_2 catalyst was the best for the low temperature SO_2 deactivation resistance. The high electrical conductivity change of Sb(2%)V_2O_5/TiO_2, compared to that of W(10%)V_2O_5/TiO_2 catalyst, obtained during in situ electrical conductivity study and its correlation with high catalytic activity at low temperatures suggested that the Sb(2%)V_2O_5/TiO_2 was a promising catalyst. The XPS, BETSA, and CHNS elemental analysis also confirmed the effective catalytic performance and resistance to SO_2 of Sb(2%)V_2O_5/TiO_2, compared to those of W(10%)V_2O_5/TiO_2, at low temperatures. Finally, Sb(2%) promoted V_2O_5/TiO_2 catalyst can be efficiently used as sulfur resistance catalyst at low temperatures in substitution to commercial W(10%)V_2O_5/TiO_2.

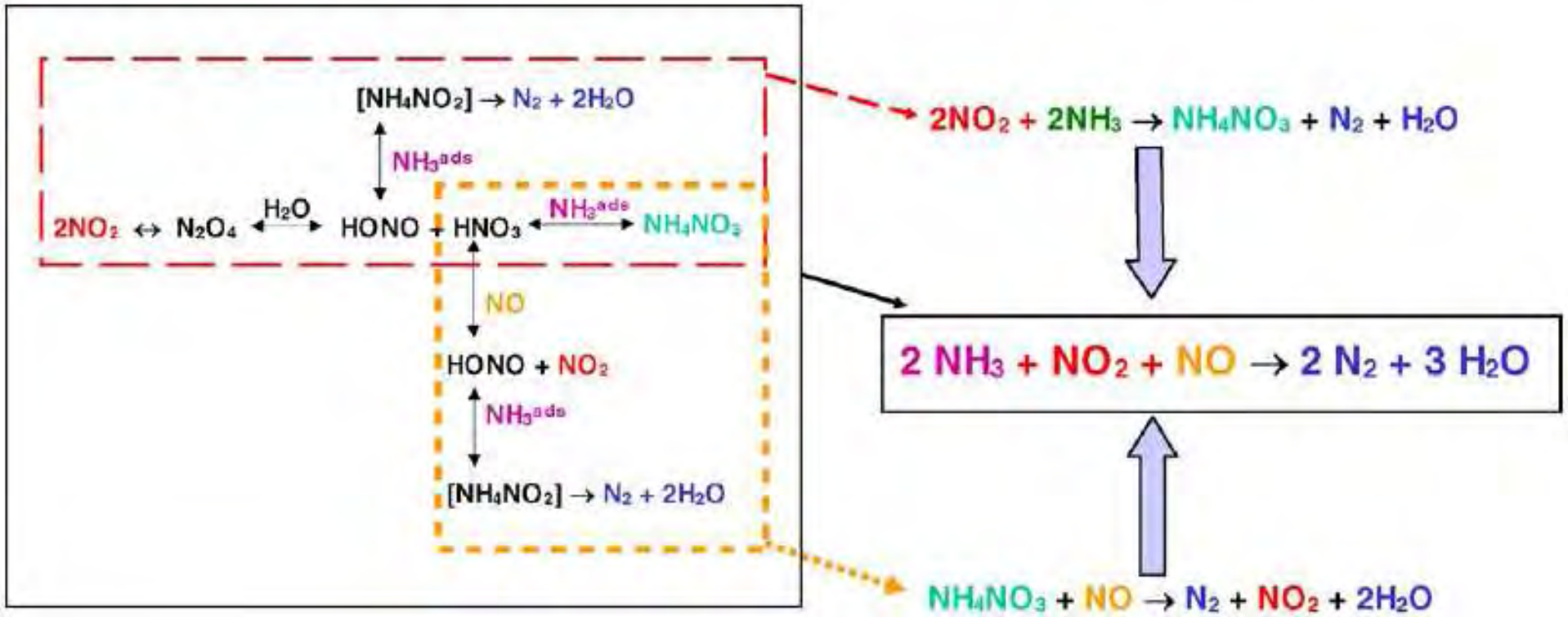

Figure 2.9 Chemistry of NH_3/NO_2 (dashed box) and of NH_3–NO/NO_2 (solid box) SCR reacting systems over V_2O_5–WO_3/TiO_2 SCR catalysts. (Nova et al., 2006)

CHAPTER III

EXPERIMENTAL

This chapter contains details about prepared on methods for TiO_2 support and V_2O_5-WO_3/TiO_2 catalysts, and various characterization techniques performed. Schematic diagram of the apparatus employed in selective catalytic reduction of nitrogen oxide by ammonia as well as experimental procedures are presented.

The scope of this study

Type of deNO_X catalyst used in this study:

– Vanadia-tungsten oxide over titania contain:
  1wt.% vanadium-8wt.% tungsten, 1wt.% vanadium -10wt.% tungsten,
  1wt.% vanadium -12wt.% tungsten, 3wt.% vanadium -8wt.% tungsten,
  3wt.% vanadium -10wt.% tungsten, 3wt.% vanadium -12wt.% tungsten,
  5wt.% vanadium -8wt.% tungsten, 5 wt.% vanadium -10wt.% tungsten,
  and 5wt.% vanadium -12wt.% tungsten

– Addition of Mn and Ce over V_2O_5- WO_3/TiO_2:
  2mole% cerium-2mole% manganese,
  2mole% cerium -5mole% manganese,
  5mole% cerium -2mole% manganese,
  and 5mole% cerium -5mole% manganese

– Addition of Mn and Cu over V_2O_5- WO_3/TiO_2:
  2mole% copper-2mole% manganese,
  2mole% copper-5mole% manganese,
  5mole% copper-2mole% manganese,
  and 5mole% copper-5mole% manganese

– Addition of Mn and Fe over V_2O_5- WO_3/TiO_2:
  2mole% iron-2mole% manganese,
  2mole% iron -5mole% manganese,
  5mole% iron -2mole% manganese,
  and 5mole% iron-5mole% manganese

3.1 Catalyst preparation

3.1.1 Preparation of titanium dioxide by a sol-gel method

Titanium dioxide was prepared using a sol-gel method, and titanium isopropoxide (Aldrich Chemical, Milwaukee, WI) was employed as a precursor. The first, nitric acid, 70 % (Asia Pacific Specialty Chemical Limited) 7.33 cm^3 was added to 1000 $cm^3$of distillated water. While the acid solution was stirred, titanium isopropoxide 83.5 cm^3 was added slowly. The suspension was stirred continuously at room temperature for about 3-4 days until clear sol was obtained. After that, the sol was dialyzed in a cellulose membrane with a molecular weight cutoff of 3500 (Spectrum companies, Gardena, CA) by distilled water until pH of sol was about 3.3 - 3.5, dialyzed titania sol was dried at 110°C for 24 hours, crushed, grinded, and then calcined at 350°C for 2 hours.

3.1.2 Preparation of vanadium-tungsten over titania catalyst

V_2O_5-WO_3/TiO_2 catalyst was prepared by the conventional wet impregnation method. The amount of calculated ammonium metavanadate (>99.999%; Aldrich Chemical) and ammonium metatungstete hydrate (>99.99%; Aldrich Chemical) were dissolved into hot de-ionized water, continuously stirred and heated at 80°C. Amount of oxalic acid anhydrous (Fuka chemica) equal to mole of vanadium was added into the solution to increase solubility of ammonium metavanadate. Mixture solution was stirred until solution was clear-blue aqueous solution. Amount of calculated TiO_2 was added into the solution slowly and continuously stirred and heated for evaporate water until they was paste and thick. They was dried in oven at 110°C over night, crushed, grinded and then calcined in air at 550°C for 2 hours. This type catalyst was denoted by symbols 1V8W to refer to 1wt.%V_2O_5-8wt.%WO_3/TiO_2.

3.1.3 Impregnation of manganese and other metal (Cerium, Copper, and iron)

After testing activities of the V_2O_5-WO_3/TiO_2 catalysts to find the catalyst that has highest NO conversion in wide temperature range. Manganese nitrate and one of the others metal nitrate salt (cerium nitrate, copper nitrate, and iron nitrate) were

dissolved into de-ionized water. The mixture solution was dropped onto the chosen catalyst and mixed the paste until they were looked like uniform. The paste was dried in air at room temperature for 6-8 hours, in oven at 110°C over night. They were crushed, grinded and then calcined in air at 500°C for 2 hours.

3.2 The catalytic activity testing system

The catalytic activity was measured at steady state by 7 mm ID stainless tubular fixed bed reactor. Temperature of furnace was controlled by a digital temperature controller. The diagram of the system is exhibited schematically in Figure 3.1. The total flow rate of feed gas mixture was about 188.5-192.4 cm^3/min, upon the high of bed. Each feed gas stream was controlled by using mass flow controller. Prepared catalyst was tested by passing feed gas stream through the catalyst bed, was packed on quartz wool. NO_X concentration in outlet stream was measured by NO_X analyzer (NOA-7000, SHIMADZU).

Reaction condition for test of SCR activity:	
Reaction temperature	50 - 450°C
Operation pressure	1 atm
Gas hourly space velocity	40000 hr^{-1}

Component of feed gas mixture:	
Nitrogen oxide	60, 90, 120, and 500 ppm
Ammonia	60, 90, 120, and 500 ppm
Oxygen	3 vol.%
Nitrogen	balance

In this study, the activity testing of catalysts was divided into dry condition such as low and high NO concentration, low and high gas hourly space velocity and wet condition.

3.2.1 Activities of V_2O_5-WO_3/TiO_2 catalysts under high reactant concentrations and high space velocity

SCR of NO by NH_3 over V_2O_5-WO_3/TiO_2 catalysts with various compositions in the reaction temperature range of 100-450°C were presented. The composition of feed gas stream was 500 ppm NO, 500 ppm NH_3, 3 vol.% O_2, and balancing N_2. The gas hourly space velocity of feed was set at 40000 hr^{-1}. The reaction temperature was varied between 100-450 °C. No water was present in the feed.

3.2.2 Activities of V_2O_5-WO_3/TiO_2 catalysts under low reactant concentrations and moderate space velocity region

SCR of NO by NH_3 over V_2O_5-WO_3/TiO_2 catalysts with various compositions in the reaction temperature range of 100-450°C were presented. The inlet concentrations of NO and NH_3 were varied in the range of 60-120 ppm. The feed also contained 3 vol.% O_2 and balancing N_2. The gas hourly space velocity of feed was set at 20000 hr^{-1}. The reaction temperature was between 100-450 °C. No water was present in the feed.

3.2.3 Activities of the V_2O_5-WO_3/TiO_2 catalyst under variable space velocity

SCR of NO by NH_3 over the 3V12W catalyst in the reaction temperature range of 100-450°C were presented. The inlet concentrations of NO and NH_3 were varied in the range of 60-120 ppm. The feed also contained 3 vol.% O_2 and balancing N_2. The gas hourly space velocity of feed was varied at the values of 3000, 6000, 10000, and 20000 hr^{-1}. The reaction temperature was between 100-450 °C. No water was present in the feed.

3.2.4 Activities of 3V12W that were promoted with Mn and another metal catalysts

3V12W catalysts that were promoted with manganese and another metal are presented. The catalysts contained manganese and cerium at the concentration of either 2 mole% or 5 mole% each. Feed gas stream contained 500 ppm NO, 500 ppm

NH_3, 3 vol.% O_2, and balancing N_2. The reaction temperature was varied between 50-450°C.

3.2.5 Activities of the 3V12W catalysts that were promoted with manganese and another metal with water vapor present in feed (wet condition)

The promoted 3V12W catalysts chosen for this portion of the experiment were the ones that exhibited the best performance in a wide temperature range for each pair of metal (see section 4.2.1 to 4.2.3). For wet condition, saturated water vapor was added into feed gas stream about 5, 10, and 15 mole%.

3.3 Characterization of catalyst

3.3.1 Surface area measurement

The specific surface area was determined by nitrogen adsorption method. The single point specific surface area of the catalysts was measured by Micromeritics ChemiSorb 2750 using nitrogen as the adsorbate. The operating conditions were shown below.

Sample weight	:	0.2 g
Degas temperature	:	200^{o}C for as-synthesized sample

3.3.2 X-ray diffraction (XRD)

The XRD patterns of catalysts were performed by using SIEMENS D-5000 diffractrometer with CuKα radiation in the 2θ range of 20-80°. The XRD spectrum is used to identify the crystal structure of catalyst.

3.3.3 Determination of composition of catalyst using Inductively Coupled Plasma-Optical Emission Spectroscopy (ICP-OES)

The percentage of metal loading of each catalyst prepared in this study was analyzed by Inductively-coupled plasma optical emission spectroscopy (ICP-OES). The amount of metal on the surface of titanium dioxide was measured with an Inductively Coupled Plasma Atomic Emission Spectrometer (ICP-AES) Perkin Elmer model PLASMA-1000. About 0.02 g of catalyst was dissolved in 10 cm^3 hydrofluoric acid 49%, stir until all solid are solution then make volume up to 100 cm^3 using

deionized water by the volumetric flask which has the volume of 100 cm^3. The concentration of sample is about 1-24 ppm ($mg.l^{-1}$).

3.3.4 X-ray photoelectron spectrometer (XPS)

For each and every element, there will be a characteristic binding energy associated with each core atomic orbital i.e. each element will give rise to a characteristic set of peaks in the photoelectron spectrum at kinetic energies determined by the photon energy and the respective binding energies. The binding energies (E_b) reference for the peak positions the C-1s peak occurred at a binding energy of 285 eV.

The presence of peaks at particular energies therefore indicates the presence of a specific element in the sample under study - furthermore, the intensity of the peaks is related to the concentration of the element within the sampled region.

3.3.5 Temperature programmed desorption (NH_3-TPD)

Temperature programmed desorption (TPD) using NH_3 as a probe molecule performed in a Micromeritic ChemiSorb 2750 automated system attached with ChemiSoft TPx software. The amount of NH_3 adsorbed on the surface was determined by thermal conductivity detector.

Approximately 0.2 grams of sample was placed in quartz tube in a temperature-controlled furnace. Helium gas with a flow rate 15 ml/min was fed through sample. The sample was heated from room temperature to 250°C with a heating rate of 10°C/min and held for two hours to remove moisture. Then the sample was cooled down to room temperature. After that, 15 vol.% NH_3 in helium gas was flowed through sample at a flow rate of 15 ml/min in stead of helium, and held for 1 hour. Subsequently, helium gas was fed through the sample for two hours. Finally, the sample was heated from room temperature to 650°C with heating rate of 10°C/min. The signal from this step was recorded every one second and stored on a microcomputer.

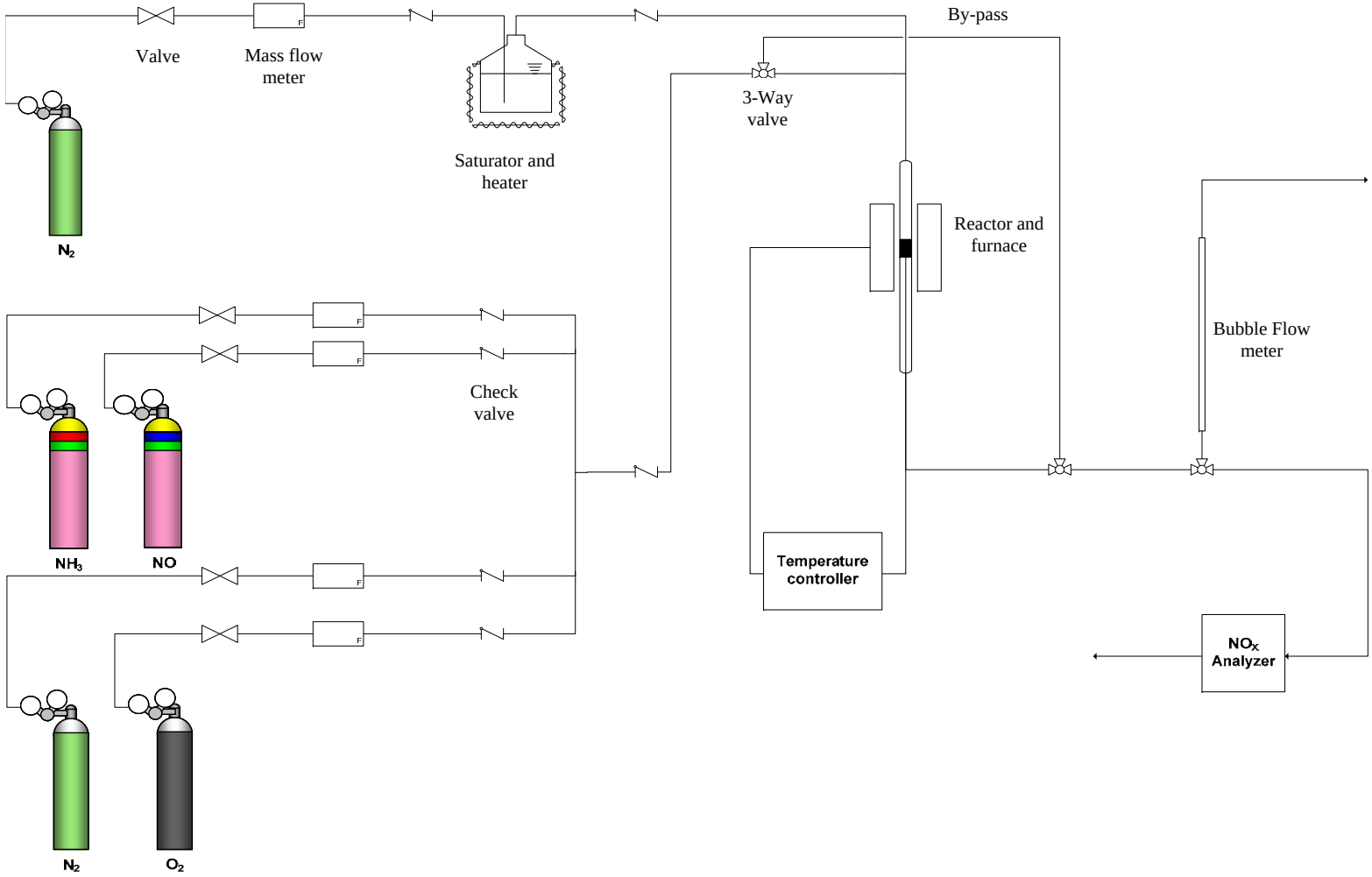

Figure3.1 Flow diagram of the reactor system for SCR of NO byNH_3

CHAPTER IV

RESULT AND DISCUSSION

In this chapter selective catalytic reduction of nitrogen oxide by ammonia over V_2O_5-WO_3/TiO_2 catalysts and promoted catalysts were investigated. This chapter is divided into two main parts. The first part discusses characterizations and activity of V_2O_5-WO_3/TiO_2 catalysts in three different conditions. The second part discusses characterization and activities of promoted catalysts under dry and wet conditions. The activity of catalysts for selective catalytic reduction was studied as a function of reaction temperature.

4.1 V_2O_5-WO_3/TiO_2 catalysts

In this section, prepared V_2O_5-WO_3/TiO_2 catalysts were characterized by XRD to analyze crystal structure, nitrogen adsorption to determine specific surface area, NH_3-TPD to determine amounts of acid site on the catalyst surface, XPS to determine oxidation states of vanadium and tungsten on the catalyst surface, and ICP-OES to determine the amounts of metal loading of catalyst. And the catalytic activity was measured as NO conversion in reaction temperature ranging from 100 to 450°C.

4.1.1 Characterization of V_2O_5-WO_3/TiO_2 catalysts

4.1.1.1 X-ray diffractometry

XRD patterns of various V_2O_5-WO_3/TiO_2 catalysts are shown in Figures 4.1 to 4.3. The catalysts contained anatase TiO_2 primarily with small amounts of rutile and brookite phase. No peaks corresponding to V_2O_5 or WO_3 were observed, suggesting that both vanadium and tungsten were highly dispersed on the titania surface.

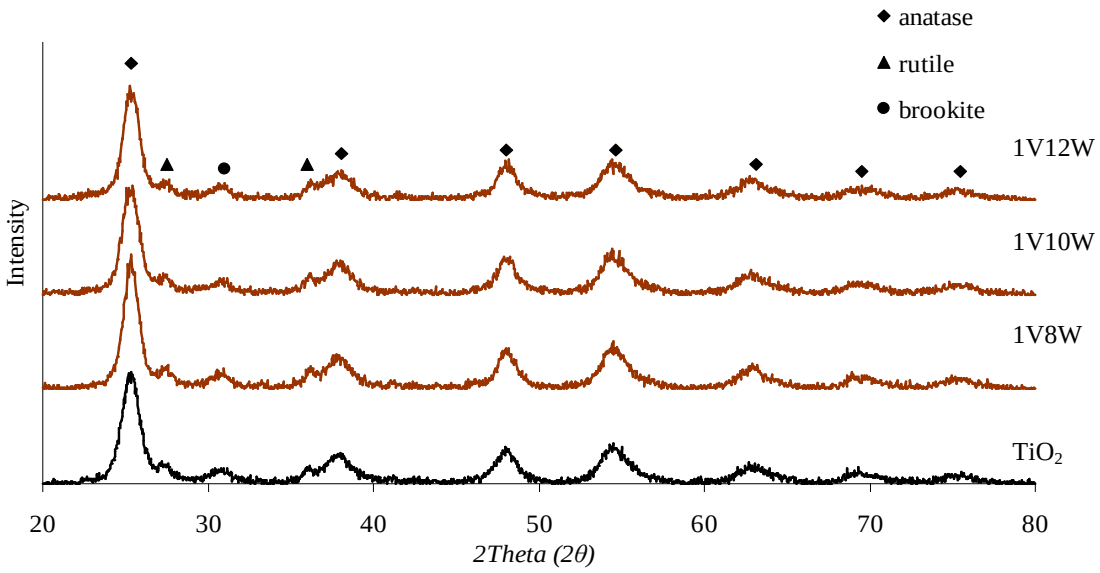

Figure 4.1 XRD patterns of V_2O_5-WO_3/TiO_2 catalysts with 1 wt.% vanadium

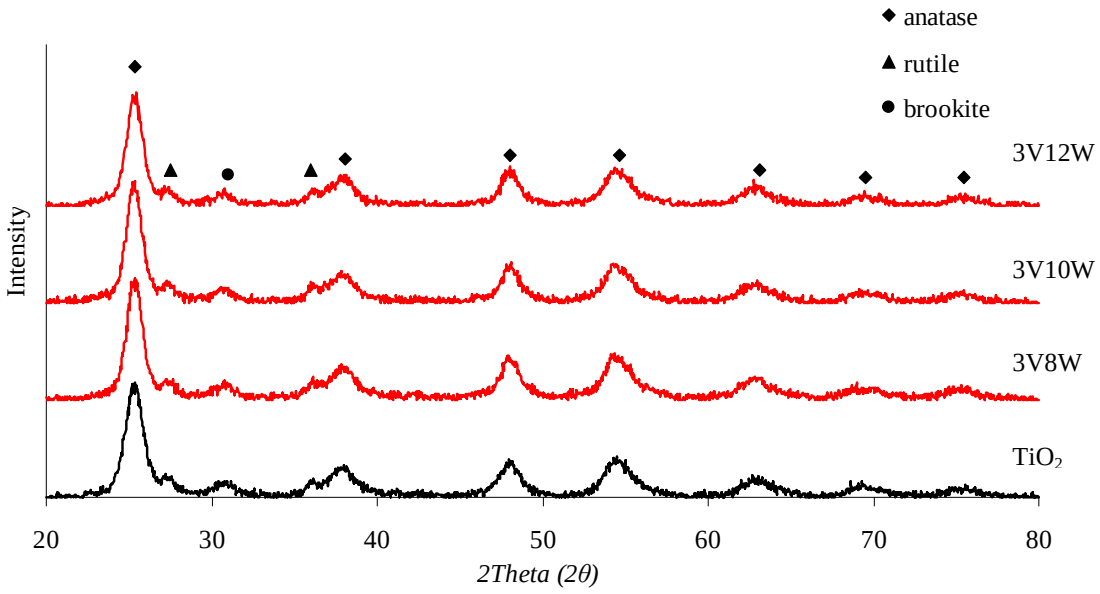

Figure 4.2 XRD patterns of V_2O_5-WO_3/TiO_2 catalysts with 3 wt.% vanadium

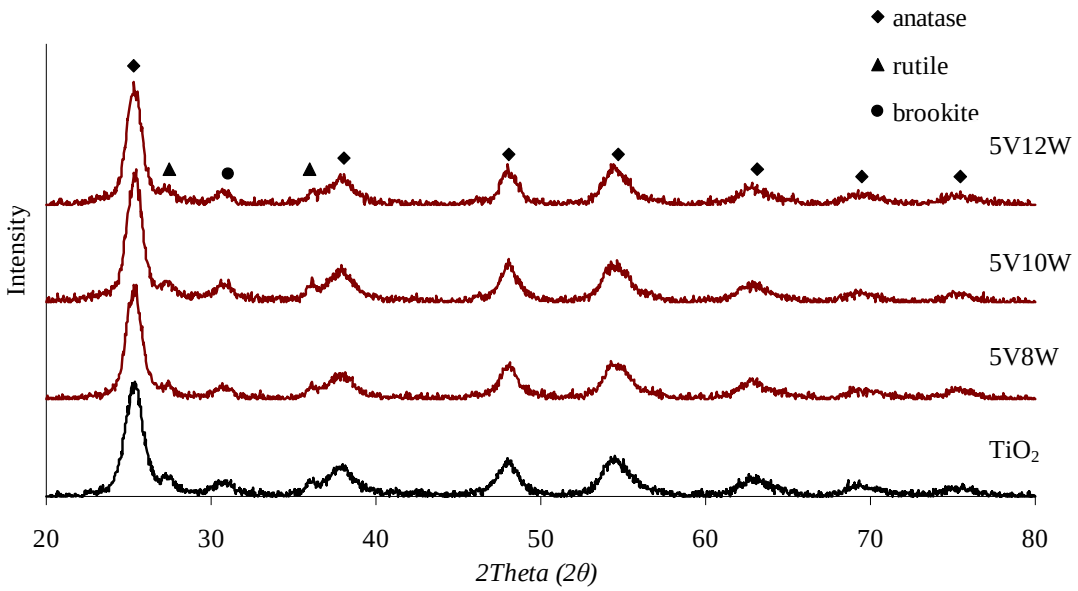

Figure 4.3 XRD patterns of V_2O_5-WO_3/TiO_2 catalysts with 5 wt.% vanadium

4.1.1.2 Specific surface area and crystallite size of catalysts

The most common procedure for determining surface area of a solid is based on adsorption and condensation of nitrogen at liquid nitrogen temperature. This method is also called BET (Brunauer Emmett Teller) method. About 0.2 grams of catalyst used in measurement. BET specific surface area of the catalyst and crystallite size of titania in the catalyst are shown in Table 4.1. Increasing the amount of vanadium or tungsten loading lowered the specific surface area of the catalyst, compared with that of pure titania support. The crystallite sizes of titania in the catalyst became slightly larger and were in the range of 6.0 - 8.2nm. The crystallite size was calculated from XRD peak width using Debye-Scherrer equation. The crystallite size grew larger when vanadium or tungsten was added.

Table 4.1 BET surface areas and crystallite size of the V_2O_5-WO_3/TiO_2 catalysts

Catalyst Sample	BET surface area (m^2/g)	Crystallite size [a] (nm)
TiO_2 supported	91.2	6.2
1V8W	73.7	8.2
1V10W	69.1	6.0
1V12W	50.4	7.0
3V8W	66.3	7.6
3V10W	63.3	7.0
3V12W	60.4	7.1
5V8W	67.1	7.2
5V10W	63.7	7.6
5V12W	52.9	7.6

[a] Calculated by Debye-Scherrer equation from XRD spectra

4.1.1.3 Temperature programmed desorption using NH_3 as a probe molecule (NH_3-TPD)

Temperature program desorption was a commonly used technique for the titration of surface acid sites. The strength of an acid site could be related to the corresponding desorption temperature of ammonia, while the total amount of ammonia desorption after saturation coverage permits quantification of the number of acid sites at the surface (Kung et al.,1985). The temperature-programmed desorption profiles for the V_2O_5-WO_3/TiO_2 catalysts are displayed in Figure 4.7. From the TPD profiles, the amounts of acid sites were calculated from the area under the curve and were listed in Table 4.2

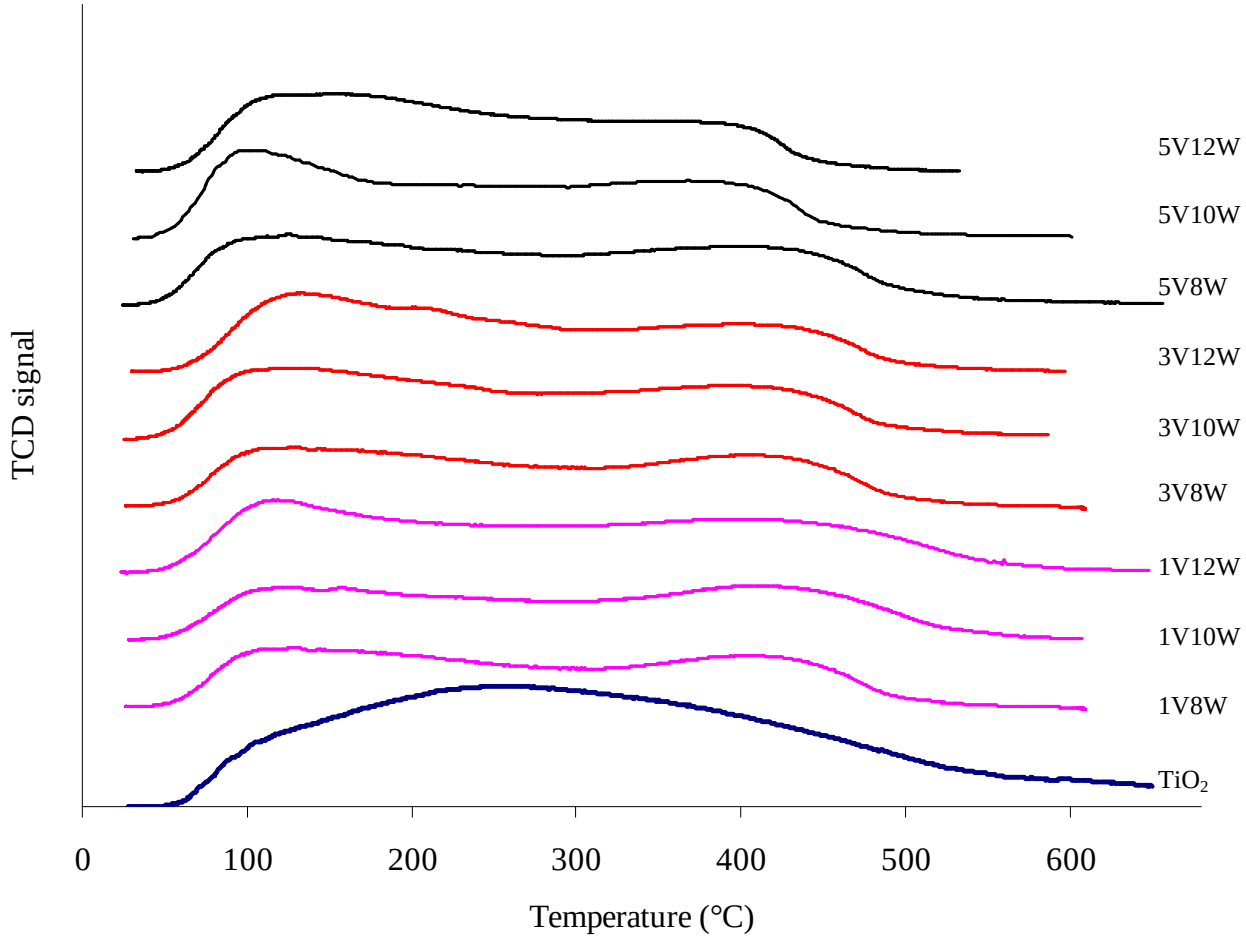

Figure 4.4 NH_3-TPD profiles of various V_2O_5-WO_3/TiO_2 catalysts.

The evolution of ammonia occurred over a temperature ranging from room temperature to about 600 °C due to the presence of adsorbed ammonia species with different thermal stability. All curves exhibited two peaks corresponding to weakly and strongly bound ammonia. When performing the ammonia adsorption at about 50°C, a huge amount of ammonia desorbed from all samples between 100 and 250°C, which was lower than that reported by Nicrosia et al. [2008]. The second peak of the ammonia desorption was observed at 350–500°C, of which the location varied among the sample.

Table 4.2 Amounts of acid site on various V_2O_5-WO_3/TiO_2 catalysts.

Sample	Amount of acid site (μmol H^+/g)
TiO_2	24764
1V8W	7582
1V10W	6934
1V12W	8283
3V8W	6779
3V10W	7609
3V12W	7566
5V8W	8339
5V10W	8140
5V12W	7461

4.1.1.4 X-ray Photoelectron Spectroscopy (XPS)

XPS analysis was carried out not only to examine the surface species on the V_2O_5-WO_3/TiO_2 catalysts but also to determine the relative amounts of elements on the surface. The V_2O_5-WO_3/TiO_2 catalysts exhibited the signals of vanadium, titanium, oxygen, and tungsten in term of binding energies. The peaks of V 2p signals appeared around a binding energy of 514-519 eV, and the binding energy for W 4f electron was around 35-40 eV [Najbar et al., 2000]. The binding energies of the three oxidation states of vanadium, ie.V(III), V(IV), and V(V) were 515.6, 516.6, and 517.5eV, respectively.

The binding energies of the two states of tungsten, ie.W(V) and W(VI)) were 34.7 and 35.4 eV, respectively. In this study, the binding energies for both vanadium and tungsten were slightly higher than those reported. The binding energy of vanadium was in the range of 515.24 - 518.031 eV and that of tungsten was in the range of 35.145 – 38.01 eV. The binding energy, the percentages of atomic concentration, and full width at half maximum (FWHM) of V $2p_{3/2}$ and W $4f_{7/2}$ are presented in Table 4.4 and Table 4.5, respectively. The deconvoluted XPS spectra for the V $2p_{3/2}$ and W $4f_{7/2}$ core level regions for V_2O_5-WO_3/TiO_2 catalysts are displayed in Figure 4.8-4.13. From XPS spectra of vanadium $2p_{3/2}$, the sample of 1 wt. % vanadium trended to be V(III) and V(IV) more than V(V). The sample of 3 and 5 wt. % vanadium trended to be V(IV) and V(V).

4.1.1.5 Composition of vanadium and tungsten of V_2O_5-WO_3/TiO_2

Amounts of vanadium and tungsten loading were determined by inductively coupled plasma-optical emission spectroscopy (ICP-OES). The composition of the catalysts was displayed in Table 4.3

Table4.3 The compositions of V_2O_5-WO_3/TiO_2 catalysts as determined from ICP-OES

Sample	Vanadium content (%wt.)	Tungsten content (%wt.)
1V8W	1.057	8.190
1V10W	1.043	9.838
1V12W	1.067	12.105
3V8W	3.300	8.105
3V10W	3.230	10.005
3V12W	3.276	12.114
5V8W	5.420	7.950
5V10W	5.320	10.125
5V12W	5.286	11.659

Table 4.4 Results from XPS for vanadium over V_2O_5-WO_3/TiO_2 catalysts

sample	V $2p_{3/2}$								
	V(III)			V(IV)			V(V)		
	BE	FWHM	% atomic	BE	FWHM	% atomic	BE	FWHM	% atomic
1V8W	515.78	1.083	0.10	516.57	1.145	0.07	-	-	-
1V10W	515.24	0.461	0.07	516.31	0.788	0.12	-	-	-
1V12W	-	-	-	516.67	1.213	0.17	517.89	0.402	0.04
3V8W	-	-	-	516.60	1.592	0.70	517.33	1.173	0.07
3V10W	-	-	-	517.16	1.178	0.55	518.00	0.747	0.08
3V12W	-	-	-	517.09	1.331	0.35	518.03	0.658	0.06
5V8W	-	-	-	516.80	1.171	0.35	517.82	1.338	0.88
5V10W	-	-	-	516.20	1.014	0.19	517.19	1.478	1.14
5V12W	-	-	-	516.70	1.659	0.82	517.90	0.793	0.16

Table 4.5 Results from XPS for tungsten over V_2O_5-WO_3/TiO_2 catalysts

Sample	W $4f_{7/2}$					
	W (V)			W (VI)		
	BE	FWHM	% atomic	BE	FWHM	% atomic
1V8W	35.72	1.933	1.33	37.62	1.843	1.39
1V10W	35.45	2.185	2.39	37.33	1.797	1.36
1V12W	35.70	1.885	1.96	37.68	1.987	1.92
3V8W	35.15	1.892	1.38	37.01	1.759	1.32
3V10W	35.79	1.702	1.90	37.63	1.969	1.45
3V12W	36.15	2.005	1.85	37.97	1.78	1.44
5V8W	36.09	2.415	1.74	38.01	1.903	1.34
5V10W	35.71	1.948	1.50	37.57	1.851	1.61
5V12W	35.62	2.372	2.67	37.56	1.894	1.33

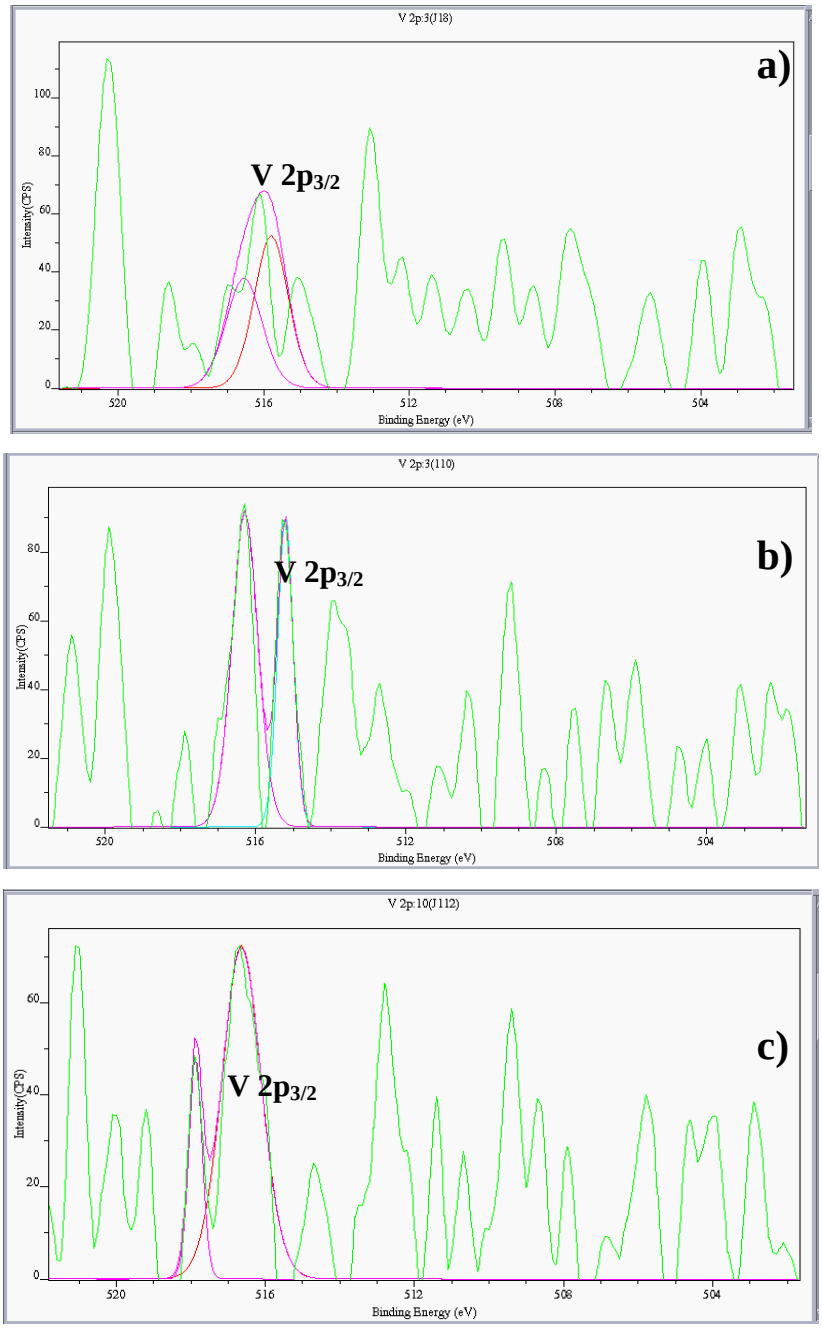

Figure4.5 The deconvolution of XPS spectra of vanadium (V $2p_{3/2}$) in a)1V8W, b)1V10W, and c)1V12W catalyst**s**

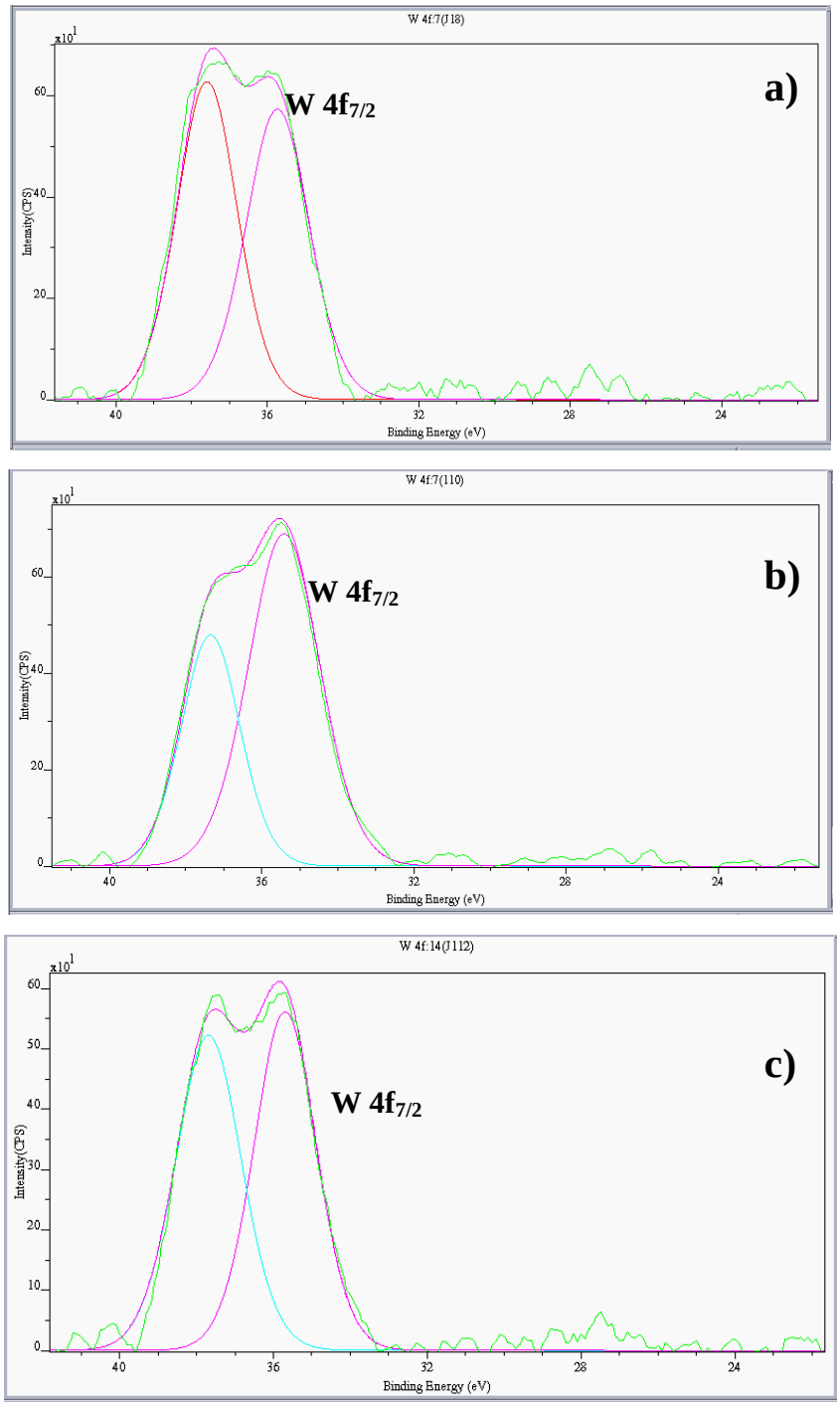

Figure4.6 The deconvolution of XPS spectra of Tungsten (W $4f_{7/2}$) in a)1V8W, b)1V10W, and c)1V12W catalysts

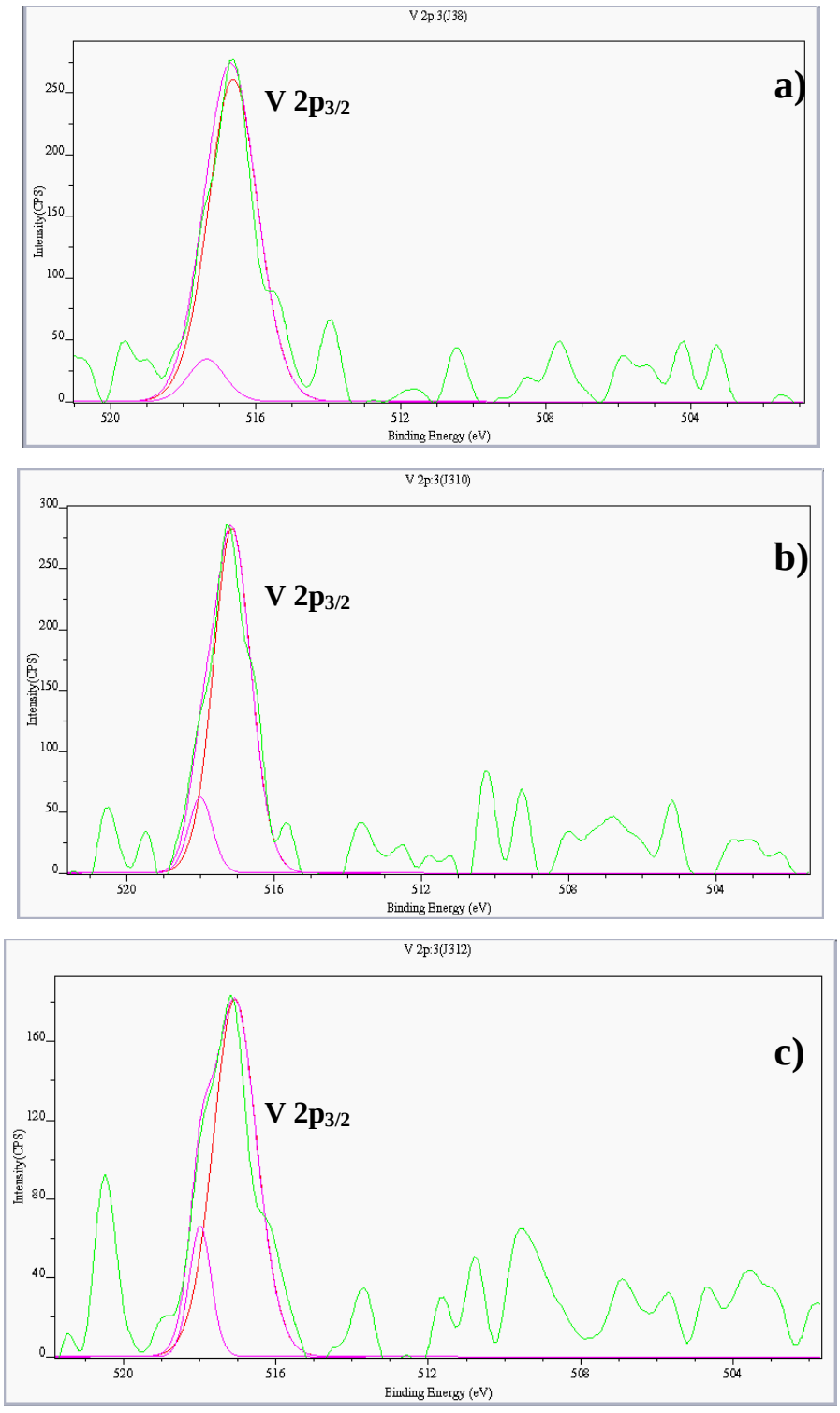

Figure4.7 The deconvolution of XPS spectra of vanadium (V $2p_{3/2}$) in a)3V8W, b)3V10W, and c)3V12W catalysts

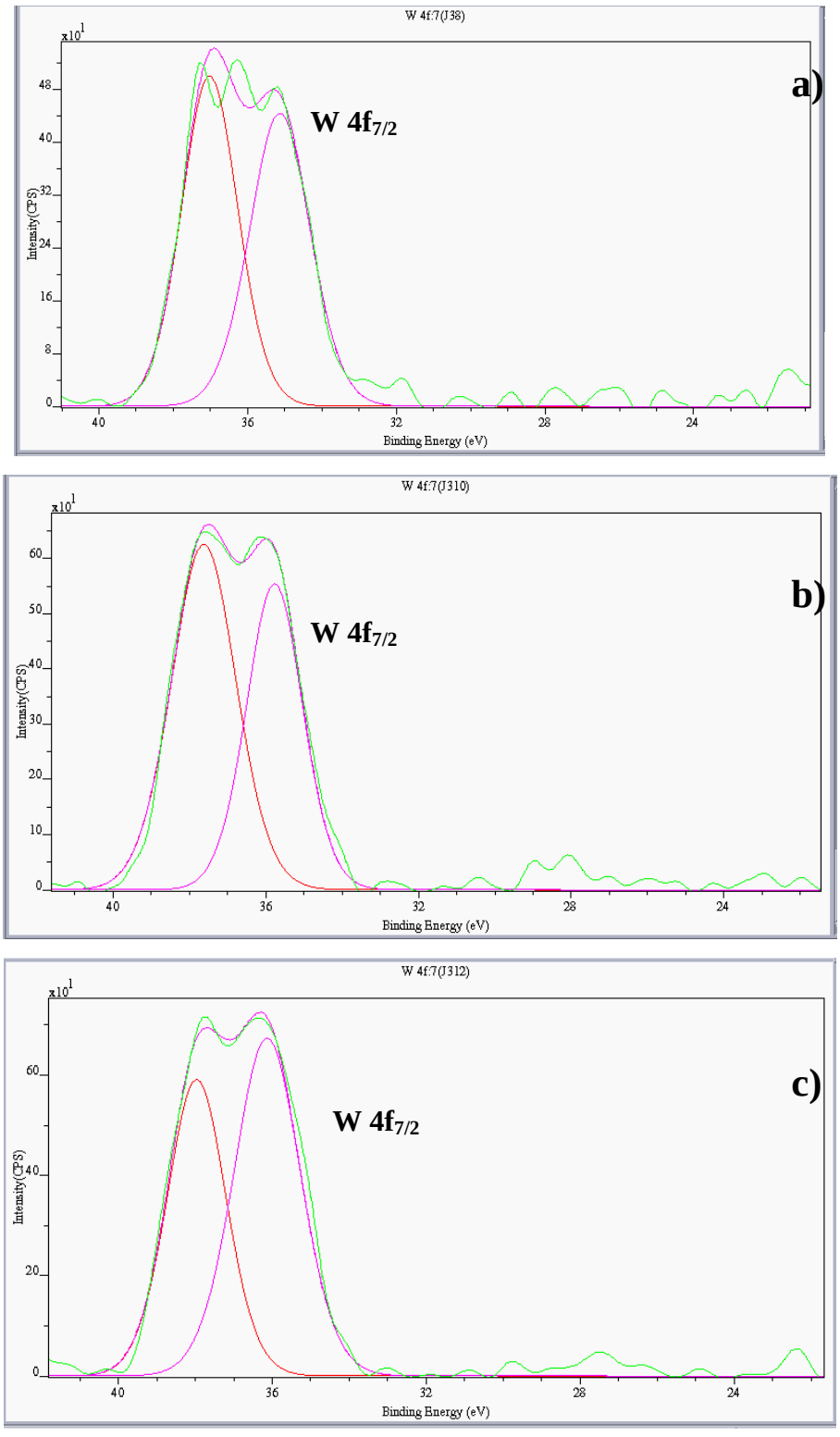

Figure4.8 The deconvolution of XPS spectra of Tungsten (W $4f_{7/2}$) in a)3V8W, b)3V10W, and c)3V12W catalysts

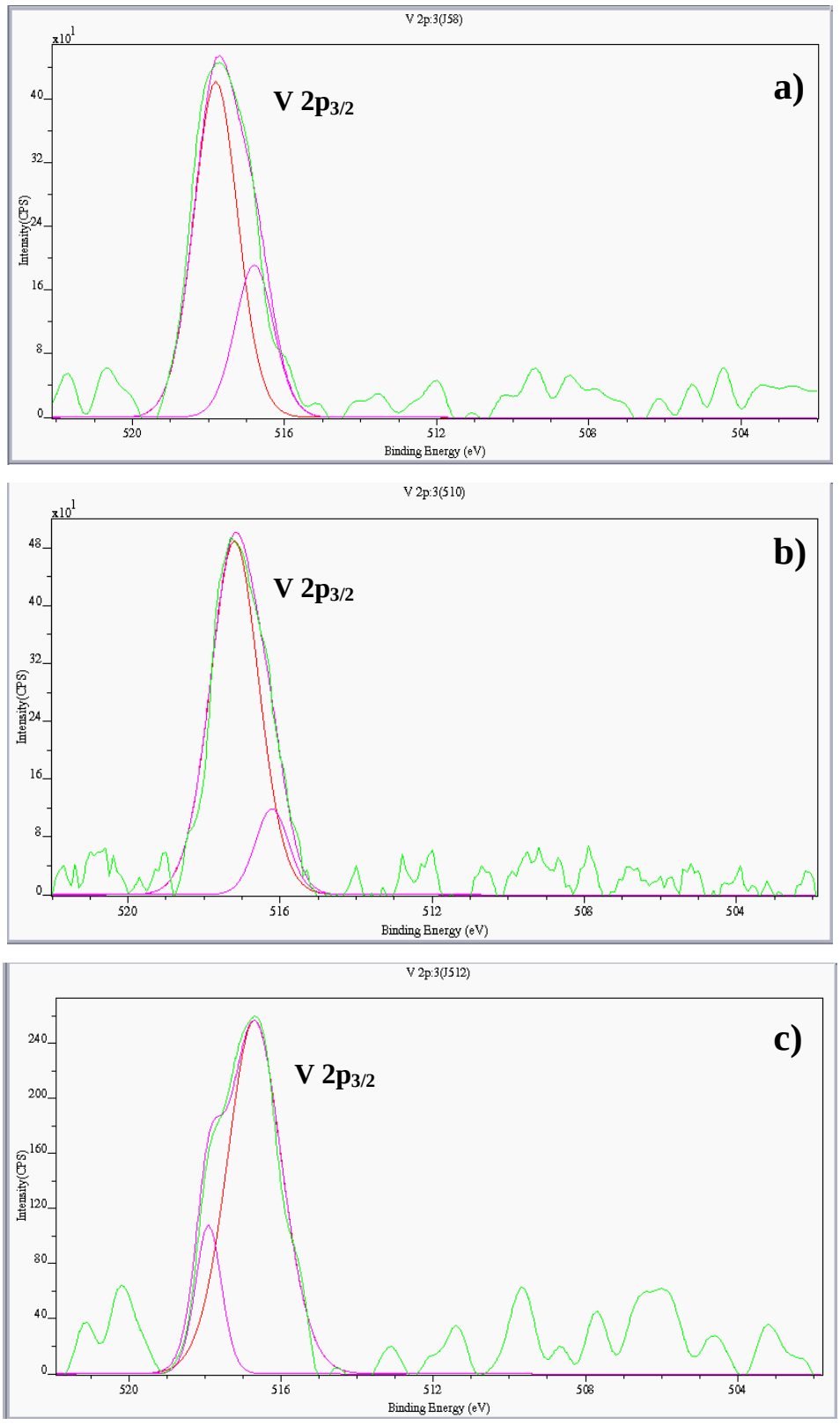

Figure4.9 The deconvolution of XPS spectra of vanadium (V $2p_{3/2}$) in a)5V8W, b)5V10W, and c)5V12W catalysts

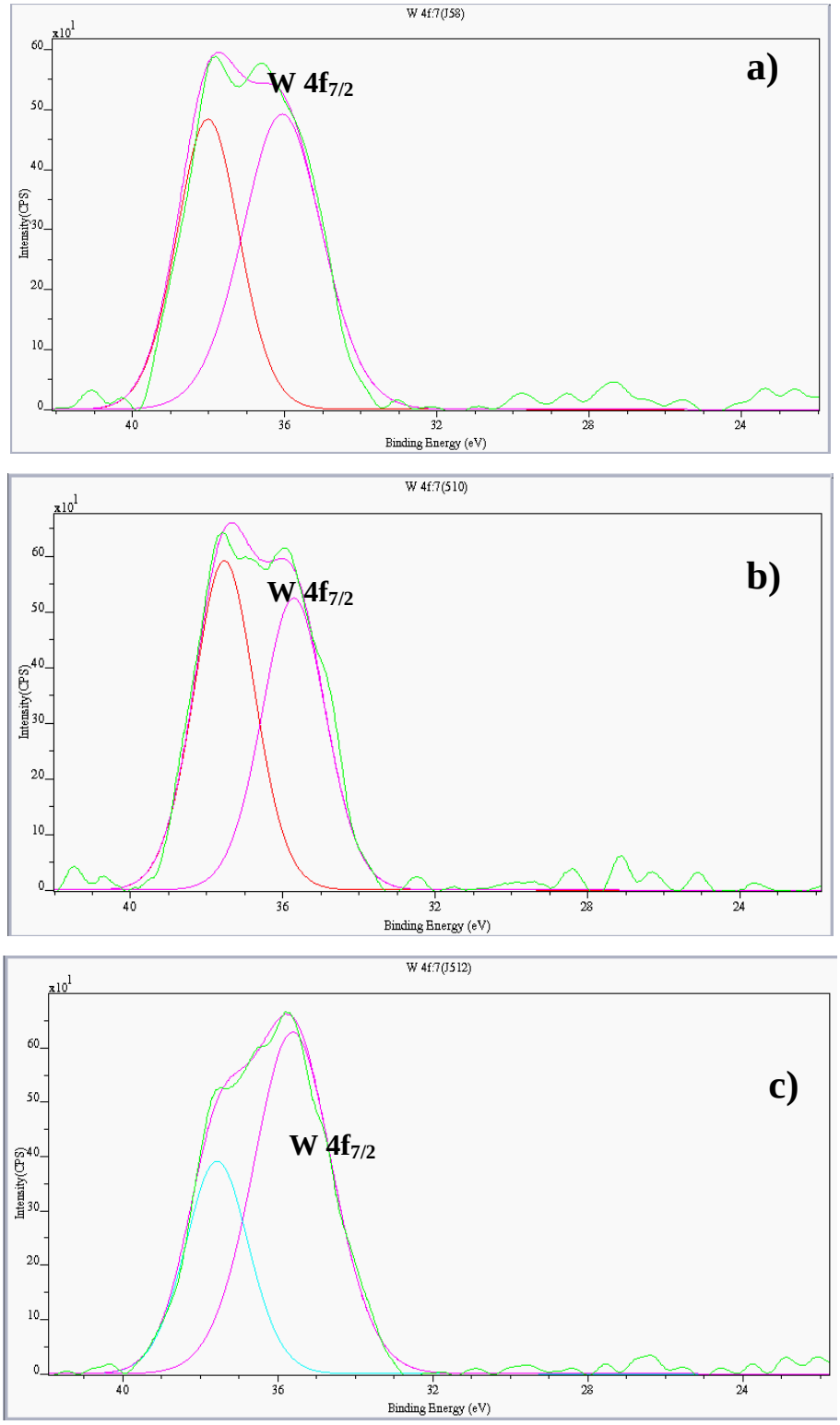

Figure4.10 The deconvolution of XPS spectra of Tungsten (W $4f_{7/2}$) in a)5V8W, b)5V10W, and c)5V12W catalysts

4.1.2 Selective catalytic reduction of NO by NH_3 over V_2O_5-WO_3/TiO_2catalysts

This section presents the catalytic activities of V_2O_5-WO_3/TiO_2 catalysts under three conditions. The first part presents NO conversion of V_2O_5-WO_3/TiO_2 catalysts under high space velocity and high reactant concentrations to find the composition of catalyst that gave rise to high conversion in wide reaction temperature range. This optimum composition was selected for subsequent experiments involving promotion of the two metals. The second part presents NO conversion of V_2O_5-WO_3/TiO_2 catalysts with inlet NO concentrations of 60, 90, and 120 ppm and under moderate space velocity. The third part investigated the effect of space velocity for the SCR reaction over the 3V12W catalyst.

4.1.2.1 Activities of V_2O_5-WO_3/TiO_2 catalysts under high reactant concentrations and high space velocity

The results of SCR of NO by NH_3 over V_2O_5-WO_3/TiO_2 catalysts with various compositions in the reaction temperature range of 100 - 450°C were presented. The composition of feed gas stream was 500 ppm NO, 500 ppm NH_3, 3 vol.% O_2, and balancing N_2. The gas hourly space velocity of feed was set at 40000 hr^{-1}. The reaction temperature was varied between 100-450 °C. No water was present in the feed. Figures 4.14 to 4.16 displayed NO conversion for SCR of NO by NH_3 over various V_2O_5-WO_3/TiO_2 catalysts.

When the reaction temperature was raised, the NO conversion increased with the temperature up to 350°C and then decreased. These results agreed with those reported by Bourikas and coworkers [2004]. A decline in conversion at high temperature, combined with the observed continuous increase of NH_3 consumption, suggested that besides the main reaction (Equation 4.1), there were other side reactions involving NH_3 but not NO, like Equations 4.2 to 4.4, which took place at high reaction temperatures over that catalyst [Bourikas et al.,2004]:

$$4NO + 4NH_3 + O_2 \rightarrow 4N_2 + 6H_2O \quad (4.1)$$

$$4NH_3 + 3O_2 \rightarrow 2N_2 + 6H_2O \quad (4.2)$$

$$2NH_3 + 2O_2 \rightarrow N_2O + 3H_2O \quad (4.3)$$

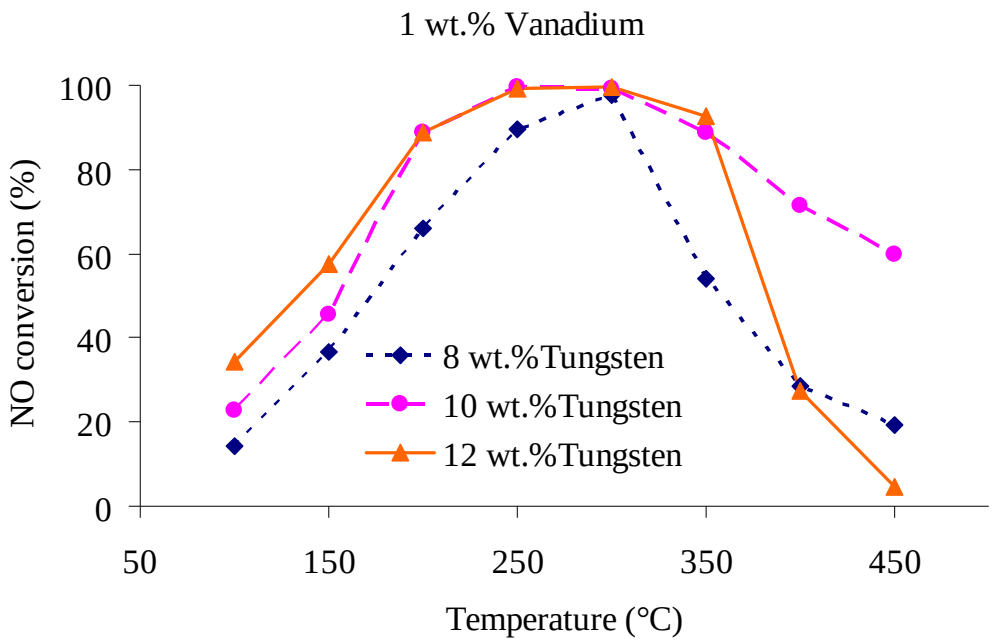

Figure 4.11 NO conversion for SCR of NO by NH_3 over V_2O_5-WO_3/TiO_2 catalysts containing 1 wt.% vanadium.

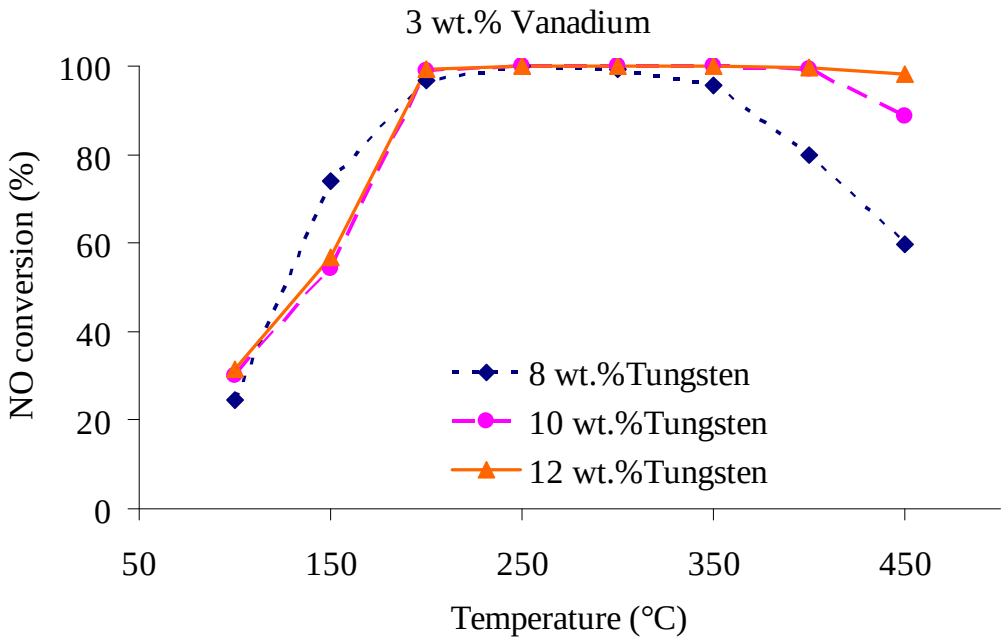

Figure 4.12 NO conversion for SCR of NO by NH_3 over V_2O_5-WO_3/TiO_2 catalysts containing 3 wt.% vanadium.

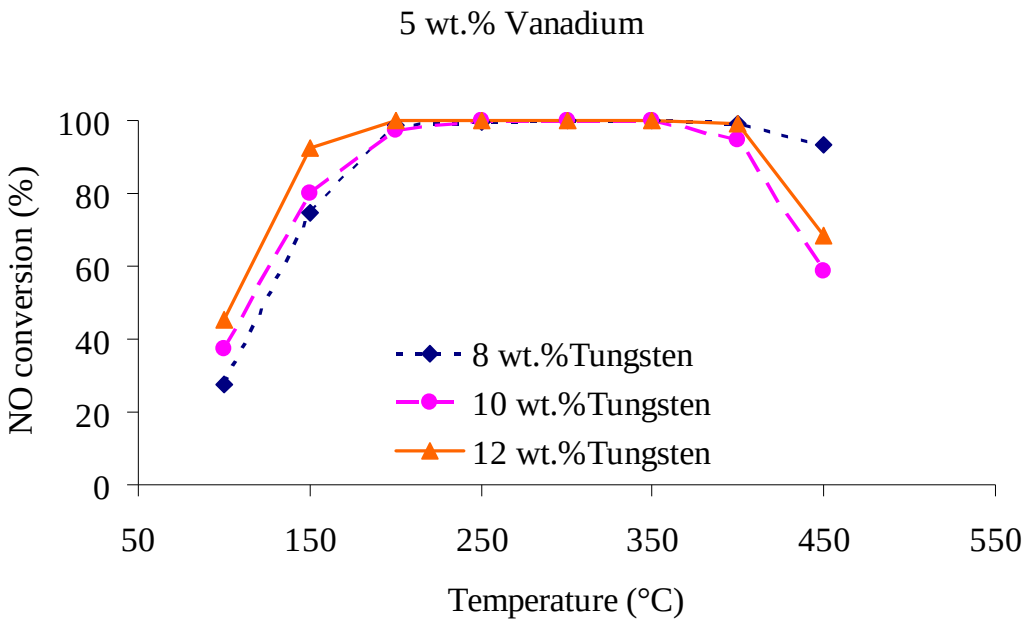

Figure 4.13 NO conversion for SCR of NO by NH_3 over V_2O_5-WO_3/TiO_2 catalysts containing 5 wt.% vanadium.

$$4NH_3 + 5O_2 \rightarrow 4NO + 6H_2O \qquad (4.4)$$

Inspection of Figures 4.12 to 4.14 suggested that the catalyst that exhibited the highest catalytic activity was V_2O_5-WO_3/TiO_2 catalyst with 3 wt.% vanadium and 12 wt.% tungsten (or 3V12W catalyst). NO conversion over the 3V12W catalyst reached almost 100% at 200°C and remained at that level up to 450°C.

4.1.2.2 Activities of V_2O_5-WO_3/TiO_2 catalysts under low reactant concentrations and moderate space velocity region

In this section the results of SCR of NO by NH_3 over V_2O_5-WO_3/TiO_2 catalysts with various compositions in the reaction temperature range of 100-450°C were presented. The inlet concentrations of NO and NH_3 were varied in the range of 60-120 ppm. The feed also contained 3 vol.% O_2 and balancing N_2. The gas hourly space velocity of feed was set at 20000 hr^{-1}. The reaction temperature was between 100-450 °C. No water was present in the feed. Figures 4.14 to 4.16 displayed NO conversion for SCR of NO by NH_3 over various V_2O_5-WO_3/TiO_2 catalysts.

For all catalysts, the NO conversion increased as the reaction temperature was raised up to 200°C and then decreased when the temperature exceeded 300°C. However, for low initial concentration of NO the catalysts containing 1 wt.% vanadium appeared to retain their activities in the high temperature region (T > 300°C) better than other series of catalysts. At low temperature, high initial NO concentration has a lower NO conversion than low initial NO concentration. At high temperature, high initial NO concentration has a higher NO conversion than low initial NO concentration.

4.1.2.3 Activities of the V_2O_5-WO_3/TiO_2 catalyst under variable space velocity

In this section the results of SCR of NO by NH_3 over the 3V12W catalyst in the reaction temperature range of 100-450°C were presented. The inlet concentrations of NO and NH_3 were varied in the range of 60-120 ppm. The feed also contained 3 vol.% O_2 and balancing N_2. The gas hourly space velocity of feed was varied at the values of 3000, 6000, 10000, and 20000 hr^{-1}. The reaction temperature was between 100-450 °C. No water was present in the feed.

Figures 4.18 to 4.20 displayed NO conversion for SCR of NO by NH_3 over 3V12W catalyst when the gas hourly space velocity was varied in the range of 3000 – 20000 hr^{-1}. For 3V12W catalyst, the NO conversion increased as the reaction temperature was raised up to 200°C and then decreased when the temperature exceeded 300°C. NO conversion decreased as gas hourly space velocity was raised.

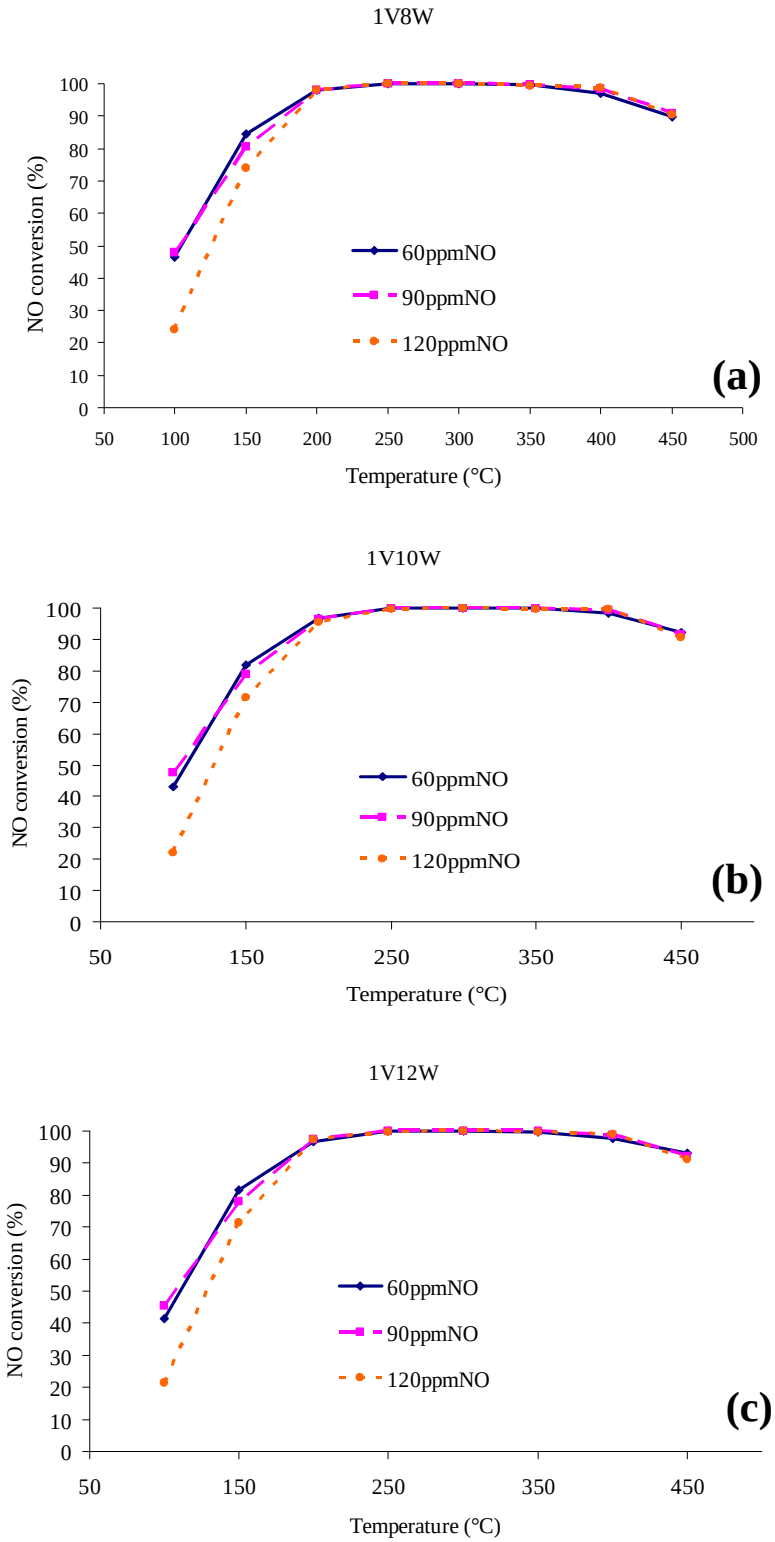

Figure 4.14 NO conversion for SCR of NO by NH_3 over (a) 1V8W, (b) 1V10W, and (c) 1V12W catalysts. The initial of NO in the feed was varied in the range of 60-120ppm.

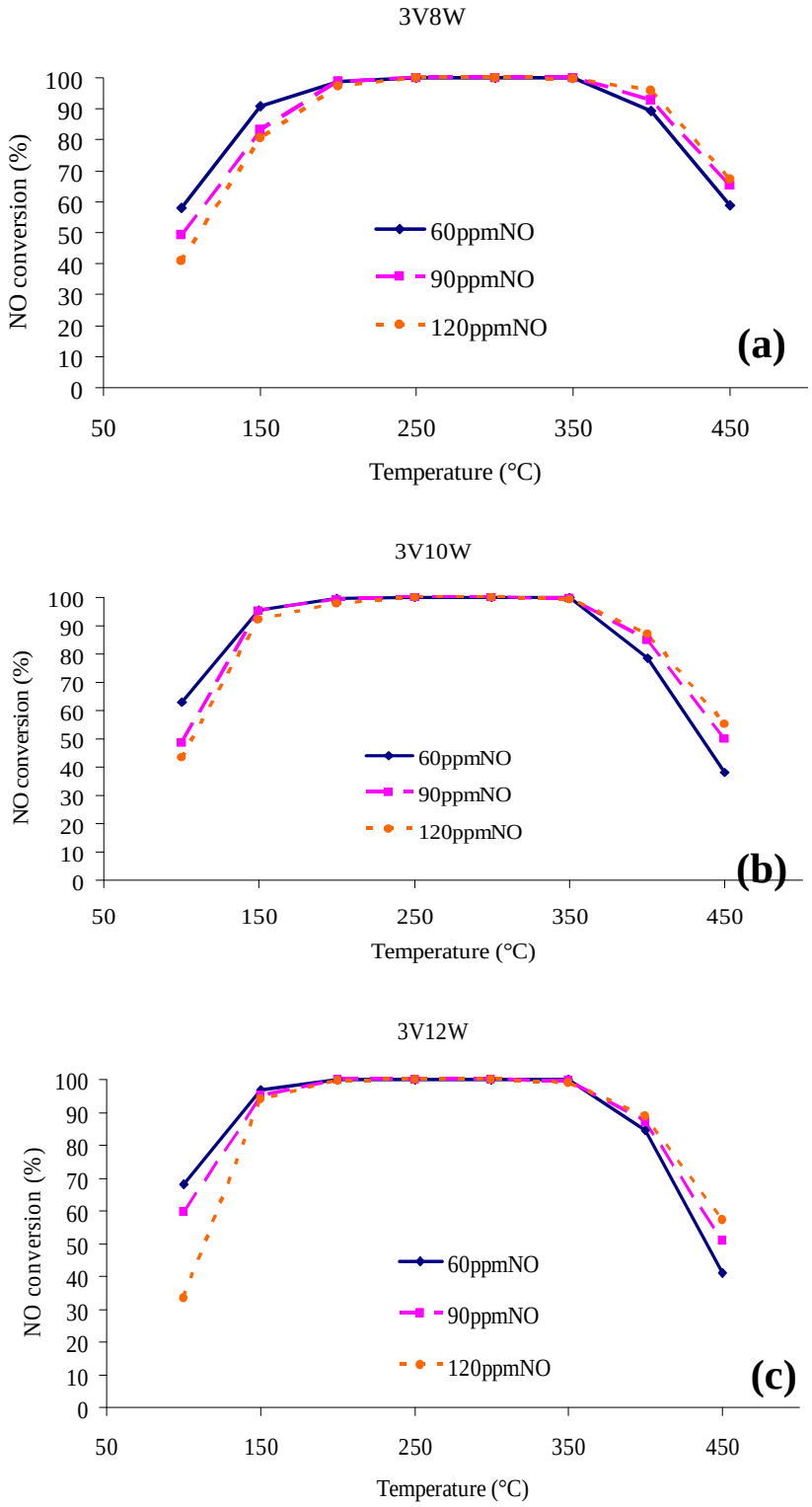

Figure 4.15 NO conversion for SCR of NO by NH_3 over (a) 3V8W, (b) 3V10W, and (c) 3V12W catalysts. The initial of NO in the feed was varied in the range of 60-120ppm.

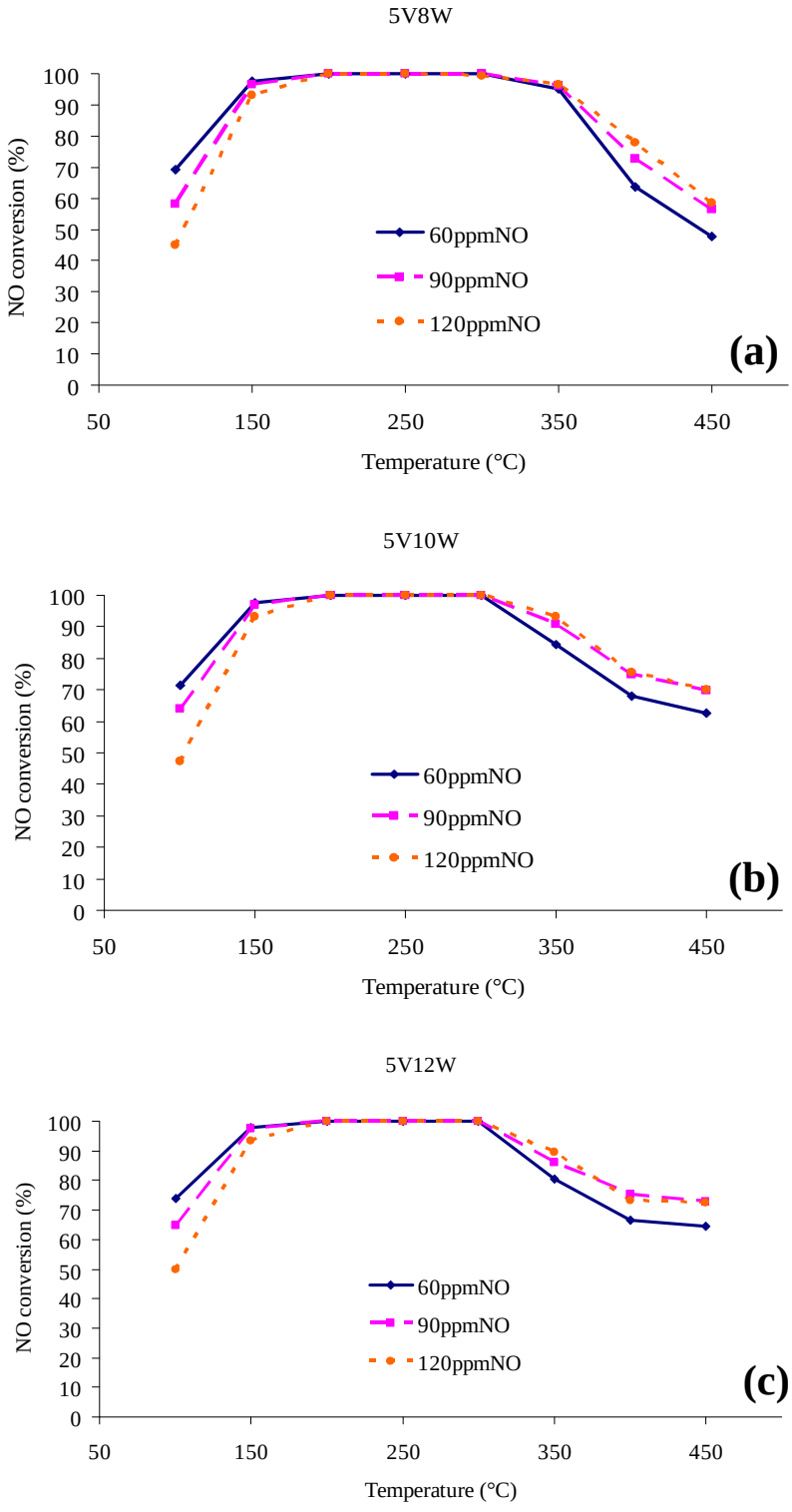

Figure 4.16 NO conversion for SCR of NO by NH_3 over (a) 5V8W, (b) 5V10W, and (c) 5V12W catalysts. The initial of NO in the feed was varied in the range of 60-120ppm.

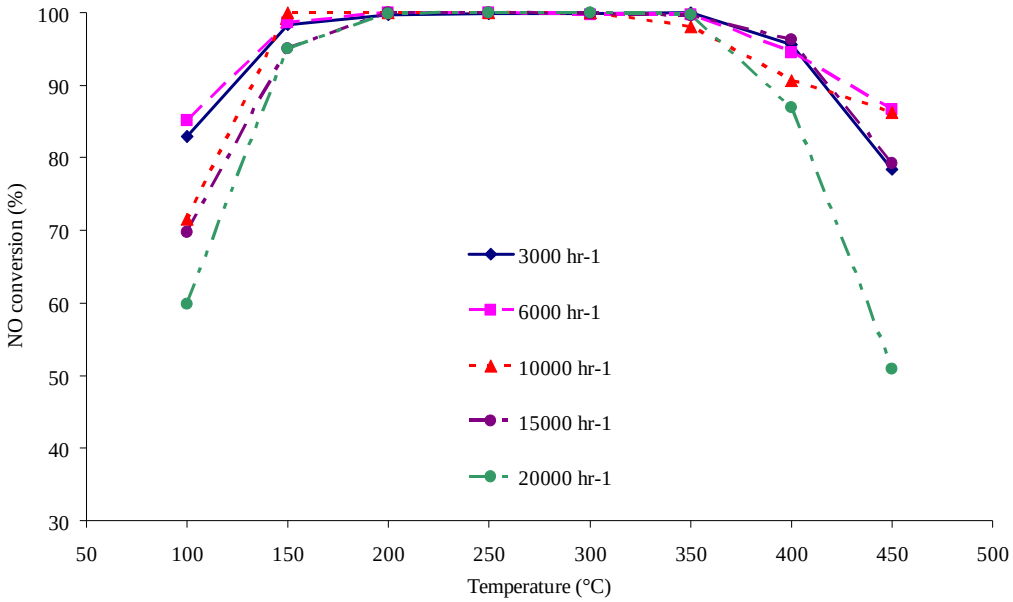

Figure 4.17 NO conversion for SCR of NO by NH_3 over the 3V12W catalyst. The initial of NO in the feed is 60 ppm. The gas hourly space velocity was varied in the range of 3000-20000 hr^{-1}.

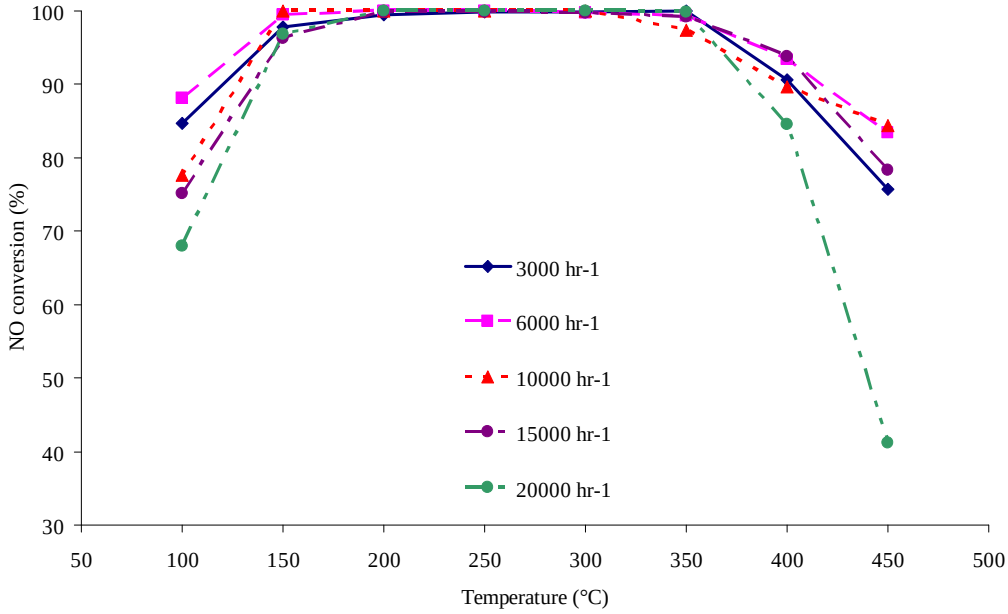

Figure 4.18 NO conversion for SCR of NO by NH_3 over the 3V12W catalyst. The initial of NO in the feed is 90 ppm. The gas hourly space velocity was varied in the range of 3000-20000 hr^{-1}.

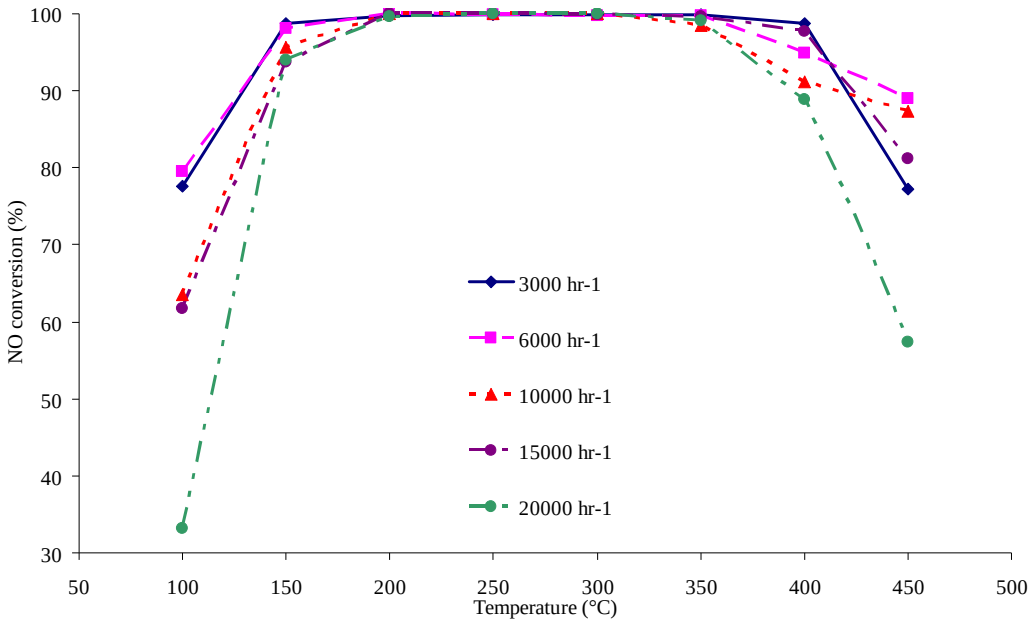

Figure 4.19 NO conversion for SCR of NO by NH_3 over the 3V12W catalyst. The initial of NO in the feed is 120 ppm. The gas hourly space velocity was varied in the range of 3000-20000 hr^{-1}.

4.2 Manganese and another metal modified 3V12W catalysts

In this section, the 3V12W catalyst was promoted with manganese and another metal. The promoted catalysts were characterized by XRD to analyze crystal structure, nitrogen adsorption to determine the specific surface area, NH_3-TPD to determined amounts of acid site over catalyst surface, XPS to determine the oxidation states of vanadium and tungsten over catalyst surface, and ICP-OES to determine the amounts of metal loading of catalyst. And the catalytic activity for NO conversion was measured at a reaction temperature ranging from 50°C to 450°C.

4.2.1 Characterization of manganese and another metal catalyst

4.2.1.1 X-ray diffractometry

XRD patterns of various manganese and another metal catalysts are shown in Figures 4.20 to 4.22. The catalysts contained anatase TiO_2 primarily with small amounts of rutile and brookite phase. No peaks corresponding to V_2O_5, WO_3, manganese oxide, cerium oxide, copper oxide, or iron oxide were observed.

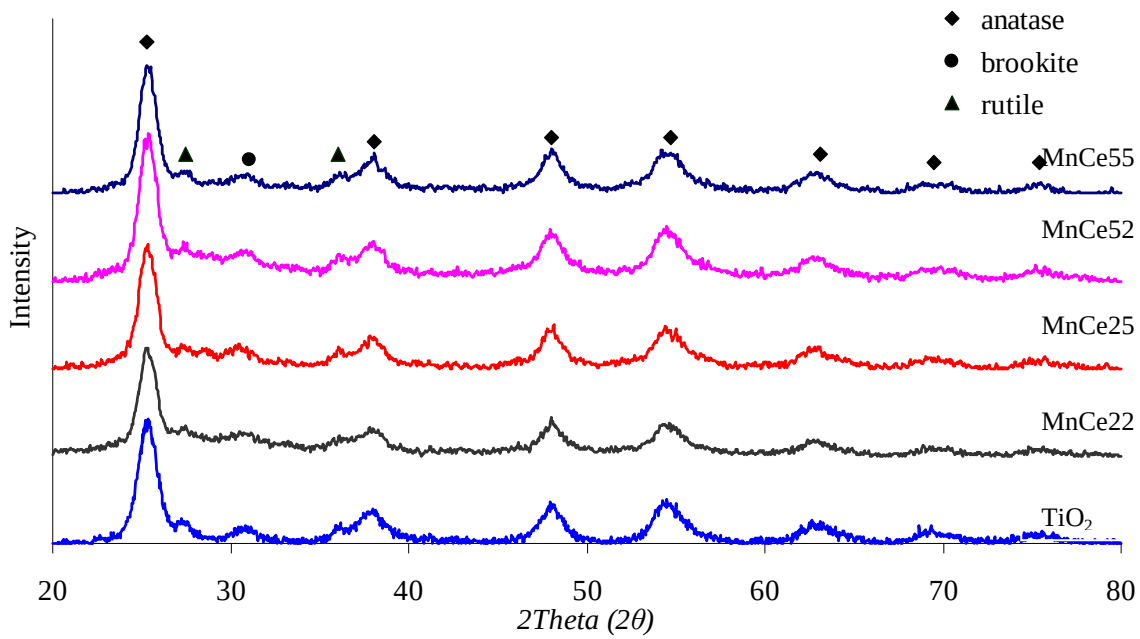

Figure 4.20 XRD patterns of the 3V12W catalysts that were promoted with manganese and cerium.

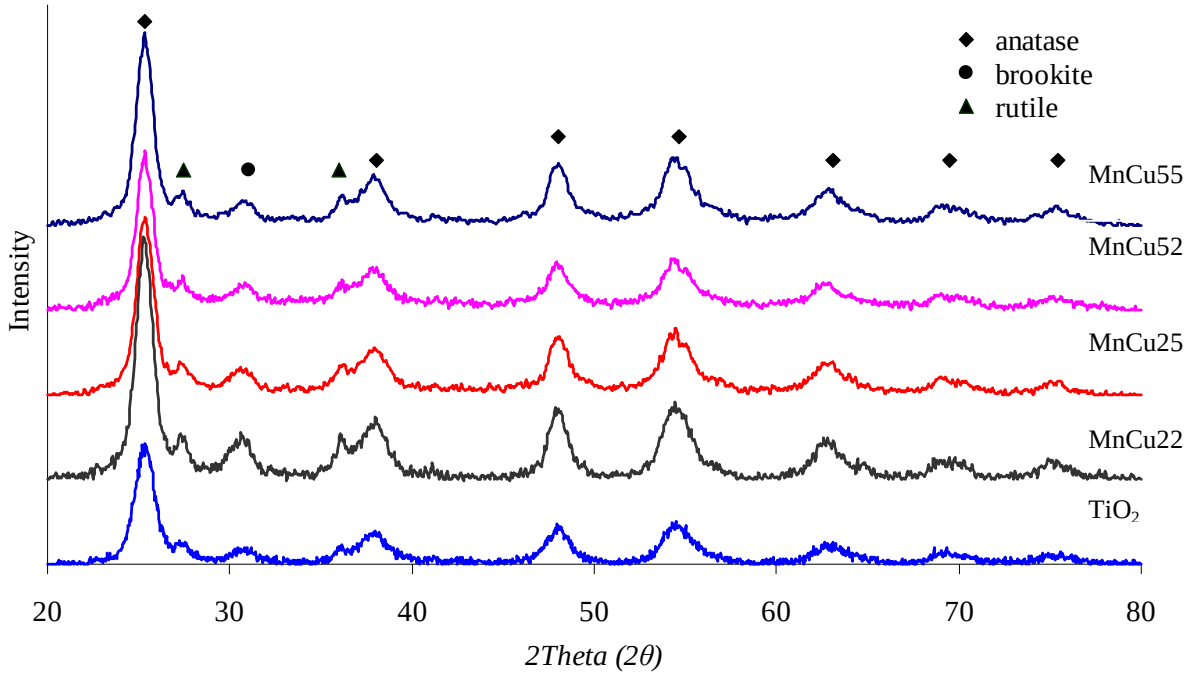

Figure 4.21 XRD patterns of the 3V12W catalysts that were promoted with manganese and copper.

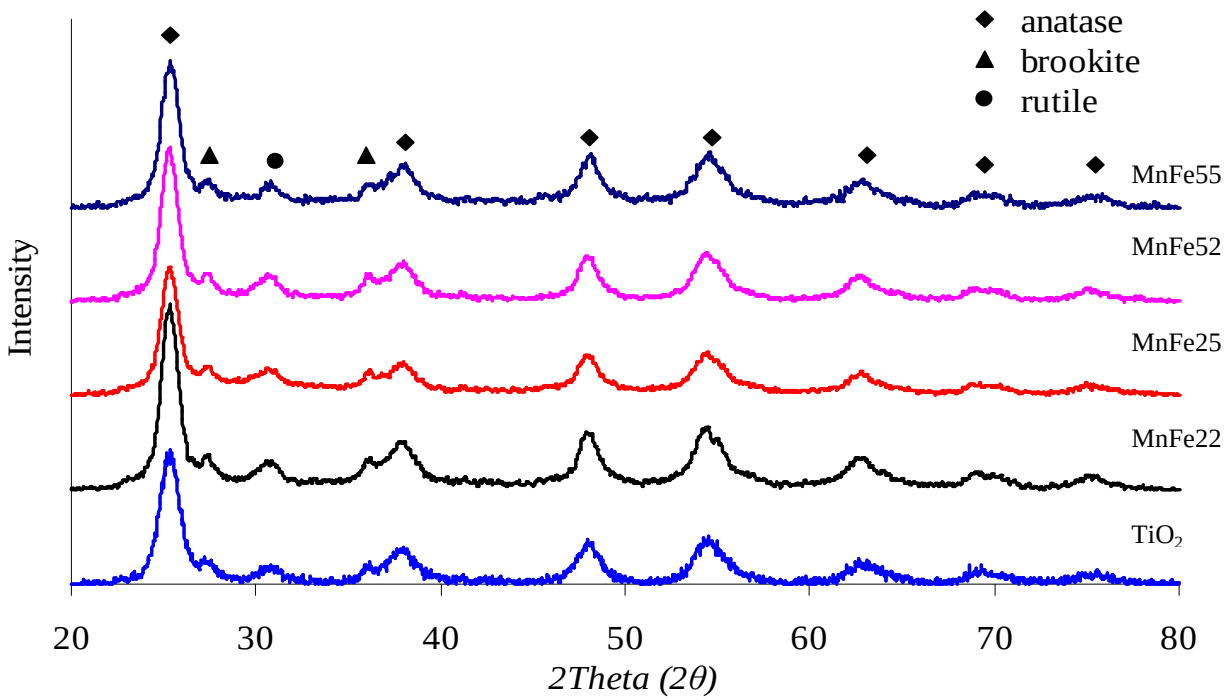

Figure 4.22 XRD patterns of the 3V12W catalysts that were promoted with manganese and iron.

4.2.1.2 Specific surface area and crystallite size of the 3V12W catalysts that were promoted with manganese and another metal

The most common procedure for determining surface area of a solid is based on adsorption and condensation of nitrogen at liquid nitrogen temperature. This method is also called BET (Brunauer Emmett Teller) method. About 0.2 grams of catalyst used in measurement. BET specific surface area of the catalyst and crystallite size of titania in the catalysts are shown in Table 4.6. Increasing the amount of manganese and another metal loading was higher the specific surface area of the catalysts, compared with 3V12W catalyst. The crystallite sizes of titania in the catalyst became slightly larger and were in the range of 7.1 - 7.7 nm. The crystallite size was calculated from XRD peak width using Debye-Scherrer equation.

Table 4.6 BET surface areas and crystallite size of the 3V12W catalysts that were promoted with manganese and another metal (cerium, copper, and iron)

Catalyst Sample	BET surface area (m^2/g)	Crystallite size [a] (nm)
3V12W	60.4	7.1
MnCe22	72.3	7.3
MnCe25	61.8	7.6
MnCe52	69.5	7.1
MnCe55	61.4	7.7
MnCu22	70.7	7.5
MnCu25	67.2	7.2
MnCu52	65.9	7.5
MnCu55	62.0	7.6
MnFe22	80.6	7.3
MnFe25	73.8	7.1
MnFe52	67. 2	7.5
MnFe55	60.4	7.2

[a] Calculated by Debye-Scherrer equation from XRD spectra

4.2.1.3 Temperature programmed desorption using NH_3 as a probe molecule (NH_3-TPD)

Temperature program desorption was a commonly used technique for the titration of surface acid sites. The strength of an acid site could be related to the corresponding desorption temperature of ammonia, while the total amount of ammonia desorption after saturation coverage permits quantification of the number of acid sites at the surface [Kung et al.,1985]. The temperature-programmed desorption profiles for the manganese and another metal catalysts are displayed in Figures 4.24 to 4.26. From the TPD profiles, the amounts of acid sites were calculated from the area under the curve and were listed in Table 4.7

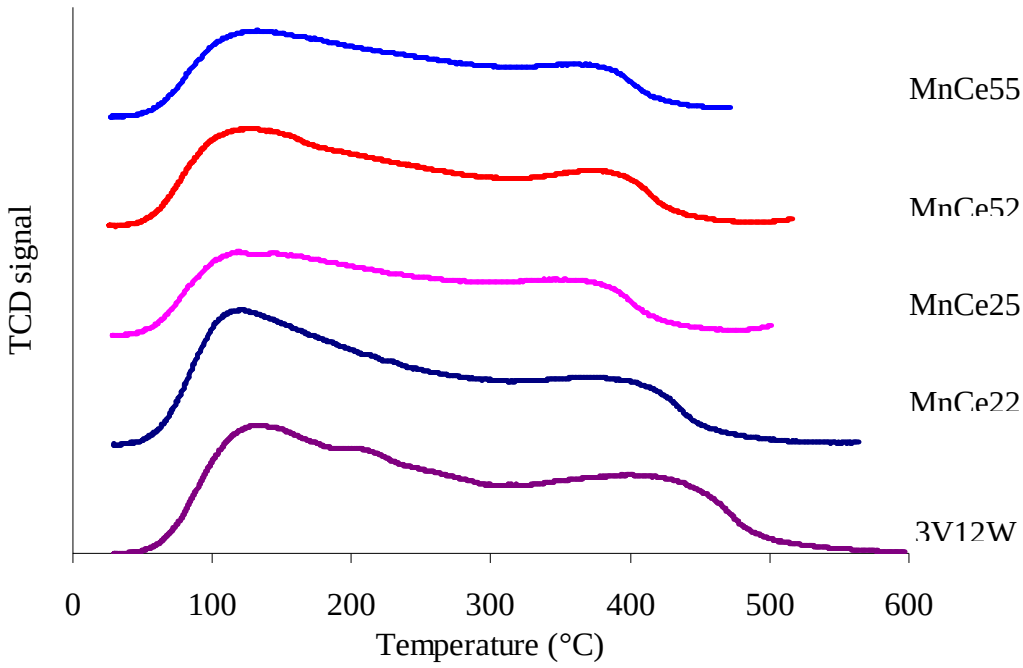

Figure 4.23 NH_3-TPD profiles of the 3V12W catalyst that were promoted with manganese and cerium

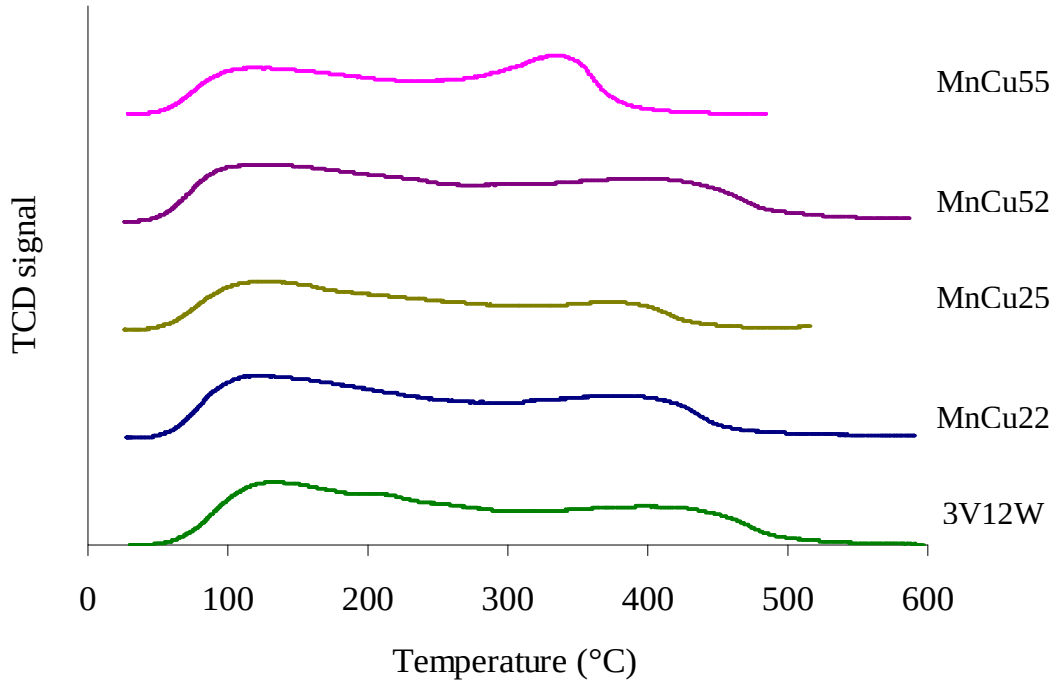

Figure 4.24 NH_3-TPD profiles of the 3V12W catalyst that were promoted with manganese and copper

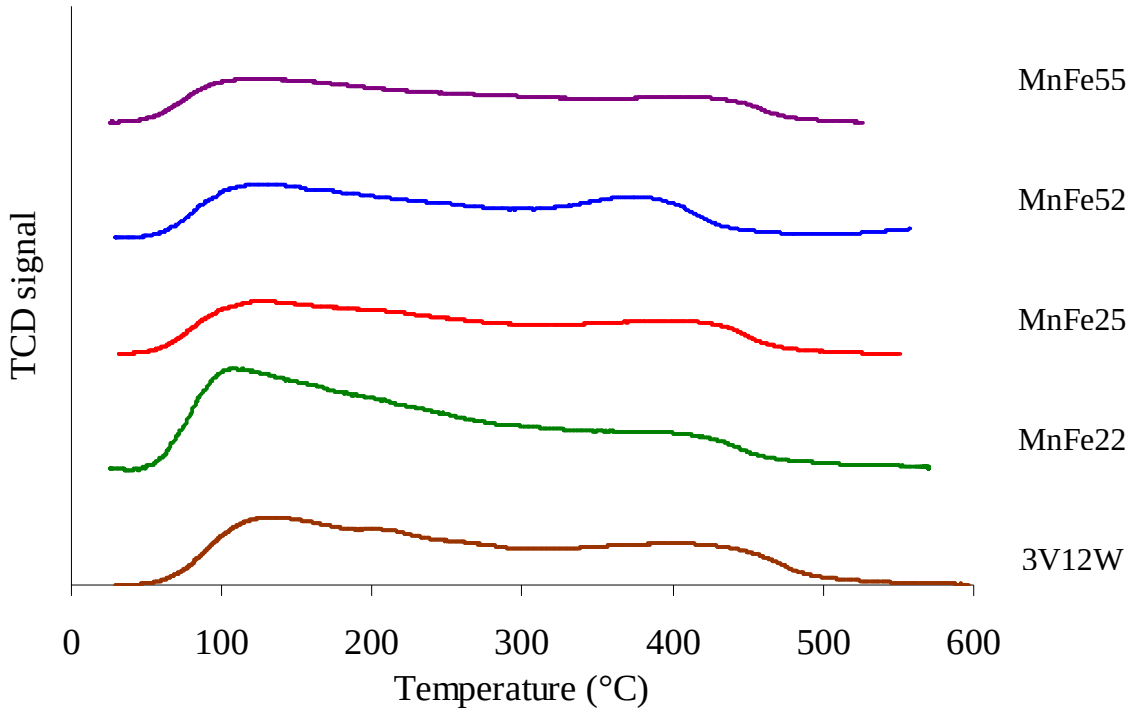

Figure 4.25 NH_3-TPD profiles of the 3V12W catalyst that were promoted with manganese and iron

Three series of loading manganese and other metal over 3V12W catalysts were measured surface acidity with NH_3 temperature program desorption, as condition of using in measurement of vanadium catalyst. They were found, surface acidity of catalyst decrease when increase manganese or another metal loading over 3V12W catalyst, reduce from 7566.62 to 4221.44 μmol H^+/g of lowest surface acidity of MnCe55 catalyst.

4.2.1.4 X-ray Photoelectron Spectroscopy (XPS)

The V_2O_5-WO_3/TiO_2 promoted with manganese and another metal catalysts were for the signals of vanadium, titanium, oxygen, tungsten, manganese, and another metal in term of binding energies. The binding energy of the three oxidation states of vanadium (V(III), V(IV), and V(V)) were 515.6, 516.6, and 517.5eV, respectively. The binding energy of the two states of tungsten (W(V) and W(VI)) were 34.7 and 35.4 eV, respectively. For 3V12W catalyst promote with manganese and another metal, the binding energy of vanadium was in the range of 515.82 - 518.45 eV and

that of tungsten was in the range of 35.50 – 38.38 eV. The binding energy, the percentage of atomic concentration, and FWHM of V $2p_{3/2}$ and W $4f_{7/2}$ are presented in Table 4.8and Table 4.9, respectively.

Table 4.7 Amounts of acidity of the 3V12W catalyst that were promoted with manganese and another metal (cerium, copper, and iron)

Sample	Amounts of acid site (μmol H^+/g)
3V12W	7566
MnCe22	6640
MnCe25	4555
MnCe52	4712
MnCe55	4221
MnCu22	6977
MnCu25	6081
MnCu52	6213
MnCu55	5577
MnFe22	8699
MnFe25	5695
MnFe52	5434
MnFe55	4773

Table4.8 Results from XPS for vanadium over 3V12W catalyst promoted with manganese and another metal.

sample	V $2p_{3/2}$								
	V(III)			V(IV)			V(V)		
	BE	FWHM	% atomic	BE	FWHM	% atomic	BE	FWHM	% atomic
3V12W	-	-	-	517.09	1.331	0.35	518.03	0.658	0.06
MnCe22	516.13	0.378	0.02	-	-	-	517.07	1.498	0.61
MnCe25	-	-	-	-	-	-	517.18	0.749	0.76
MnCe52	-	-	-	516.65	1.127	0.19	517.59	1.128	0.45
MnCe55	-	-	-	517.43	1.566	0.40	518.38	1.332	0.18
MnCu22	-	-	-				517.13	1.337	0.58
MnCu25	-	-	-	517.40	1.371	0.44	518.20	0.882	0.08
MnCu52	-	-	-				517.20	0.772	0.51
MnCu55	-	-	-	516.98	1.108	0.45	517.80	0.55	0.05
MnFe22	-	-	-	516.92	0.747	0.15	517.82	1.092	0.52
MnFe25	516.08	0.709	0.04	-	-	-	517.42	1.446	0.53
MnFe52	515.82	0.715	0.03	-	-	-	517.88	1.347	0.63
MnFe55	-	-	-	517.40	1.272	0.50	518.45	0.619	0.07

Table4.9 Results from XPS for tungsten over 3V12W catalyst promoted with manganese and another metal.

Sample	W $4f_{7/2}$					
	W (V)			W (VI)		
	BE	FWHM	% atomic	BE	FWHM	% atomic
3V12W	36.15	2.005	1.85	37.97	1.78	1.44
MnCe22	35.98	2.45	2.69	37.82	1.376	0.98
MnCe25	36.39	2.256	2.13	38.28	1.815	1.28
MnCe52	35.87	2.142	2.01	37.75	1.902	1.60
MnCe55	36.21	2.496	2.14	38.21	1.604	0.86
MnCu22	-	-	-	37.34	2.127	3.80
MnCu25	-	-	-	37.96	1.602	3.27
MnCu52	36.08	2.305	2.22	37.98	1.609	1.11
MnCu55	35.50	2.409	2.32	37.48	1.827	1.08
MnFe22	-	-	-	38.08	1.531	3.91
MnFe25	35.78	2.087	2.39	37.68	1.601	1.44
MnFe52	36.35	2.077	2.17	38.38	1.76	1.38
MnFe55	35.82	2.056	2.16	37.72	1.607	1.29

4.2.1.5 Metal contents in the 3V12W catalysts that were promoted with manganese and another metal

Amounts of metals in the catalyst were determined using inductively coupled plasma-optical emission spectroscopy (ICP-OES). The results were listed in Table 4.10. The result showed that both ICP-OES and calculating amount of metal in catalysts were proximate.

Table 4.10 The compositions of 3V12W catalysts that were promoted with manganese and another metal as determined from ICP-OES.

Sample	Vanadium content (%wt.)	Tungsten content (%wt.)	Manganese content (%wt.)	Cerium content (%wt.)	Copper content (%wt.)	Iron content (%wt.)
MnCe22	3.25	11.88	1.63	0.33	-	-
MnCe25	3.27	11.86	1.58	5.91	-	-
MnCe52	3.24	11.64	3.88	2.18	-	-
MnCe55	3.24	11.94	4.08	5.69	-	-
MnCu22	3.28	11.95	1.38	-	1.60	-
MnCu25	3.29	12.20	1.57	-	4.44	-
MnCu52	3.22	11.61	3.80	-	1.87	-
MnCu55	3.24	12.10	4.05	-	4.95	-
MnFe22	3.21	11.78	1.47	-	-	1.47
MnFe25	3.22	11.68	1.54	-	-	3.84
MnFe52	3.25	11.84	3.85	-	-	1.48
MnFe55	3.26	11.98	3.96	-	-	3.93

4.2.2 Selective catalytic reduction of NO by NH_3 over 3V12W catalysts that were promoted with manganese and another metal

This section presents the catalytic activities of the 3V12W catalysts that were promoted with manganese and another metal for SCR of NO by NH_3 under high reactant concentrations and high space velocity at a reaction temperature ranging from 50°C to 450°C.

4.2.2.1 Activities of 3V12W that were promoted with Mn and Ce catalysts

The catalytic activities of the 3V12W catalysts that were promoted with manganese and cerium are presented. The catalysts contained manganese and cerium at the concentration of either 2 mole% or 5 mole% each. Feed gas stream contained 500 ppm NO, 500 ppm NH_3, 3 vol.% O_2, and balancing N_2. The reaction temperature was varied between 50-450°C.

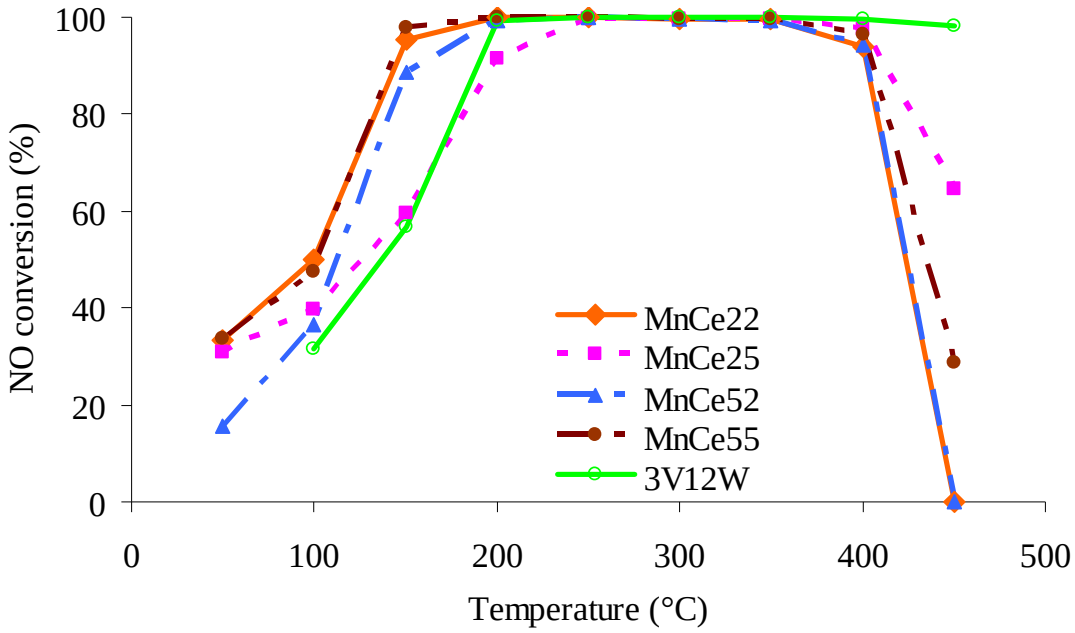

Figure 4.26 NO conversion for SCR of NO by NH_3 over the 3V12W catalysts that were promoted with manganese and cerium catalysts.

4.2.2.2 Activities of 3V12W that were promoted with Mn and Cu catalysts

The catalytic activities of the 3V12W catalysts that were promoted with manganese and copper are presented. The catalysts contained manganese and cerium at the concentration of either 2 mole% or 5 mole% each. Feed gas stream contained 500 ppm NO, 500 ppm NH_3, 3 vol.% O_2, and balancing N_2. The reaction temperature was varied between 50-450°C.

4.2.2.3 Activities of 3V12W that were promoted with Mn and Fe catalysts

The catalytic activities of the 3V12W catalysts that were promoted with manganese and iron are presented. The catalysts contained manganese and cerium at the concentration of either 2 mole% or 5 mole% each. Feed gas stream contained 500 ppm NO, 500 ppm NH_3, 3 vol.% O_2, and balancing N_2. The reaction temperature was varied between 50-450°C.

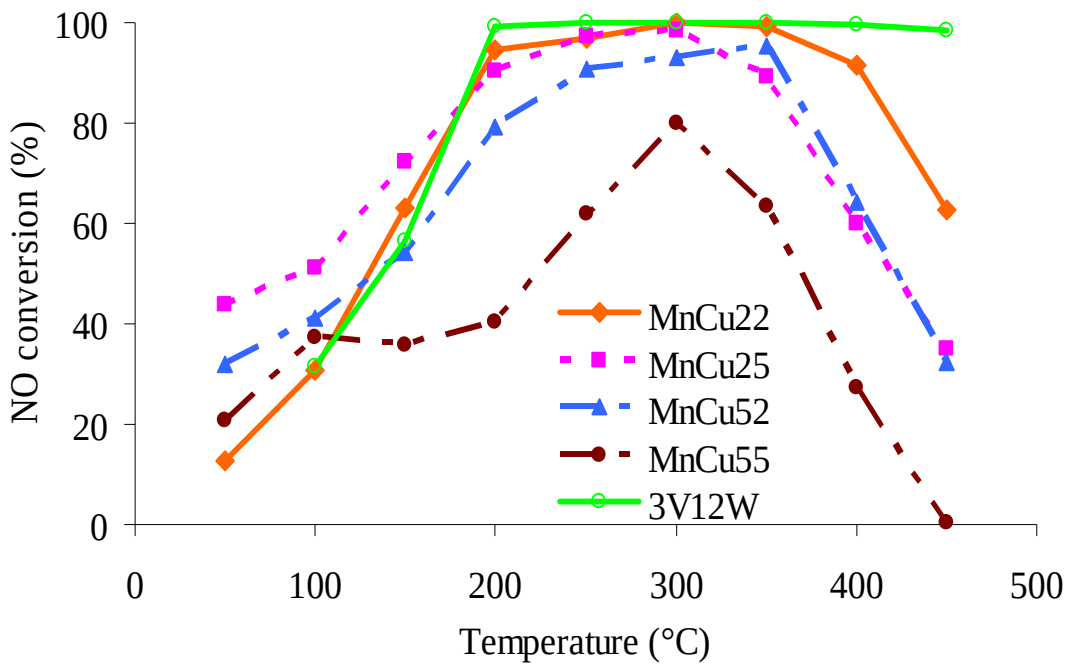

Figure 4.27 NO conversion for SCR of NO by NH_3 over 3V12W promoted with manganese and copper catalysts.

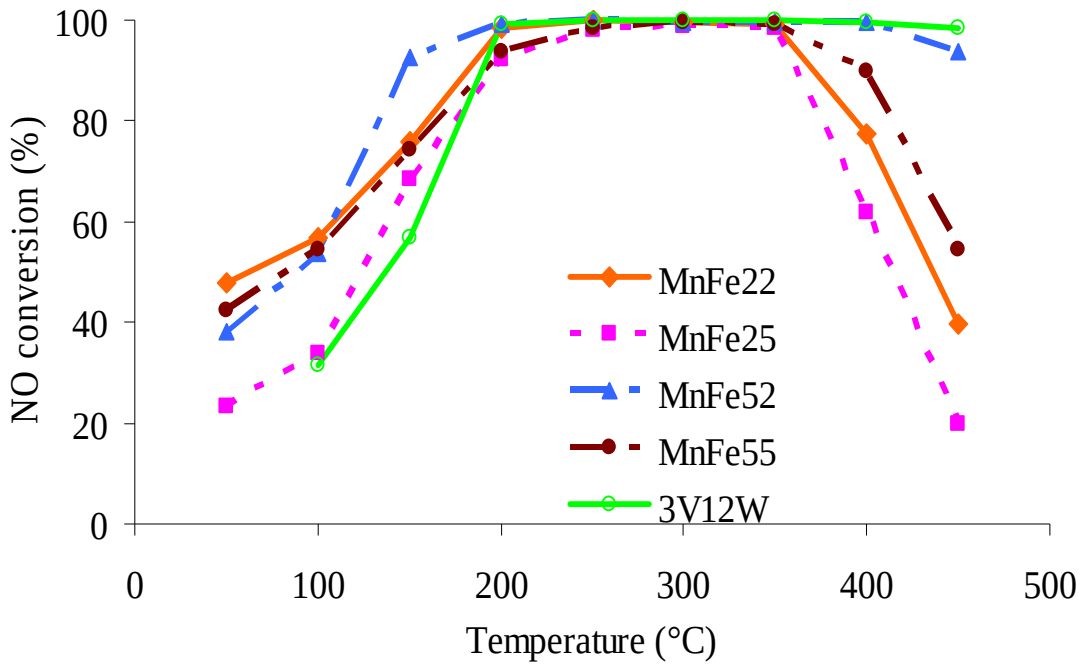

Figure 4.28 NO conversion for SCR of NO by NH_3 over 3V12W promoted with manganese and iron catalysts.

From these results, the promotion of manganese and another metal enhanced the catalytic activity at a temperature below 200°C. These binary metal loading were reported that can to improve activity in low temperature region [Wu et al.,2008; Kang et al.,2006; and Qi et al.,2003]. These metals oxidized NO to NO_2 and NO_2 reacted with NO and NH_3. This reaction was called fast SCR. With lower activation energy, fast SCR occurred more easily than the common SCR.

In the high temperature region however, the promotion of manganese and another metal lowered the NO conversion. This may be attributed to the oxidation of NH_3, which occurred at high temperature [Bourikas et al.,2004].

4.2.2.4 Activities of the 3V12W catalysts that were promoted with manganese and another metal with water vapor present in feed (wet condition)

The promoted 3V12W catalysts chosen for this portion of the experiment were the ones that exhibited the best performance in a wide temperature range for each pair

of metal (see section 4.2.1 to 4.2.3). The catalysts being tested were MnCe55, MnCu25, MnFe52, and 3V12W (as a bench mark).

From Figure 4.30 the presence of water vapor in the feed lowered the catalytic activity of the 3V12W catalyst. The decline in the activity was greater when more water vapor was presented. Inspection of Figure 4.31 to 4.33 suggested that the promotion of manganese and another metal appeared to maintain the catalytic activity of the catalysts even when water vapor was present in the feed.

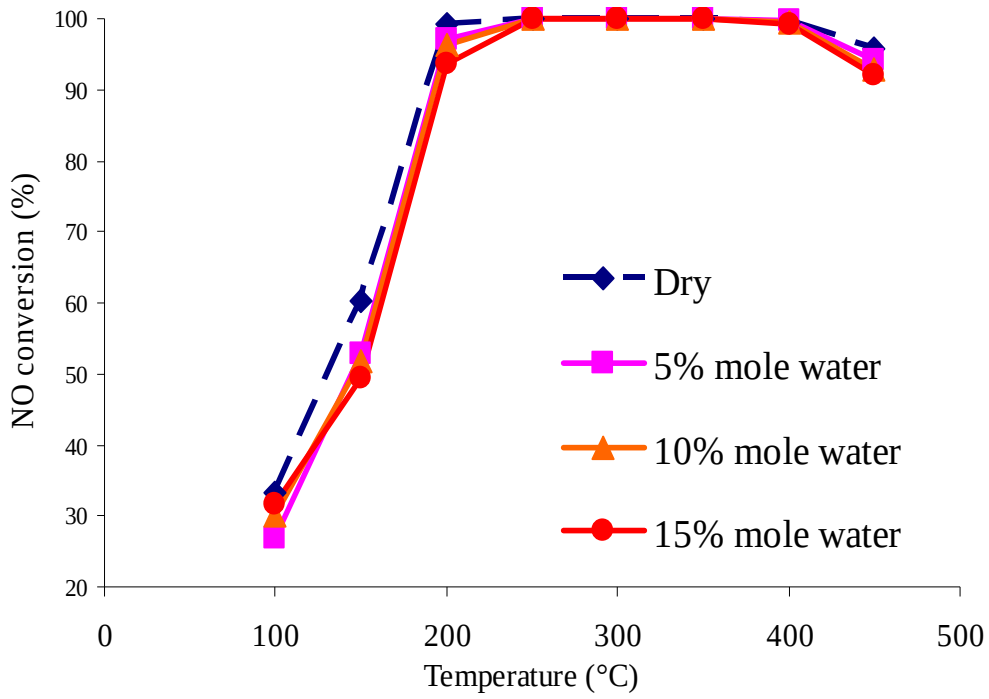

Figure 4.29 NO conversion for SCR of NO by NH_3 over the 3V12W catalyst under wet condition.

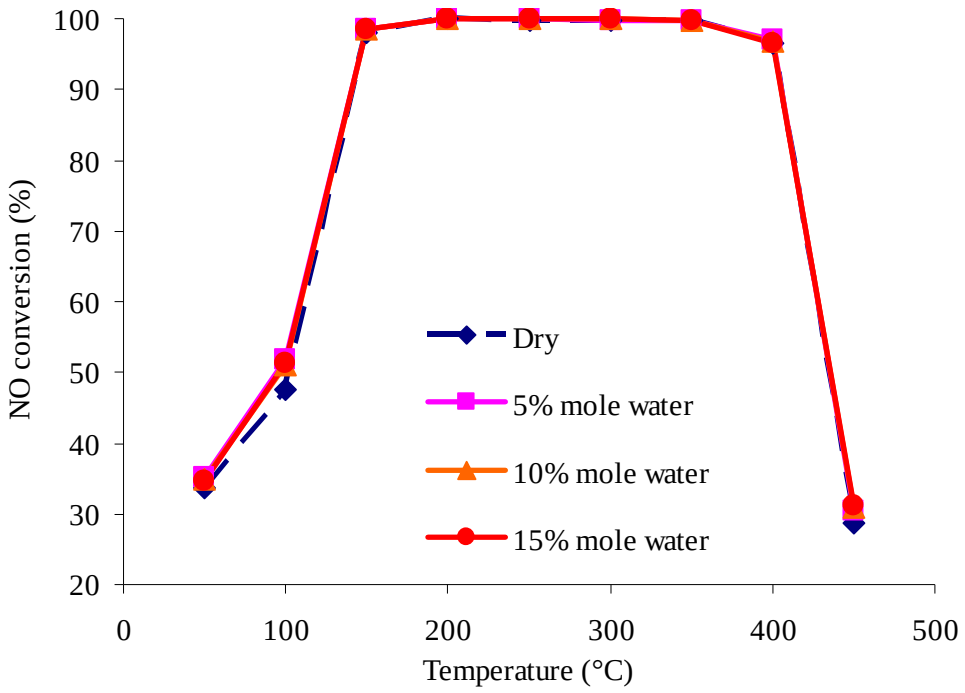

Figure 4.30 NO conversion for SCR of NO by NH_3 over the MnCe55 catalyst under wet condition.

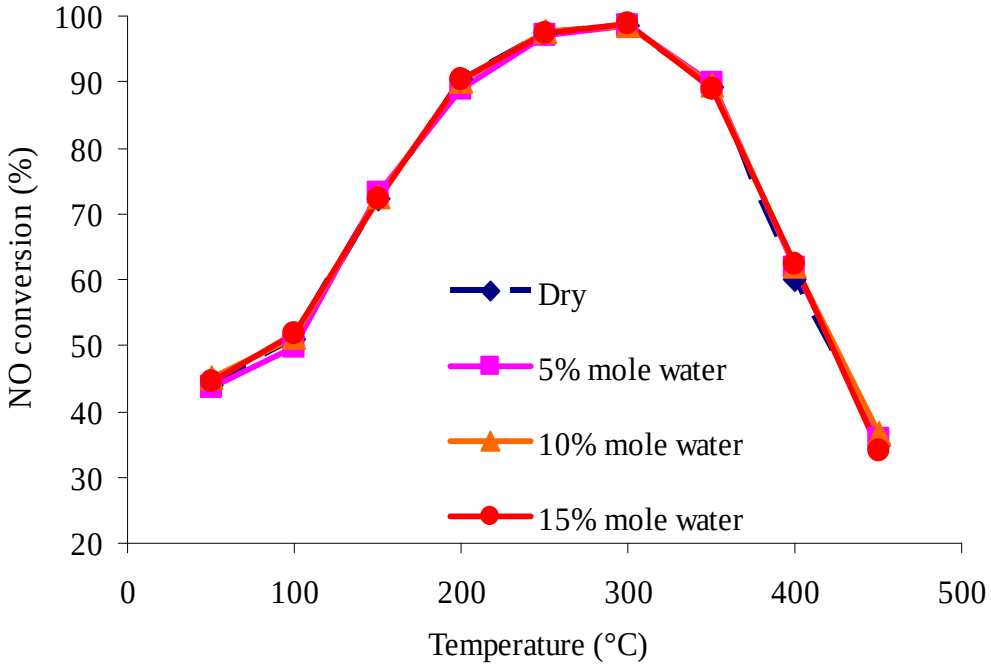

Figure 4.31 NO conversion for SCR of NO by NH_3 over MnCu25 catalyst under wet condition.

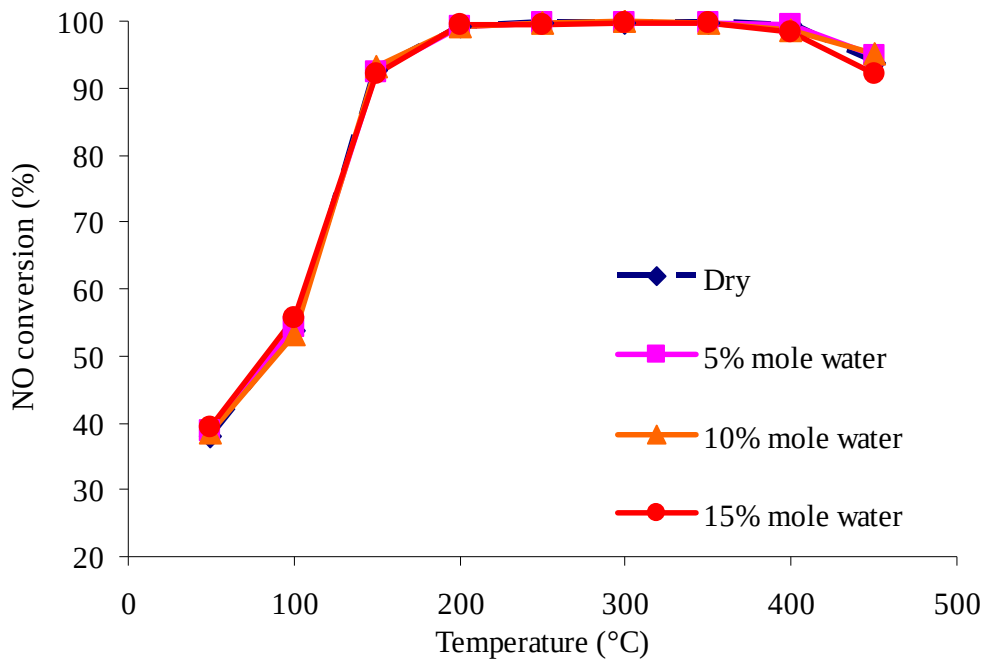

Figure 4.32 NO conversion for SCR of NO by NH_3 over MnFe52 catalyst under wet condition.

CHAPTER V

CONCLUSIONS AND RECOMMENDATIONS

In this chapter, section 5.1 provides the conclusions obtained from the experimental results. Additionally, recommendations for further study are given in section 5.2.

5.1 Conclusions

- Vanadium and tungsten loading reduce surface area of pure TiO_2.
- Vanadium increases NO conversion in lower and higher temperature region.
- Tungsten increases reaction temperature window.
- At low temperature (<200°C), higher NO concentration in feed, NO conversion decrease.
- At high temperature (>350°C), higher NO concentration in feed, NO conversion increase.
- Mn and another metal promoted increase surface area of 3V12W catalyst but decrease surface acidity of catalysts.
- Manganese and cerium or iron are appropriate promoter for low temperature SCR of NO.

5.2 Recommendations

1. Other species of reaction must be specified to determine selectivity of reaction.
2. Lewis and Brønsted acid site should be investigated with in-situ NH_3/pyridine adsorption in further.
3. Effect of SO_2 in feed stream must be investigated.
4. NO oxidation to NO_2 test should be investigated in further for fast SCR reaction study.
5. Monolithic type of this catalyst must be studied for use in SCR unit of industrial.

REFERNCES

Baraket, L., Ghorbel, A. and Grange, P. Selective catalytic reduction of NO by ammonia on V_2O_5–SO_4^{2-}/TiO_2 catalysts prepared by the sol–gel method. Applied Catalysis B: Environmental 72 (2007):37–43.

Bosch, H., and Janssen, F.J.J.G., "Formation and control of nitrogen oxide", Catalysis Today, 2 (1988):369-532.

Bourikas, B., Fountzoula, Ch., Kordulis, Ch. Monolayer transition metal supported on titania catalysts for the selective catalytic reduction of NO by NH_3. Applied Catalysis B: Environmental 52 (2004):145–153.

Busca, G., Lietti, L., Ramisa, G., and Bertic, F. Chemical and mechanistic aspects of the selective catalytic reduction of NO_X by ammonia over oxide catalysts: A review. Applied Catalysis B: Environmental 18 (1998):1-36.

Djerad, S., Tifouti, L., Crocoll, M., and Weisweiler, W. Effect of vanadia and tungsten loadings on the physical and chemical characteristics of V_2O_5-WO_3/TiO_2 catalysts. Journal of Molecular Catalysis A: Chemical 208 (2004):257–265.

Kanongchaiyot, N. Effect of tungsten and potassium on the V_2O_5/TiO_2 catalyst for selective catalytic reduction of NO with NH_3. Master's Thesis, Department of Chemical Engineering, Graduate School, Chulalongkorn University, 1998.

Kang, M., Park, E. D., Kim, J. M., and Yie, J. E. Cu–Mn mixed oxides for low temperature NO reduction with NH_3. Catalysis Today 111 (2006): 236–241.

Kim,Y. A., Choi, J.H.,, Scott, J., Chiang, K., and Amal, R. Preparation of high porous Pt–V_2O_5–WO_3/TiO_2/SiC filter for simultaneous removal of NO and particulates. Powder Technology 180 (2008):79–85.

Kobayashi, M., and Hagi, M. V_2O_5-WO_3/TiO_2-SiO_2-SO_4^{2-} catalysts: Influence of active components and supports on activities in the selective catalytic reduction of NO by NH_3 and in the oxidation of SO_2. Applied Catalysis B: Environmental 63 (2006):104–113.

Kung, M. C. and Kung, H. H. IR studies of NH_3, Pyridine, CO, and NO adsorbed on transition metal oxides. Catal. Rev. Sci. Eng. 27 (1985): 425-460.

Lietti, L., Alemany, J. L., Forzatti, P., Busca, G., Ramis, G., Giamello, E., and Bregani F. Reactivity of V_2O_5-WO_3/TiO_2 catalysts in the selective catalytic reduction of nitric oxide by ammonia. Catalysis Today 29 (1996):143-148.

Lintz, H. G., and Turek, T. Intrinsic kinetics of nitric oxide reduction by ammonia on vanadia/titania catalyst. Applied Catalysis 85 (1992): 13-25.

Najbar, M., Brocławik, E., Góra., Camra, J., Białas, A., and Wesełucha-Birczyńska, A. Evolution of the surface species of the V_2O_5 –WO_3 catalysts. Chemical Physics Letters 325 (2000):330–339.

Nicosia, D., Czekaj, I., and Kröcher, O. Chemical deactivation of V_2O_5/WO_3–TiO_2 SCR catalysts by additives and impurities from fuels, lubrication oils and urea solution

Part II. Characterization study of the effect of alkali and alkaline earth metals. Applied Catalysis B: Environmental 77 (2008):228–236.

Nova, I., Ciardelli, C., Tronconi, E., Chatterjee D., and Bandl-Konrad, B. NH_3–NO/NO_2 chemistry over V-based catalysts and its role in the mechanism of the Fast SCR reaction. Catalysis Today 114 (2006):3–12.

Ozera, N., and Lampert, C. M. Electrochromic performance of sol-gel deposited WO_3-V_2O_5 films. Thin Solid Films 349 (1999):205-211.

Phil, H. H., Reddy, M. P., Kumar, P. A., Ju, L. K., and Hyo, J. S. SO_2 resistant antimony promoted V_2O_5/TiO_2 catalyst for NH_3-SCR of NO_X at low temperatures. Applied Catalysis B: Environmental 78 (2008):301–308.

Qi, G. and Yang, R. T. Low-temperature selective catalytic reduction of NO with NH_3 over iron and manganese oxides supported on titania. Applied Catalysis B: Environmental 44 (2003):217–225.

Tronconi, E., Lietti, L., Forzatti, P., and Malloggi, S. Experimental and theoretical investigation of the dynamics of the SCR - DeNOx reaction. Chemical Engineering Science 51(1996):2965-2970.

Topsøe, N. Y., Topsøe, H., Dumesic, J. A. Vanadia/Titania Catalysts for Selective Catalytic Reduction (SCR) of Nitric-Oxide by Ammonia : I. Combined Temperature-Programmed in-Situ FTIR and On-line Mass-Spectroscopy Studies Journal of Catalysis. 151(1995):226-240.

Topsoe N. Y., Dumesic J. A., Topsoe H. Vanadia-Titania Catalysts for Selective Catalytic Reduction of Nitric-Oxide by Ammonia : II. Studies of Active Sites and Formulation of Catalytic Cycles. Journal of Catalysis. 151(1995):241-252.

Vargas, M. A. L., Casanova, M., Trovarelli, A., and Busca, G. An IR study of thermally stable V_2O_5-WO_3 -TiO_2 SCR catalysts modified with silica and rare-earths (Ce, Tb, Er). Applied Catalysis B: Environmental 75 (2007):303–311.

Wu, Z., Jiang, B., and Liu, Y. Effect of transition metals addition on the catalyst of manganese/titania for low-temperature selective catalytic reduction of nitric oxide with ammonia. Applied Catalysis B: Environmental 79 (2008):347–355.

Xu ,W., Yu, Y., Zhang, C., and He, H. Selective Catalytic Reduction of NO by NH_3 over a Ce/TiO_2 Catalyst. Catalysis Communications 9 (2008):1453–1457.

Yang, R.T., and Li, W. J. Ion-Exchanged Pillared Clays: A New Class of Catalysts for Selective Catalytic Reduction of NO by Hydrocarbons and by Ammonia. Journal of Catalysis, 155 (1995):414-417.

APPENDICES

APPENDIX A

CALCULATION FOR CATALYST PREPARATION

Preparation of V_2O_5-WO_3-TiO_2 are shown as follows:

Reagent:
- Titania powder prepared by a sol-gel method.
- Ammonium metavanadate 99.999%, NH_4VO_3 (Aldrich)
- Ammonium metatungsteae hydrate 99.99%, $(NH_4)_6H_2W_{12}O_{40}\cdot xH_2O$ (Aldrich)
- Oxalic acid hydrate (Fluka)

Calculation for the preparation of V_2O_5-WO_3-TiO_2

Example calculation for the preparation of 3 wt.%Vanadium-12 wt.%Tungsten/TiO_2

Based on 5 g of catalyst used, the composition of the catalyst will be as follows:

vanadium	=	0.03×5	=	0.15g
tungsten	=	0.12×5	=	0.6 g
TiO_2	=	5-0.15-0.6	=	4.25 g

Vanadium 0.15 g was prepared from NH_4VO_3 and molecular weight of V is 50.1961 g/mole

$$NH_4VO_3 \text{ required} = \frac{NH_4VO_3 \times vanadium\ required}{MW\ of\ V}$$

$$= (116.98 / 50.1961) \times 0.03 = 0.06991 \text{ g}$$

Tungsten 0.6 g was prepared from NH_4VO_3 and molecular weight of W is 183.85 g/mole

$(NH_4)_6H_2W_{12}O_{40}\cdot xH_2O$ required =

$$\frac{(NH_4)_6H_2W_{12}O_{40}\cdot xH_2O \times \textit{tungsten required}}{12 \times \textit{MW of W}}$$

$= 2956.3 \times 0.6/(183.85 \times 12) =$ 0.804 g

Oxalic acid require equal to two time of mole of vanadium

Mole of vanadium = 0.15/50.1961 = 0.00299 mole

Molecular weight of oxalic acid equal to 126.07 g/mole

Oxalic acid required = 0.00299×126.07 = 0.3656 g

Calculation for preparation of manganese and another metal on V_2O_5-WO_3-TiO_2

Reagent:
- Manganese(II)Nitrate hydrate 99.99%, $Mn(NO_3)_2\cdot xH_2O$ (Aldrich)
- Cerium(III) nitrate hexahydrate 99.99%, $Ce(NO_3)_3\cdot 6H_2O$ (Aldrich)
- Cupric nitrate hydrate ≥99.99%, $Cu(NO_3)_2\cdot 2.5H_2O$(Aldrich)
- Iron(III) nitrate nonahydrate≥99.999%, $Fe(NO_3)_2\cdot 9H_2O$(Aldrich)

Molecular of manganese = 54.938 g/mol

Molecular of cerium = 141.116 g/mol

Molecular of copper = 63.546 g/mol

Molecular of iron = 55.845 g/mol

Molecular of $Mn(NO_3)_2\cdot xH_2O$ = 178.95 g/mol

Molecular of $Ce(NO_3)_3\cdot 6H_2O$ = 434.22 g/mol

Molecular of $Cu(NO_3)_2\cdot 2.5H_2O$ = 232.59 g/mol

Molecular of $Fe(NO_3)_2\cdot 9H_2O$ = 404.00 g/mol

Amount of a pair of metal based on V_2O_5-WO_3-TiO_2

Example prepare 2 mole% manganese- 2 mole% cerium over 3V12W

Using 3V12w catalyst for prepare = 2 g

Mole of vanadium = $(2 \times 0.03 / 50.1961)$

= 0.001195 mole

Mole of tungsten = $(2 \times 0.12 / 183.85)$

= 0.0013054 mole

Mole of titanium = $(2 - 0.06 - 0.24) / 79.867$

= 0.021285 mole

Total mole of 3V12W = 0.02379 mole

From solve equation two variable

Given A = $mole\%\ of\ \ Mn \div (100 - mole\%\ of\ \ Mn)$

B = $mole\%\ of\ \ Ce \div (100 - mole\%\ of\ \ Ce)$

And T = total mole of 3V12W

Then Mole of manganese required = $AT(B+1)/(1-AB)$

And mole of another metal (Ce) = $B(T + mole\ of\ \ Mn)$

A = $2 \div (100 - 2)$

= 0.020408

B = 0.020408

So Mole of manganese required = $\dfrac{0.020408 \times 0.02379 \times (0.020408 + 1)}{1 - (0.020408 \times 0.020408)}$

= 0.00049562 mole

And Mole of cerium required = $0.020408 \times (0.02379 + 0.00049562)$

= 0.00049562 mole

$Mn(NO_3)_2 \cdot xH_2O$ required = $(0.00049562 \times 178.95)$

= 0.0887g

$Ce(NO_3)_3 \cdot 6H_2O$ required = $(0.00049562 \times 434.22)$

= 0.2152g

APPENDIX B

DATA AND CALCULATION OF ACID SITE

Table B1 Reported total peak area from Micromeritrics Chemisorb 2750

Sample	Total peak are
1V8W	3.24535
1V10W	2.97547
1V12W	3.57507
3V8W	2.883473
3V10W	3.213651
3V12W	3.221219
5V8W	3.694145
5V10W	3.43798
5V12W	3.17811
MnCe22	2.85611
MnCe25	1.972881
MnCe52	2.002312
MnCe55	1.791801
MnCu22	2.986687
MnCu25	2.616947
MnCu52	2.727489
MnCu55	2.376658
MnFe22	3.91208
MnFe25	2.473868
MnFe52	2.287237
MnFe55	2.070345

Calculation of total acid sites

For pure 3V12W sample, total acid site is calculated from the following steps.

1. Conversion of total peak area to peak volume

Conversion from Micromeritrics Chemisorb 2750 is equal 77.5016 ml/area unit. Therefore, total peak volume is derived from

Total peak volume = 77.5016 x total peak area
= 77.5016 x 3.221219
= 249.648 ml

2. Calculation for adsorbed volume of 15% NH_3

Adsorbed volume of 15% NH_3 = 0.15 x total peak volume
= 0.15 x 249.648 ml
= 37.447 ml

3. Calculation of total acid sites

$$\text{Total acid sites} = \frac{(absorbed\ volume, ml) \times 101.325\ Pa}{(8.314 \times 10^{-3} \frac{Pa \cdot ml}{K \cdot \mu mol}) \times 298\ K \times (weight\ ofcatalyst, g)}$$

For pure titania sample, 0.1048 g of this sample was measured, therefore

$$\text{Total acid sites} = \frac{16.2109\ ml \times 101.325\ Pa}{(8.314 \times 10^{-3} \frac{Pa \cdot ml}{K \cdot \mu mol}) \times 298 K \times (0.0.2024\ g)}$$

$$= 7566.62\ \mu mol\ H^{+}/g$$

APPENDIX C

CALCULATION OF THE CRYSTALLITE SIZE

Calculation of the crystallite size by Debye-Scherrer equation

The crystallite size was calculated from the half-height width of the highest intensity diffraction peak of XRD patterns of transition alumina.

From Debye-Scherrer equation:

$$D = \frac{K\lambda}{\beta \cos\theta} \qquad (C.1)$$

where D = Crystallite size, Å

K = Crystallite-shape factor = 0.9

λ = X-ray wavelength, 1.5418 Å for CuKα

θ = Observed peak angle, degree

β = X-ray diffraction broadening, radian

The X-ray diffraction broadening (β) is the pure width of a powder diffraction free from all broadening due to the experimental equipment. α-Alumina is used as a standard sample to observe the instrumental broadening since its crystallite size is larger than 2000 Å. The X-ray diffraction broadening (β) can be obtained by using Warren's formula.

From Warren's formula:

$$\beta = \sqrt{B_M^2 - B_S^2} \qquad (C.2)$$

where B_M = The measured peak width in radians at half peak height.

B_S = The corresponding width of the standard material.

Example: Calculation of the crystallite size of titania

The half-height width of 101 diffraction peak = 0.93125^{o}

= 0.01625 radian

The corresponding half-height width of peak of α-alumina = 0.004 radian

The pure width = $\sqrt{B_M^2 - B_S^2}$

= $\sqrt{0.01625^2 - 0.004^2}$

= 0.01577 radian

β = 0.01577radian

2θ = 25.56^{o}

θ = 12.78^{o}

λ = 1.5418 Å

The crystallite size = $\frac{0.9x\,1.5418}{0.01577\ \cos 12.78}$ = 90.15Å

= 9 nm

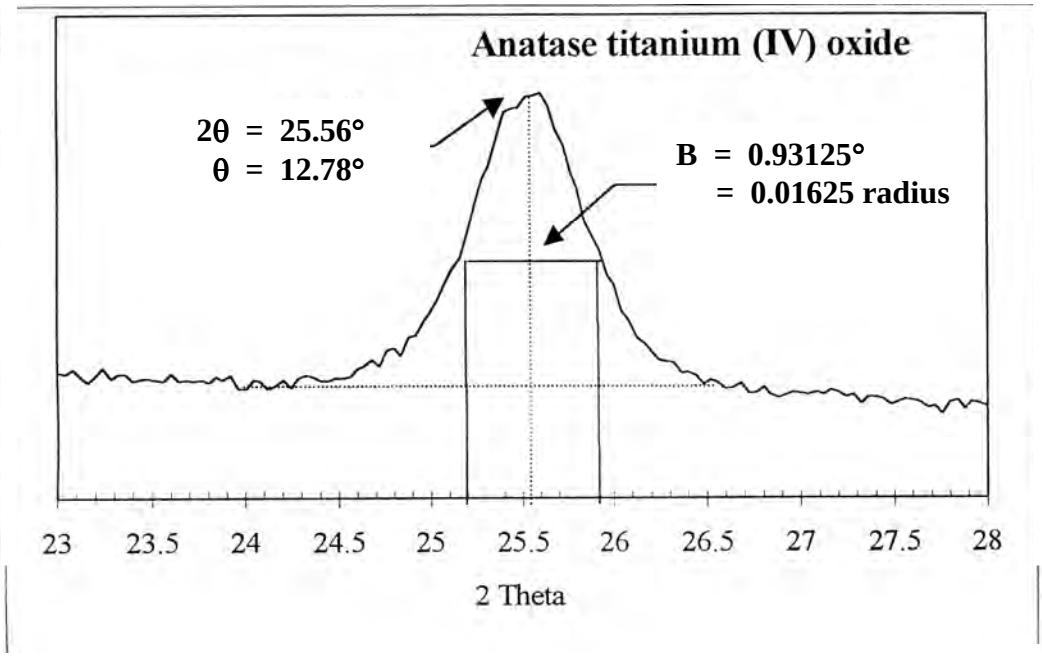

Figure C.1 The 101 diffraction peak of titania for calculation of the crystallite size

B

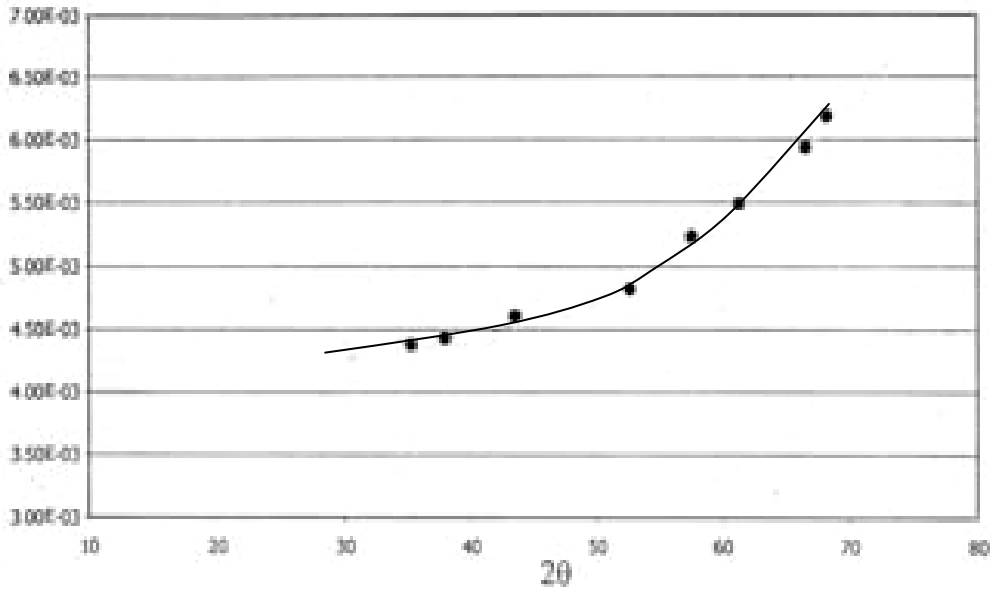

Figure C.2 The plot indicating the value of line broadening due to the equipment. The data were obtained by using α-alumina as standard.

LIST OF PUBLICATION

Izkun Arunyakasemsuk and Akawat Sirisuk. Selective catalytic reduction of NO with NH_3 over V_2O_5-WO_3/TiO_2 catalyst. 2nd SUT graduate conference, Suranaree University of Technology, January 21-22, 2009.

VITA

Mr. Izkun Arunyakasemsuk was born on May 24, 1983 in Sukhotai, Thailand. He finished high school from Sawanananwittaya School, Sawankhalok, Sukhotai, and received the bachelor's degree in Chemical Engineering from Faculty of Engineering, King Mongkut's Institute of Technology North Bangkok. He continued his master's study at Chulalongkorn University in June, 2007.